Studies on Photoreceptor-Horizontal Cell Synaptic Transmission by Analysing Spontaneous EPSCs in the Retinal Horizontal Cells of the Carp

Hajime HIRASAWA

A dissertation submitted to the Doctoral Program
in Biological Sciences, the University of Tsukuba
in partial fulfillment of the requirements
for the degree of Doctor of Philosophy in Science

June 2001

Abstract

The visual processing is originated from the synaptic transmission from retinal photoreceptors (PRs). An analysis of miniature spontaneous excitatory postsynaptic current (sEPSC) of retinal horizontal cell (HC) should be essential to investigate the vesicular transmitter release from PR to HC. However, the quantal sEPSC events on HCs have not yet been studied, since an adequate voltage clamp recording from HCs in the retina has not been established, probably due to their extensive electrical coupling between adjacent HCs. In the present study, at first, I aimed to record and to analyze sEPSCs of H1 HCs, with pharmacological agents to suppress the electrical coupling. Next, I aimed to investigate the regulatory mechanisms of PR-HC synaptic transmission, based on the sEPSC analysis of HCs. Especially, I focused on the importance of 1) presynaptic regulation by metabotropic glutamate receptor (mGluR) and 2) postsynaptic regulation by receptor desensitization, to the PR-HC synaptic transmission.

sEPSCs were recorded under whole-cell voltage clamp from carp H1 HCs uncoupled by dopamine. Red light steps, which hyperpolarize presynaptic cones and reduce glutamate release, induced outward current responses accompanied by a suppression of sEPSCs. sEPSCs decayed exponentially with a mean time constant of 0.71 ± 0.07 ms and had a reversal potential near 0 mV. Power spectral analysis of sEPSCs revealed a similar decay time constant. They were suppressed by a non-NMDA receptor antagonist, CNQX at 10 μM, and a relatively specific AMPA receptor antagonist, GYKI52466 at 20 μM. The presence of sEPSCs suggests that the release of glutamate from cone synaptic terminals is vesicular. The reduction in mean sEPSC frequency with red light was not accompanied by a significant change in the mean sEPSC conductance increase (482 ± 59 pS), suggesting that a decrease in the vesicular release rate from cones does not alter the vesicular glutamate concentration (quantal contents). The results suggest that the spontaneous events in H1 cells were contributed by non-NMDA (possibly AMPA) type glutamate receptors modulated by the red cone input.

To investigate the presynaptic regulation of PR-HC synapse, the mGluR-mediated synaptic

regulation at PR-HC synapse was tested by analysing sEPSCs of H1 HCs. Red light steps or the application of 100 μM cobalt reduced the frequency of sEPSCs without affecting their peak amplitude, consistent with hyperpolarization or the suppression of Ca^{2+} entry into cone synaptic terminals reducing vesicular transmitter release. Conversely, postsynaptic blockade of H1 HC AMPA receptors by 500 nM CNQX reduced the amplitude of sEPSCs without affecting their frequency. The selective group III mGluR agonist L-2-amino-4-phosphonobutyrate (L-APB) (20μM) reduced the frequency of sEPSCs with a slight reduction in amplitude, in H1 HCs dialysed with the protein kinase inhibitor, H-7. This action was antagonized by 500 μM (s)-2-methyl-2-amino-4-phosphonobutyrate (MAP4), a group III mGluR selective antagonist. The reduction of sEPSC frequency induced by L-APB was restored by application of 200 μM 4-aminopyridine (4-AP), a blocker of voltage-dependent potassium channels. These results suggest that the activation of group III mGluRs suppresses transmitter release from cone presynaptic terminals, via 4-AP sensitive pathway. They also suggest that negative feedback, operating via mGluR autoreceptors, may limit excessive glutamate release from cone synaptic terminals.

Desensitization of postsynaptic HC AMPA receptors was investigated using cyclothiazide (CTZ), an inhibitor of AMPA receptor desensitization. 100 μM CTZ depolarized H1 HCs and increased the amplitude of light responses, without prominent changes in their kinetics. sEPSCs in H1 HCs were observed in the presence of 2.5 mM heptanol, an uncoupling agent of gap junctions. 20 μM GYKI52466 blocked the sEPSCs, consistent with the sEPSCs being mediated by AMPA receptors. 100 μM cobalt suppressed the frequency of sEPSCs without changing their mean peak amplitude, suggesting that calcium-dependent transmitter release from cones was not affected by heptanol. CTZ increased the total inward charge transferred per sEPSC by increasing the sEPSC decay time constant 2-fold, without a significant change in their frequency and mean peak amplitude. This suggests that the depolarizing effect of CTZ on H1 HCs was due to blocking desensitization of AMPA receptors, increasing the inward current induced by glutamate released

from cone synaptic terminals. The desensitization of glutamate receptors may function to extend the dynamic range of H1 HC light responses.

An analysis of HC sEPSC, of which frequency is reduced by light stimulation, revealed the feature of asynchronous vesicular transmitter release from photoreceptors. The frequency of vesicular transmitter release can be modulated by a presynaptic regulation of mGluRs, resulting in the regulation of HC light responses. The postsynaptic AMPA receptor on HCs is desensitized by glutamate released from photoreceptors, resulting in the regulation of HC light responses. The asynchronous transmitter release from PRs should be essential for the graded light response of horizontal cells, because the release rate can change gradually and successively. The analyses of HC sEPSC clearly showed that the regulation of HC light response can be regulated by both of pre- and postsynaptic factors; presynaptic transmitter release and postsynaptic receptor sensitivity. The sEPSC analyses of HCs should be useful to investigate not only the vesicular synaptic transmission at PR-HC synapse, but also the elementary postsynaptic process for graded potential signalling.

Acknowledgements

At first, I would like to express special thanks to Prof. MasahiroYamada of Electrotechnical Laboratory (ETL), who recently moved to Tokyo Metropolitan Institute of Technology, for his introduction to neurophysiology and supervision to complete this dissertation.

I am grateful to Dr. Richard A. Shiells of University College London for his great support and help during the course of my study, without whose help my study would never have been completed.

I would like to thank Prof. Takehiko Saito, Prof. Yoshimasa Tanaka and associate Prof. Kei Nakatani of the Institute of Biological Sciences, Tsukuba University, for their critical reading of the manuscript and for helpful suggestions.

I also would like to thank members of Dr. MasahiroYamada's Laboratory in ETL for their supports, discussions and suggestions. Especially, I would like to thank Dr. Kaoru Katoh for his encouragement and useful advices to complete my study.

Finally, my thanks go to my parents Osamu and Tsuya for their generosity and assuring my education.

Abbreviations

AC: amacrine cell

AMPA: α-amino-3-hydroxy-5-methyl-4-isoxazole propionic acid

BC: bipolar cell

CNQX: 6-cyano-7-nitroquinoxaline

CNS: central nervous system

CTZ: cyclothiazide

DA: dopamine

DMSO: dimethylsulfoxide

FFT: fast Fourier transform

GC: ganglion cell

GYKI52466: 1-(4-aminophenyl)-4-methyl-7,8-methylenedioxy-5H-2,3-benzodiazepine

HC: horizontal cell

L-APB: L-2-amino-4-phosphonobutyric acid

LED: light emitting diode

MAP4: 2-amino-2-methy-4-phosphonobutyric acid

mGluR: metabotropic glutamate receptor

NMDA: N-methyl-D-asparatate

PR: photoreceptor cell

sEPSC: spontaneous excitatory postsynaptic current

4-AP: 4-aminopyridine

Table of Contents

Chapter 1. General introduction

1.1 Vertebrate retina

1) Histrogical and physiological properties of retinal neurons

The vertebrate retina possesses three neural layers, 1) outer nuculear layer, 2) inner nucular layer and 3) ganglion cell layer (**Fig. 1.1**). Outer nuculear layer consists of two types of photoreceptor cells called rod and cone photoreceptors (PRs). Inner nuculear layer consists of three kinds of neurons called horizontal cells (HCs), bipolar cells (BCs) and amacrine cells (ACs). Ganglion cell (GC) layer consists of ganglion cells. Besides neurons described above, the retina possesses Müller cells, one of glial cells, which contribute to the metabolism of the retina. Light passes through transparent retinal neural layers and is finally absorbed by photopigments in the outer segments of PRs. Photopigments consists of rhodopsin in rod PRs and iodopsin in cone PRs. The absorbed light energy triggers the conformational change of the photopigment, which starts the second messenger cascade (especially cGMP) leading to the hyperpolarization of PRs by the closure of cGMP-gated channels. After all, the depolarized photoreceptors in the dark (at around –20~30 mV) are hyperpolarized by light stimulus, which reduces Ca^{2+} current influx mediated by voltage dependent Ca^{2+} channels in the axon terminal. The reduction of Ca^{2+} influx regulates the transmitter release from PRs to the postsynaptic second order neurons including HCs and BCs. The vertical signal originated from PRs is transferred to BCs and thereafter GCs, and the spiking signal encoded at GCs is finally transferred to CNS for visual processings. On the other hand, lateral signal pathways are mediated by HCs and ACs. HCs are considered to modulate the PR-BC synaptic transmission. ACs are considered to modulate the BC-GC synaptic transmission. PRs, HCs and BCs generate the graded potential change according to the light stimulation. The outer retina is, therefore, considered to possess analog signal processings. While HCs show sign-preserving light response according to the hypepolarization of PRs, BCs possesses sign-preserving and -inverting light responses in OFF-centre and ON-centre BCs, respectively. The spiking signal of GCs, encoding the visual information processed by retinal circuit, is propagated to the CNS, and the propagation of spikes is convenient for the propagation of long

distance communication in the neural circuits.

2) Photoreceptor-horizontal cell synaptic transmission

The physiological functions of second order neuron HCs are proposed as follows. First, the HC integrates PR responses, which contributes to the spatial integration of visual processing. Second, this integrated light response of HCs can act as the feedback signal to the PR light responses, which can control the light response range of PRs. Moreover, the feedback system from HCs to PRs is assumed to convert color signals into color opponent signals in BCs.

In the teleost retina, the rod and cone pathways are segregated at HCs (Kaneko & Yamada, 1972). Cone-driven horizontal cells in carp retina categorized into H1, H2 and H3 subtypes, according to their characteristic spectral responses (**Fig. 1.2**). H1 cells, concerned in the present thesis, are considered to receive predominant synaptic input from red-sensitive cones since the spectral response of H1 cells in cyprinid retina is very similar to that of red-sensitive cones (Djamgoz, 1984; Yamada & Yasui, 1988; Yamada et al., 1999). The ratio of red, green and blue cone synaptic contacts onto H1 cells in goldfish is considered to be 9: 5: 2, respectively (Stell et al., 1975).

The PR-HC synapse is one of the most representative synapse for graded potential signaling. The first step of visual processing is originated from the signal transduction at photoreceptor cells. The photoisomerization of visual pigment results in the reduction of intracellular cGMP, which induces the closure of cGMP-gated cation channels. Thus, the membrane potential of photoreceptor cells shows depolarization (-20~30 mV) in darkness and hyperpolarization by light stimulation (Tomita et al., 1967). The membrane potential changes in graded manner according to the light intensity. In order to transfer the graded response of PRs to postsynaptic second order neurons, the graded synaptic transmission is performed in their synapses.

The graded synaptic transmission from PRs to HCs has been extensively investigated by voltage measurement of HCs in isolated retina. According to original scheme proposed by

Trifonov (1968) and Tomita (1970), neurotransmitter from photoreceptors is tonically released in darkness and acts to depolarize horizontal cells. The following substantial evidence also supports the original proposal by Trifonov and Tomita. 1) Extrinsic current-induced depolarization of PRs results in the depolarization of HCs (Byzof & Trifonov, 1968). 2) External application of divalent cations such as Co^{2+} or Mg^{2+} suppresses transmitter release, results in the hyperpolarization of HCs (Dowling & Ripps, 1973; Kaneko & Shimazaki, 1975). 3) Light stimulation increases the input resistance of HCs accompanied by the membrane hyperpolarization (Byzof & Trifonov, 1981; Yasui & Yamada, 1989; Miyachi & Murakami, 1989). 4) Glutamate, a candidate of the neurotransmitter released from PRs, depolarizes HCs in intact retina (Murakami et al., 1972) and dissociated HCs (Lasater & Dowling, 1982; Tachibana, 1985). 5) Electrical stimulation of isolated PRs induces NMDA-channel activity in outside-out patches (Copenhagen & Jahr, 1989). Recently, GYKI53655 or GYKI52466, selective AMPA receptor antagonists, blocked glutamate response of isolated HCs (Eliasof and Jahr, 1997; Lu et al., 1998) and suppressed HC-light response in the isolated retina (Yang et al., 1998). Therefore, it is widely believed that the vertebrate PRs tonically release transmitter (glutamate) to HCs in darkness and reduce the release by light-induced hyperpolarization.

1.2 Synaptic transmission

1) Quantal transmitter release

The neurotransmitter release at chemical synapses is triggered by Ca^{2+} influx through voltage dependent Ca^{2+} channels, which is opened by the presynaptic depolarization. Originally, Fatt and Katz (1952) discovered the miniature end plate potential (mEPP) at frog neuromuscular junctions (**Fig. 1.3A**) and proposed that the release of neurotransmitter is quantized. The miniature potential has also been observed at all of myoneural junctions, and similar miniature events have also been reported at neuronal synapses in CNS (Bekkers &

Stevens, 1989). From 90's, the patch-clamp recording in brain slices enabled synaptic current recording with high-time resolution and, therefore, provided a miniature spontaneous excitatory or inhibitory postsynaptic current (sEPSC, sIPSC or mEPSC, mIPSC) in neuronal synapses (Bekkers et al., 1990; Silver et al., 1992) (**Fig. 1.3B**). Spontaneous miniature postsynaptic current (sPSC) is also generally believed to be due to the quantal transmitter release, although some arguments are proposed that some sPSCs are due to multi-quantal transmitter release (Paulsen & Heggelund, 1994). The quantitative analysis of sEPSC, therefore, is essential to understand the activities of excitatory synaptic transmission.

2) Graded synaptic transmission vs. evoked synaptic transmission

Evoked synaptic transmission at spiking synapses, such as neuromuscular junctions or CNS synapses, shows synchronous transmission by brief spike-like depolarization in presynaptic neurons. According to classical synaptic transmission theory proposed by Katz and his colleagues, the brief and robust depolarizarion of presynaptic terminals elicits synchronous and massive transmitter release in a 'pulse' like fashion. Moreover, they confirmed the variance of postsynaptic potential could be described by the multiple of the amplitude of mEPP (del Castillo & Katz, 1954). Thus, at evoked synapses, the amplitude of postsynaptic voltage response is considered to be proportional to the number of transmitter vesicles release.

In contrast, synaptic transmission at graded synapses, such as retinal photoreceptor-second order neuron synapses, shows tonical transmission during stational deporarization at presynapse (Juusola et al., 1996). The transmitter release is regulated by graded voltage change at presynaptic terminals. At the outer retina, the membrane potential of PRs is depolarized in darkness and hyperpolarized during light stimulation. The second order neurons receiving synaptic input from PRs, therefore, show graded responses according to the graded change of light intensity. Thus, it is assumed that transmitter from photoreceptors is released tonically in darkness and that the amount of transmitter is successively reduced by light stimulation. The graded synaptic

transmission, therefore, may possess unique synaptic mechanisms distinct from the evoked synaptic transmission.

3) Quantal synaptic transmission from photoreceptors has not been described well

The synaptic terminals of PRs and BCs in the vertebrate retina possess unique structure called 'ribbon synapse'. Neurotransmitter vesicles are released continuously at the ribbon synapses during their depolarization, which is distinct from the transmission form of conventional synapses, and this synapse possesses different properties in their morphology and in their synaptic vesicle proteins (Morgans, 2000).

Moreover, the transmitter from PRs should be released in vesicular manner, because axon terminals of PRs have huge number of synaptic vesicles in their cytoplasm (Gray & Pease, 1971; Matsumura et al., 1981). Asynchronous excitatory quantal events have not been observed at HCs, although the asynchronous transmitter release is performed at isolated rod synapse (Reike and Schwartz, 1996). There has been little evidence of shot events induced by vesicular neurotransmitter release from PRs, although voltage noise fluctuation analysis in OFF-bipolar cells, based on the Campbell's theorem, could estimate the transmitter release rate (Ashmore & Copenhagen, 1983).

1.3 Synaptic regulation

The efficiency of synaptic transmission can be controlled by several modulators. The synaptic modulation is important process for synaptic plasticity. The synaptic modulation can include both of synaptic activation and regulation. Especially, synaptic regulation can play a role in the adjustment of synaptic strength, and therefore can be one of the principal phenomena for controlling neural systems. Mainly, there are two kinds of synaptic regulation: presynaptic regulation and postsynaptic regulation.

1) Presynaptic regulation

Presynaptic regulation is the regulatory mechanism to control transmitter release rate and, therefore, it can play a role in the adjustment of synaptic strength or the prevention of excessive transmitter release. Activation of presynaptic receptors, such as prinergic and muscarinergic receptors, mediates a part of synaptic regulation at many synapses, and some experimental evidence showed that presynaptic modulators inhibit Ca^{2+} channels or activate K^{+} channels at presynaptic neurons (Wu & Saggau, 1997).

Activation of presynaptic metabotropic glutamate receptors (mGluR), a class of G-protein coupled glutamate receptors, can also play a role in presynaptic inhibition at several CNS synapses (Anwyl 1999; Cartmell & Schoepp; 2000). Recently, it is reported that the presynaptic activation of kainate type receptors can also regulate a synaptic transmission (Frerking & Nicoll, 2000). Therefore, glutamate, an excitatory neurotransmitter, can be presynaptic regulator for the synaptic transmission. In the retinal neurons, immunohistochemical studies propose the existence of presynaptic mGluR on the axon terminal of PRs (Koulen et al., 1999) and BCs (Brandstätter et al., 1996). Nevertheless, their physiological functions have not yet been described, because electrophysiological recordings to determine synaptic modulation site have not been established at these graded potential synapses.

2) Postsynaptic regulation

Postsynaptic regulation is the mechanism to regulate the response of postsynaptic receptors, and it can also play a role in the adjustment of synaptic strength or the prevention of excessive sensitivity to the released neurotransmitter. The synaptic current is controlled by postsynaptic modulation of receptors, such as single channel conductance or opening probability. Receptor desensitization, a reduction of responsiveness during long application of transmitter, can also regulate the postsynaptic current, and therefore the efficacy of synaptic transmission. At spiking neurons, the desensitization of postsynaptic receptors can regulate the decay and amplitude of

postsynaptic response (Jones & Westbrook, 1996). At the graded potential neurons, however, the functions of postsynaptic receptor desensitization have poorly been understood, although kainate receptor desensitization at OFF-BCs is considered to regulate the operating range of postsynaptic responses (DeVries & Schwartz, 1999).

In order to discuss the mechanism of synaptic modulation, the modulation site should be determined. At the evoking synapse, the analysis of CV (coefficient of variance) of postsynaptic response enables to determine the synaptic modulation site (Clements & Silver, 2000). Alternatively, an analysis of miniature spontaneous postsynaptic current (sPSC) is also used for this determination, because the frequency of sPSC reflects the activity of transmitter release from presynapses. In contrast, at the graded potential synapse, the analysis to determine the synaptic modulation site has not been established with a conventional analysis of postsynaptic current.

1.4 Purpose of the present study

The analysis of sEPSCs on HC should be essential to investigate the vesicular transmitter release from PRs to HCs. However, the quantal sEPSC events in HCs have not been studied yet, since an adequate voltage clamp recording from HCs in the retina has not been established, probably due to their extensive electrical coupling between adjacent HCs. At first, I aimed to record the postsynaptic current of HCs with pharmacological procedures, using either dopamine or heptanol, to suppress the electrical coupling in order to minimize leakage current through the electrical coupling. Next, I aimed to investigate the regulatory mechanisms of PR-HC synaptic transmission, based on the HC sEPSC analysis. Especially, I focused on the importance of 1) presynaptic regulation via mGluR and 2) postsynaptic regulation by postsynaptic receptor desensitization onto the PR-HC synaptic transmission. After all, main purposes of this thesis are as follows,

1) To establish the recording and analysis of sEPSCs in graded potential neurons, HCs.

2) To investigate the mGluRs-mediated synaptic regulation at PR-HC synapse, based on sEPSC analysis.
3) To investigate the role of desensitization of postsynaptic receptors in graded potential signaling at PR-HC synapse, based on sEPSC analysis.

In the **Chapter 2**, I report the physiological and pharmacological properties of sEPSCs of HC in sliced retina.

In the **Chapter 3**, I show that L-APB, a selective agonist of type III mGluR, can regulate transmitter release from cone PRs by the analyses of the sEPSC frequency and amplitude in HCs.

In the **Chapter 4**, I investigate the contribution of receptor desensitization to the graded synaptic transmission at PR-HC synapse, using modulatory drug of postsynaptic receptors.

Chapter 2. Analysis of spontaneous EPSCs in retinal horizontal cells of the carp

2.1 Introduction

Horizontal cells (HCs) are second order neurons receiving their main synaptic drive from photoreceptors. These second order neurones are non-spiking neurones responding with only graded potentials for neural processing. HCs in carp retina receive synaptic input from rods and cones via separate pathways (Kaneko & Yamada, 1972).

Neurotransmitter from photoreceptors is tonically released in darkness and acts to depolarize horizontal cells. The release of the transmitter, glutamate, from photoreceptor cells (Copenhagen & Jahr, 1989) is reduced by light resulting in hyperpolarizing responses to light in H1 cells. Whilst there are a few instances reporting the presence of NMDA receptors in isolated HCs in catfish retina (O'Dell & Christensen, 1989), other work has shown non-NMDA type glutamate receptors to be the major glutamate receptor type mediating synaptic input into cone-driven HCs (Lasater, 1990; Ishida et al., 1984; Ishida & Neyton, 1985). The non-NMDA receptors respond to glutamate receptor agonists with a pharmacology which closely resembles that of cloned AMPA receptors (Hollmann & Heinemann, 1994). Glutamate-receptor channel kinetics in dissociated HCs have been studied using either the power spectrum of current noise (Ishida & Neyton, 1985) or single-channel recordings (Lasater, 1990), revealing fast and slow channels. Recently, desensitization of AMPA receptors also in dissociated HCs was studied with rapid drug applications (Eliasof & Jahr, 1997; Lu et al., 1998).

Because of difficulties in the measurement of synaptic currents of HCs in the retina due to their extensive electrical coupling, only a few voltage clamp studies of H1 cells have been made using double barrelled micro-electrodes, using dopamine to reduce electrical coupling (Low et al., 1991; Yamada et al., 1992). These studies revealed that the reversal potential of light-induced current was near zero, but interestingly, responses to different wavelengths in the red, green and blue ranges had different kinetics. However, this method could not detect rapid current events resulting from the quantal release of transmitter, due to filtering by the high resistance micro-electrodes. In contrast, whole-cell patch clamp recording from CNS slices (Edwards et al., 1989) or retinal slices

(Shiells & Falk, 1990) could measure synaptic currents with high time resolution whilst preserving the synaptic connections and responses to light, respectively. Since the glutamate in photoreceptor synaptic terminals is stored in the form of synaptic vesicles, quantal events might be expected to occur in second-order neurones.

The ultrastructure of the cone to horizontal cell synapse is stereotyped but in unusual fashion across vertebrates: a horizontal cell process invaginates into the cone pedicle and ends in close apposition to a synaptic ribbon at the apex of the invagination (Downing et al., 1986). It is generally considered that a quantal release of synaptic vesicles would result in spontaneous excitatory postsynaptic current (sEPSC) at excitatory synapses of CNS, as well as miniature end plate potential at neuromuscular junctions (Fatt & Katz, 1952). A brief description of sEPSCs at OFF-bipolar cells is one and only electrophysical evidence for clustered release of transmitter from photoreceptors (Maple et al., 1994), but not in horizontal cells.

In this chapter, I describe the properties of post-synaptic currents of H1 cells in retinal slices of carp using whole-cell patch clamp recording.

2.2 Materials and Methods

1) Retinal slice preparation and superfusion

Slices of retina were prepared as described by Werblin (1978) and Shiells & Falk (1990) from carp (*Cyprinus carpio*) kept under natural day light conditions. Light adapted fish (200-250g) were pithed and the eyes were enucleated and hemi-sected. To remove the vitreous humour, the eyecups were gently washed for 3 - 4 min with Ringer's solution containing 120 unit/ml collagenase and 465 unit/ml hyaluronidase (Sigma Ltd.).

The eyecup was cut into 4 pieces. Retina was detached from the piece of eyecup onto filter paper (pore size 0.45 μm: Millipore Corp) and was sectioned into 200 μm thick slices. These were superfused with Ringer's solution containing (mM): 102 NaCl, 2.6 KCl, 1 $CaCl_2$, 1 $MgCl_2$, 28 $NaHCO_3$, 5 glucose and 5 HEPES, adjusted to pH 7.5 when bubbled with 95% O_2: 5% CO_2. In all experiments, control Ringer contained 15-20 μM dopamine (DA), which was used to uncouple the gap junctions of H1 cells, with 75-100 μM ascorbic acid added to reduce oxidation. 6-cyano-7-nitroquinoxaline (CNQX, an antagonist of non-NMDA receptors) (RBI Ltd.) or 1-(4-aminophenyl)-4-methyl-7,8-methylenedioxy-5H-2,3-benzodiazepine (GYKI52466, a relatively selective antagonist of AMPA receptors) (Sigma Ltd.) was dissolved in DMSO (final concentration: <0.1%), and then added to the superfusate, and all experiments were conducted at room temperature (21-23°C). It took 25-30 min to make slice preparations under slightly dim room light. The slices were viewed using an upright microscope (Olympus, BX50WI) with infrared illumination (>850 nm) and monitored on a CRT display with a CCD camera (C5985, Hamamatsu Photonics).

2) Light stimulation

Retinal slices were illuminated with red- and blue-diffuse light emitting diodes (LED's)(DHR6610 and GNB4510, Iwasaki Electric Ltd., the peak wavelength at 650 nm and 450 nm, respectively). The blue light was filtered with a band pass filter (V42, Toshiba Electric Ltd.,

transmission peak at 410 nm) and the red light filtered with a sharp cut filter (R65, Hoya Optics Ltd., cut off wavelength 650 nm). The red light was filtered to selectively stimulate the red cones (Kaneko & Tachibana, 1985). The horizontal cells were identified by their characteristic morphology, spreading laterally in the outer plexiform layer, confirmed by staining with Lucifer yellow via the patch pipettes. Subtypes were distinguished by their characteristic responses to steps of red and blue light. H1 cells responded with larger outward currents to red and smaller outward current to blue light, whilst H2 and H3 cells responded with larger outward current to blue but smaller or no current to red. The intensity of red light was usually in the range 4 – 6 $\times 10^5$ quanta/μm^2/s, which elicited near saturating responses. Stronger blue light intensity was needed than red one to induce the same current amplitude.

3) Whole-cell recording

Pipettes for whole cell patch clamp recording were fabricated from standard-walled borosilicate glass (Clark Electromedical). Intracellular K^+- based solution contained (mM): 110 KCl, 1 $MgCl_2$, 5 EGTA, 1 Mg-ATP, 1 Na-GTP, 10 HEPES adjusted to pH 7.2 with KOH. H1 cells were voltage-clamped to their initial dark potentials (corrected for the tip potential) measured just after going whole-cell. Patch-pipettes had resistances of 3-6 MΩ and only recordings with a series resistance of about 10 MΩ were analysed. sEPSCs were usually recorded from cells with high input resistance (>100 MΩ) by electrodes with low series resistance (<10 MΩ). Whole cell voltage clamp recordings were obtained using an Axopatch 1-D amplifier (Axon Instruments). No series resistance compensation was employed. Signals were filtered at 2-5 kHz, digitized at 8-25 kHz. Data were stored on DAT tape and on hard disk. Inward and outward currents were referenced with respect to the current at the holding potential clamped to the resting potential of the cells. **Figure 2.1** shows the schematic diagram of whole-cell patch clamp recording from sliced retina.

4) Measurement of sEPSCs

Slow components were removed by high pass filtering at <10 Hz. Each sEPSC amplitude was measured from the zero current level to the peak point of inward current. "Baseline noise" was fitted with a Gaussian probability distribution (see **Fig. 2.3**). Each discrete sEPSC was isolated from the baseline noise by using the following criteria: (1) The peak inward current events were detected by setting a threshold level, defined as twice the standard deviation (sigma) of the baseline noise (the detection level is illustrated in **Fig. 2.3C**). (2) All events larger than this level were included if they had a rise time <1 ms and (3) if they did not arise from the decaying phase of a previous event. (4) To detect automatically the peak of discrete inward current, a moving rectangle (height about 3 pA and width 1-3 ms for measurement of interval: height about 3 pA and width 10-20 ms for amplitude measurement) was used (Origin 4.1 or 6.0 software, Microcal Ltd.). Criterion (3) was not included for the measurement of the frequency histogram. The selected threshold level remained constant for the entire analysis of the cell. Decay time constants of individual sEPSCs were calculated by fitting single exponentials. Rise time was measured as the time between 20% and 80% of peak amplitude.

5) Spectral analysis of membrane current composed of sEPSCs

To describe the power spectrum of membrane current composed of sEPSCs, the waveform of individual sEPSC, *g(t),* was approximated by double exponential functions describing decay and rise phase as follows (Segal et al., 1985);

$$g(t) = a\left[\exp(-t/\tau_d) - \exp(-t/\tau_r)\right] \quad (1)$$

where τ_d and τ_r were decay and rise time constants, and a is an amplitude factor. τ_r corresponds to 72 % of 20-80 % rise time.

Power density spectra were calculated using a Fast Fourier Transform algorithm. Each power spectral density curve in each condition was averaged. Components of the power spectral density suppressed by test stimulation, such as light or chemicals, were obtained by subtracting the power

spectrum after the test from that before the test. The power spectra were fitted with the following equation (2), a product of two Lorentzians describing waveform of the individual sEPSCs as shown in the equation (1);

$$S(f) = \frac{S_0}{\{1 + (f / f_d)^2\}\{1 + (f / f_r)^2\}} \quad (2)$$

where S(f) is the power spectral density at frequency f. S_0 is a constant, the spectral density of zero limit frequency, and f_d ($=1/2\pi\tau_d$) and f_r ($=1/2\pi\tau_r$) the cut-off corner frequencies for decay and rise phase, respectively. The curve fitting was achieved using a nonlinear least-square error algorithm.

The statistical data were shown as mean ± standard error.

2.3 Results

1) The light induced post-synaptic current of cone horizontal cells

Figure 2.2A shows the whole cell current response of an H1 cell to steps of red and blue light which elicited outward current (actually a reduction of DC inward current as shown later) responses. This was accompanied by the suppression of spontaneous EPSCs (sEPSCs, rapid inward transients) by red light but there was less reduction in sEPSC frequency in response to blue light, even though each stimulus evoked the same outward current amplitude. This paper is concerned with the study of sEPSCs recorded in the dark and on exposure to red and blue test light which elicited prominent suppression of sEPSCs. Quantitative analysis, however, was made only for the records obtained with red light. The input resistance of the H1 cells was 148.2 ±15.0 MΩ (n=14) in darkness in the presence of dopamine which reduces electrical coupling between H1 cells (Yasui & Yamada, 1989; Furukawa et al., 1997). The resistance increase induced by red light, 29.9 ± 7.6 MΩ, was greater than that by blue light, 16.1 ± 11.6 MΩ (n=6), at the same light-evoked current amplitude, confirming previous resistance measurements obtained by intracellular recording (Yasui & Yamada, 1989; Furukawa et al., 1997). Switching from voltage clamp to current clamp resulted in the smoothing of spontaneous synaptic events (**Fig. 2.2B**). This suggests that sEPSPs observed in current clamp were low-pass filtered by the electrical properties of the H1 cell membrane. By analysing the time-course of voltage responses to rectangular current pulses measured by current clamp mode, the membrane time constant was determined to be of the order of 1 ms.

2) Isolation of sEPSCs from baseline noise

I isolated sEPSCs of the H1 cell from baseline noise using the procedure shown in **Fig. 2.3**. The current trace in **Fig. 2.3Aa** is baseline noise in an H1 cell taken from the silent period of the record without sEPSC events during red light stimulation (**Fig. 2.3Ab**) which greatly suppressed the current noise. The probability density histogram of its current amplitude (**Fig. 2.3Ba**) was almost symmetrical and was fitted well by a Gaussian distribution curve (a solid line; standard deviation σ

= 3.0 pA). **Figure 2.3Ab** shows the whole period of the current recording in the presence of red light, and **Fig. 2.3Bb** is its probability density histogram of current amplitude. It was slightly skewed due to inclusion of inward sEPSCs but the outward current side was fitted well by the Gaussian distribution curve (standard deviation: σ = 2.7 pA). The current noise greatly increased in darkness (**Fig. 2.3Ac**). The probability density histogram of the current noise (**Fig. 2.3Bc**) was much more skewed due to the higher frequency of sEPSCs but the outward current side was fitted well by the Gaussian distribution curve with a larger standard deviation (σ = 4.1 pA). This part of the current noise in the graph fitted by the Gaussian distribution curve was assumed to be baseline current noise in darkness. The standard deviation of the curve for the inward current was larger in darkness than that with red light stimulation in other H1 cells (n=15). The increased baseline noise in darkness may indicate the activation of glutamate receptor channels, contributing a component of channel noise, by some accumulation of glutamate released tonically in darkness. In the following results, individual sEPSCs were isolated from the baseline noise using all the criteria described in the Methods. The fast sweep recording in red light and darkness are shown in **Fig. 2.3Ca** and **b**, respectively. The thick continuous line indicates zero current, defined from the maximum point of the probability density histogram. In order to compare the properties of sEPSCs in darkness and red light, I isolated discrete inward events (sEPSCs) exceeding 2 times the standard deviation of baseline noise (thick dashed line: 8.1 pA) in darkness (b). sEPSCs in red light were also isolated using the same threshold as in darkness.

3) Suppression of sEPSCs by red light

Figure 2.4A shows the whole cell current response of an H1 cell in darkness and in the presence of a steady red light. Red light elicited a DC steady outward current (a reduction of DC inward current) and a marked suppression of sEPSCs. **Figure 2.4B** shows the same current noise on a faster time scale. Occasionally, large sEPSCs (>50 pA) were observed both in darkness and in red light. The frequency and the peak amplitude of the sEPSCs in different light or

pharmacological conditions were compared by using the same threshold level, as described in **Fig. 2.3**. The frequency of sEPSCs was highest in darkness, 218 ± 20 Hz, and was reduced to 34 ± 6 Hz (n = 13) by red light, consistent with a reduction in vesicular glutamate release on hyperpolarization of photoreceptor terminals with light. The distributions of sEPSC intervals between events were analysed and are shown in **Fig. 2.4C** in darkness and in red light. The histograms of sEPSC intervals in darkness and in red light were fitted with single exponentials, showing that these events were randomly distributed in time, following the Poisson process. The peak amplitude histograms of sEPSCs in darkness and in red light are shown in **Fig. 2.4D**. The mean conductance increases induced by sEPSCs in darkness and red light were 482 ± 59 and 401 ± 44 pS (n=13), respectively. The mean sEPSC amplitudes in darkness and red light were not significantly different in 13 cells (P>0.11). To determine whether the reduction in frequency of sEPSCs was graded with light intensity, whole-cell currents were recorded from H1 cells in response to increasing, then decreasing, ramps in red light intensity (**Fig. 2.5A**). Sections of the recording shown in **Fig. 2.5B** on an expanded timescale were then analysed and their mean frequency was plotted against the light-induced shift in outward current (**Fig. 2.5C**). There was an inverse linear relationship between sEPSC frequency and light-induced outward current (reduction of DC inward current) in the H1 cell. The standard deviation of baseline noise was also gradually suppressed from 7.0 pA to 3.2 pA by light stimulation. A similar relationship was observed in four cells. I noted that light stimulation reduced the variance of the baseline noise but not the mean peak amplitude of sEPSCs. This indicates that light stimulation suppresses the frequency of asynchronous vesicular transmitter release, without a reduction of quantal content, and the reduction in baseline noise reflects a consequent reduction in glutamate concentration in the synaptic cleft.

4) The reversal potential of sEPSCs of the H1 cell

Figure 2.6 shows sEPSCs recorded in the dark held at different membrane potentials. The polarity of sEPSCs was reversed around 0 mV. This is similar to the reversal potential for

glutamate induced current reported in previous studies of isolated horizontal cells (Tachibana, 1985).

5) Kinetic properties of sEPSCs

Individual examples of H1 cell sEPSCs recorded in darkness and in red light are shown superimposed in **Fig. 2.7A** and **B**, respectively. The rise and decay phases of the sEPSCs were fitted with single exponentials. Mean values of the decay and rise time constants in darkness were 0.71 ± 0.02 ms and 0.10 ± 0.01 ms, respectively (n = 11). However, the rise time would be limited by the bandwidth of the recording system (2-5kHz). The decay time constants measured from a large sample of sEPSCs were plotted against peak inward current in **Fig. 2.7** in darkness (**Ba**) and in red light (**Bb**). The decay time was positively correlated with peak amplitude (correlation coefficient = 0.64, n = 10). The decay time constants of sEPSCs measured in darkness (amplitude < 80 pA) and in red light were not significantly different ($p > 0.88$).

6) sEPSCs are mediated by AMPA type glutamate receptors

To characterise the glutamate receptor type mediating cone synaptic input to H1 cells retinal slices were superfused with 20 μM GYKI52466, a relatively specific and non-competitive antagonist of AMPA receptors (Paternain et al., 1995). This suppressed the light responses, and was accompanied by an outward current (reduction of DC inward current) and decrease in input conductance (**Fig. 2.8A**), consistent with blocking the postsynaptic action of glutamate released from photoreceptors. The sEPSCs observed in the dark were almost completely suppressed by GYKI52466 (**Fig. 2.8B**, n=3) except small residual slow components. CNQX (10 μM) also suppressed both the light responses and sEPSCs.

7) Spectral analysis of sEPSCs

I compared the power spectrum of current noise, including sEPSCs, suppressed by red light and 10 μM CNQX. **Figure 2.9A** shows effects of red light stimulation on the power spectrum. **Figure 2.9Aa** and **b** are the power spectrum in darkness and red light, and **Fig. 2.9Ac** is the

difference spectrum. Subtraction of this from the noise contributed by sEPSC events in the dark isolates the spectral components contributed by the sEPSCs. Difference spectra were fitted with the product of two Lorentzians (equation (2) in Methods). A single Lorentzian did not fit well the high frequency region of spectra (a dashed line in the figure). Mean cut-off frequencies were 197 ± 7 Hz and 1520 ± 125 Hz for (dark - red light) spectra, corresponding to a decay time constant τ_d = 0.82 ± 0.02 ms and a rise time constant of τ_r = 0.11 ± 0.01 ms (n = 11). These values correspond well with the mean rise and decay time constants measured directly. **Figure 2.9B** shows effects of 10 μM CNQX on the power spectrum. **Figure 2.9Ba** and **b** are the power spectra of current in darkness and CNQX, and **Figure 2.9Bc** is the difference spectrum. With red light or CNQX, the current noise due to sEPSC events was essentially reduced to 1/f (at less than 400 Hz) or system noise (include Johnson noise and shot noise at frequency higher than 400 Hz) and small residual components. There was good agreement between mean time constants derived from the (dark - red light) or (dark - CNQX) difference spectra.

2.4 Discussion

1) Spontaneous EPSCs of H1 horizontal cells

The presence of sEPSCs in H1 cells provides clear evidence that there is vesicular release of the neurotransmitter, glutamate, from cone synaptic terminals. These rapid events were not clearly observed in current clamp recordings from horizontal cells because of filtering by their membrane time-constant, which was of the order of 1 ms. The reduction of sEPSC frequency observed with red light is consistent with hyperpolarization of cone synaptic terminals reducing the probability of vesicular release. There was an inverse linear relation between the outward current responses to ramps of red light and sEPSC frequency, suggesting that the postsynaptic voltage response is mainly determined by the frequency of arrival of sEPSCs, which raises the concentration of glutamate within the synaptic cleft. The tonic and asynchronous release of transmitter from cones would thus be crucial for generating graded light responses in the non-spiking horizontal cell. The mean frequency of sEPSCs recorded in darkness, 218 Hz, was reduced to 34 Hz by steady red irradiation. There was no significant change in their mean peak amplitude with red light, suggesting that there was no change in the mean vesicular glutamate concentration (quantal content) when their frequency of release was reduced. Red light stimulation suppressed the variance of baseline noise (probably channel noise), suggesting that light reduces the concentration of glutamate within the synaptic cleft.

2) AMPA type glutamate receptors on H1 cells

Since these rapid sEPSCs were completely blocked by the AMPA receptor antagonists and showed the same reversal potential around 0 mV, perhaps the simplest interpretation is that these sEPSCs are all generated by the same postsynaptic mechanism, by the opening of AMPA receptor channels in response to the vesicular release of glutamate. The postsynaptic responses of salamander horizontal cells have been shown to be mediated by AMPA-receptors, since they were also blocked by GYKI52466 (Yang et al., 1998).

3) Estimation of the number of channels generating the sEPSCs

The distribution of sEPSCs in time was random, following an exponential interval distribution, but showed considerable variation in both amplitude and rate of decay. Larger amplitude sEPSCs were correlated with slower decay times. Variations in sEPSC amplitudes could be due to variations in vesicle size or glutamate concentration incorporated into individual synaptic vesicles.

The sEPSCs were clearly due to multi-channel openings. A single-channel conductance of non-NMDA receptor channels was estimated to be 16.4 pS for the carp H1 cell as shown in Appendices 2. Thus, the mean amplitude of sEPSCs associated with a conductance change of 480 pS would arise from the opening of about 29 channels. In darkness, 6380 channels would open per second with a mean sEPSCs frequency of 220 Hz.

4) Estimation of release rate of synaptic vesicles from cones

Each H1 horizontal cell contacts with 16 cones in goldfish (R:9, G:5, B:2, Stell et al., 1975) and 14 cones in roach (R:7, G:6, B:1, Downing and Djamgoz, 1989). The total number of synaptic ribbons contacting with the roach H1 cell can be calculated to be about 240 since each of red-, green- and blue-sensitive cone has 22, 13 and 7 synaptic ribbons, respectively, at the axon terminal (Downing et al., 1986). Therefore, I can estimate that the release rate in darkness would be about 14-16 Hz from each cone and about 1 Hz from each synaptic ribbon to H1 cells, assuming that the number of cones contacting H1 cells in carp is similar to that of other cyprinid retina. This low release rate from individual synaptic ribbons is probably an underestimate, since the technique used here to discriminate sEPSCs from baseline noise would exclude very low amplitude sEPSCs.

5) sEPSC kinetics.

The shortest sEPSC decay time constant of 0.2 ms is probably determined by the underlying single-channel kinetics. This is similar to the inactivation time constant of AMPA receptor channels in other neurons (0.6-3.3 ms: Geiger et al., 1995; Silver at al., 1996). At other CNS synapses, free diffusion aided by glutamate transport clears glutamate so rapidly that the decay of

the AMPA receptor EPSC is limited solely by the dissociation of glutamate from the receptor (Tong & Jahr, 1994). Multi-vesicular release, studied in cultured hippocampal neurones, does not slow the decay of AMPA receptor EPSCs, suggesting that each synaptic input contributes independently to the postsynaptic conductance change (Diamond & Jahr, 1995). The rapid decay times of sEPSCs in H1 cells would suggest a similar independent input from individual cone synaptic ribbons, which are spatially isolated from one another (Saito et al., 1985; Downing et al., 1986). Single-channel recordings from isolated horizontal cells categorised non-NMDA channels into two types, 'fast channels' (mean open time 1-2 ms) and 'slow channels' (mean open time 4.5-8.8 ms) (Lasater, 1990). The very brief decay time constants measured here suggests that only the 'fast channels' are expressed at the synapse.

The photoreceptor-horizontal-bipolar cell synapse has a highly specialized ultra-structure, with horizontal cell processes deeply invaginating into rod and cone pedicles which possess synaptic ribbons. The horizontal cell dendritic processes are in very close apposition to the presynaptic release sites with a large contact area to both rod and cone ribbon synapses. This close apposition might account for the very rapid H1 cell sEPSC kinetics. The location of the ON and OFF-II type bipolar cell processes, relative to the transmitter release sites, are more distant (Saito et al., 1985), and a consequent diffusional delay could account for much slower sEPSC kinetics in dogfish OFF-bipolar cells (R. A. Shiells, in preparation). The rod-bipolar cell synapse appears to be highly specialized to reduce synaptic noise, which otherwise would limit the sensitivity of the visual system.

NMDA receptors expressed by horizontal cells which have much slower kinetics (O'Dell & Christensen, 1989; Eliasof & Jahr, 1997) would be unlikely to contribute to the immediate process of synaptic transmission from cones. The longest decay time constant of 1.4 ms associated with larger events may be due to prolongation by the diffusion process of glutamate with the larger increment of concentration. If the sEPSC signal were propagated from the neighbouring cells, the peak amplitude would have been reduced and the decay time constant would have been prolonged

by the cable properties. The sEPSCs were certainly not reduced in amplitude or filtered by the cable properties of the H1 cell because the decay time constant did not show a negative relationship with amplitude.

DeVries & Schwartz (1999) reported that kainate receptors mediate the OFF-bipolar cell light responses in mammalian retina and that most of these receptors are desensitized in darkness, having a very long (500 ms) time constant of recovery from desensitization. In contrast, non-NMDA (possibly AMPA) receptors in horizontal cells show very rapid recovery from desensitization (9 ms: Eliasof & Jahr, 1997). Dopamine has been shown to block desensitization of horizontal cell non-NMDA receptors (Schmidt et al., 1994) so it is unlikely that the sEPSC time-courses measured in the present study in the presence of dopamine were decreased by desensitization of AMPA receptors.

6) Concluding remarks

The quantal events of glutamate release from cone photoreceptors were first found in carp retina. Spontaneous excitatory postsynaptic currents (sEPSCs) in horizontal cells were detected by uncoupling the electrical coupling of horizontal cells using dopamine. The analysis of sEPSCs suggested that red cone photoreceptors asynchronously release synaptic vesicles with high frequency in darkness and reduce the frequency of release in response to graded changes without reduction of quantal content by red light stimulus. The spontaneous events in horizontal cells were contributed by non-NMDA (possibly AMPA) type glutamate receptors modulated by the red cone input.

Chapter 3. A metabotropic glutamate receptor regulates transmitter release from cone presynaptic terminals in carp retinal slices

3.1 Introduction

I have shown that sEPSCs in H1 HCs are mediated by AMPA receptors, consistent with previous studies on isolated cells (Lu et al., 1998), that these ionotropic glutamate receptors mediate fast synaptic transmission from cones (Chapter 2; Hirasawa et al., 2001). The synaptic input to ON-bipolar cells from rod photoreceptors is, however, mediated by a G-protein coupled metabotropic glutamate receptor (mGluR6), which is selectively activated by (L)-2-amino-4-phosphonobutyric acid (L-APB) (Shiells et al., 1981; Nawy & Jahr, 1990; Shiells & Falk, 1990; Nakajima et al., 1993; de la Villa et al., 1995; Shiells & Falk, 1995). This is the only known synapse where the total excitatory postsynaptic input is mediated exclusively by an mGluR, in the rod retina (Shiells, 1994).

mGluRs, however, play a role not only in mediating postsynaptic actions but are also expressed in presynaptic terminals, functioning to modulate transmitter release in the CNS (Anwyl, 1999; Cartmell & Schoepp, 2000). Three mechanisms for the down-regulation of transmitter release by mGluRs have been proposed: (1) suppressing presynaptic Ca^{2+} conductance (Takahashi et al., 1996; Koulen et al., 1999), (2) activating K^+ conductance (Sladeczek et al., 1993; Cochilla & Alford, 1998) or (3) directly inhibiting transmitter release, independently from reducing calcium influx (Scanziani et al., 1995). L-APB, an agonist of group III mGluRs (mGluR4, 6, 7 & 8), hyperpolarized HCs in isolated retina (Nawy et al., 1989; Yasui et al., 1990; Takahashi & Copenhagen, 1992; Hare & Owen, 1992). Two distinct hypotheses have been proposed to account for this action, involving either a presynaptic or a postsynaptic mechanism. Nawy et al. (1989) proposed a presynaptic effect, that APB regulates transmitter release from photoreceptor synaptic terminals, since postsynaptic HC responses to kainate were unaffected by APB. Supporting this, Koulen et al. (1999) recently reported that photoreceptor terminals in mammalian retina showed mGluR8 immunoreactivity and a reduction in intracellular calcium concentration in response to APB. Group III mGluRs are considered to function as autoreceptors, regulating synaptic transmission from photoreceptor terminals by negative feedback. Takahashi & Copenhagen

(1992), however, have proposed a postsynaptic action, since glutamate responses of isolated HCs showed suppression by APB. This postsynaptic action was, furthermore, shown to involve the activation of guanylate cyclase, increasing the level of cGMP in HCs which in turn acted to modulate a K^+ conductance via a cGMP-dependent kinase (Dixon & Copenhagen, 1997). This action is distinctly different from the mGluR6-mediated action of APB in ON-bipolar cells, which is linked via a phosphodiesterase to reduce a cGMP-activated conductance (Shiells & Falk, 1990; Nawy & Jahr, 1990; Shiells & Falk, 2000). A further postsynaptic action of APB in HCs is to activate voltage-dependent calcium currents (Linn & Gafka, 1999).

In this chapter, I show that group III mGluRs regulate synaptic transmission from photoreceptor synaptic terminals by analysing the suppression of sEPSC frequency by APB in H1 HCs in carp retinal slices. The results indicate presynaptic expression of mGluRs functioning to reduce transmitter release by inducing K^+-dependent presynaptic inhibition, consistent with the known actions of mGluR8 or mGluR4.

3.2 Materials and Methods

1) Retinal slice preparation and superfusion

Slices of retina were prepared as described in Chapter 2, and they were superfused with Ringer's solution containing (mM): 102 NaCl, 2.6 KCl, 1 $CaCl_2$, 1 $MgCl_2$, 28 $NaHCO_3$, 5 glucose and 5 HEPES, adjusted to pH 7.5 with NaOH when bubbled with 95% O_2 and 5% CO_2. In all experiments, the control Ringer contained 15-20 μM dopamine to block the gap junctions of H1 cells, with 75-100 μM ascorbic acid added to reduce oxidation. 6-cyano-7-nitroquinoxaline (CNQX, RBI Ltd.) was dissolved in DMSO and then added to the superfusate. 2-amino-2-methy-4-phosphonobutyric acid (MAP4, an antagonist of group III mGluRs, Tocris Cookson) was dissolved with 1N NaOH and then added to the superfusate. L-2-amino-4-phosphonobutyric acid (L-APB, a selective agonist of group III mGluRs, Tocris) or 4-aminopyridine (4-AP) was directly added to the superfusate. Perfusion speed was 1.4 ml/min and the volume of the recording chamber was 500 μl. All experiments were conducted at room temperature (21-23°C). The slices were viewed using an upright microscope (BX50WI, Olympus) with infrared illumination (>850 nm) and monitored on a CRT display with a CCD camera (C5985, Hamamatsu Photonics).

2) Light stimulation

Retinal slices were similarly illuminated by red- and blue-diffuse light emitting diodes (LED's) as described in Chapter 2. The horizontal cells and their subtypes were also identified by their characteristic morphology and spectral responses as described in Chapter 2. The intensity of red light was between 6-21×10^5 quanta/μm^2/s.

3) Whole-cell recording from H1 HCs

Patch pipettes for whole-cell recordings were fabricated from standard-walled borosilicate glass (Clark Electromedical). Intracellular Cs^+-based pipette solution contained (mM): 70 cesium methanesulfonate ($CsMeSO_4$), 30 CsCl, 1 $MgCl_2$, 5 EGTA, 1 Mg-ATP, 1 Na-GTP and 10 HEPES

adjusted to pH 7.2 with 3N CsOH. sEPSCs were usually recorded from cells with high input resistance (>70 MΩ) by patch electrodes with low series resistance (<12 MΩ). Whole cell voltage clamp recordings were obtained using an Axopatch 1-D amplifier (Axon Instruments).

L-APB modulates membrane currents in HCs by the activation of cGMP-dependent protein kinase (PKG) (Dixon & Copenhagen, 1997) and by increasing voltage-dependent Ca^{+} conductance (Linn & Gafka, 1999). To block these effects, 1-5-isoquinolinesulphonyl-2-methylpiperazine (H-7) a non-selective protein kinase inhibitor (Sigma), was included to the internal pipette solution and HCs were voltage clamped to potentials more negative than –50mV. No series resistance compensation was employed. Signals were low-pass-filtered at 2-5 kHz, digitized at 8-10 kHz.

4) Whole-cell recording from cones

To eliminate the possibility of a direct modulation of voltage-activated Ca^{2+} conductance in cones, whole-cell voltage clamp recordings were obtained from cones in carp retinal slices. The same patch-clamp technique was used as for recording from H1 HCs, with one modification. To clearly observe the voltage-activated Ca^{2+} conductance, the K^{+} conductance in cones was blocked using Cs^{+} and TEA in the external solution. The external solution contained (mM): 55 NaCl, 15 CsCl, 30 TEA-Cl, 1 $CaCl_2$, 1 $MgCl_2$, 28 $NaHCO_3$, 5 glucose and 5 HEPES.

5) Analysis

sEPSCs in HCs were analysed by setting a threshold detection level between 4-10 pA, defined as twice the standard deviation (σ) of the baseline noise in darkness (Chapter 2). Probability density histograms of outward current noise were fitted with Gaussian functions, allowing calculation of the standard deviation of the baseline noise. The selected threshold level remained constant for the entire analysis. All events larger than this level were included if they had a rise time <1 ms and if they did not arise from the decaying phase of previous event. The peak of sEPSCs was detected semi-automatically with a moving rectangle (Origin 6.0 software,

Microcal Ltd). The height of rectangle was set at about 3 pA, and the width was set at 1-3 ms for interval measurement or 10-20 ms for peak amplitude measurement in order not to detect overlapped peak. The statistical data were shown as means ± standard error (SEM).

3.3 Results

1) Presynaptic suppression of sEPSCs and baseline noise by light or cobalt

Figure 3.1A shows the postsynaptic current response of an H1 HC, recorded under whole-cell voltage clamp, to a step of red light. Time-expanded traces show that red light stimulation reduced the frequency of sEPSCs compared to that in darkness (**Fig. 3.1B**), consistent with light hyperpolarizing cone synaptic terminals, leading to a reduction in vesicular glutamate release. The distribution of sEPSC amplitudes was analysed by constructing probability density histograms of the postsynaptic current. The reduction in sEPSC frequency by light resulted in a reduction in the inward current density (**Fig. 3.1C: left**), whilst a reduction of baseline noise variance was associated with a decrease in outward current density (**Fig. 3.1C: right**). sEPSC events have a solely inward current polarity, whilst baseline noise has both inward and outward noise components fluctuating about zero current level. It could be predicted that the distribution of the inward components of baseline noise, obscured by inward sEPSC events in the dark when the quantal release rate is high, by assuming a similar Gaussian distribution to the measurable outward component of baseline noise (Chapter 1). The cumulative frequency histogram shows the reduction in sEPSC frequency induced by red light (**Fig. 3.1Da**, from 141 Hz to 87 Hz) but no significant difference was observed in mean peak amplitude (**Fig. 3.1Db**, from 17.7 ± 0.6 pA to 15.7 ± 0.8 pA; n = 3: $p>0.06$). While the frequency was significantly reduced by 37.4 ± 0.01 % (paired student t-test, $p<0.001$) in 3 cells, the amplitude was not changed ($p>0.05$) (**Fig. 3.1Dc**).

Similar, but more profound effects to red light stimulation were obtained on superfusion with 100 μM cobalt (**Fig. 3.2A**), which suppresses transmitter release by blocking presynaptic Ca^{2+} conductance (Dowling & Ripps, 1973; Kaneko & Shimazaki, 1975). Cobalt (100 μM) induced an outward current accompanied by a reduction in sEPSC frequency. On washout, there was recovery of sEPSC frequency and whole-cell current. Time-expanded recordings show that cobalt suppressed the sEPSCs, with a significant reduction in baseline noise (**Fig. 3.2B**). Higher

concentrations of cobalt (1-2 mM) suppressed sEPSC frequency to less than 1 Hz (not shown). Analysis of sEPSC amplitude distribution and baseline noise showed a dramatic reduction in the inward current component of the probability density histogram (**Fig. 3.2C**: left), corresponding to the large reduction in sEPSC frequency. Reduction of the outward current density reflects an accompanying reduction of the baseline noise variance (**Fig. 3.2C**: right). **Figure 3.2D** shows the time-course of averaged sEPSCs in control (black trace) and with cobalt (gray trace). The decay phase in cobalt was slightly more prolonged, but there was no change in mean peak amplitude. The cumulative frequency histogram shows reduction of the sEPSC frequency by cobalt (**Fig. 3.2Ea**, from 204 Hz to 4 Hz), with no significant difference in the mean peak amplitude (**Fig. 3.2Eb**: from 19.4 ± 0.3 pA to 18.8 ± 0.8 pA). Whilst the frequency was significantly suppressed by 95.3 ± 1.3 % ($p<0.001$) in 8 cells, the amplitude was not significantly changed (0.8 ± 5.9 %: $p>0.8$) (**Fig. 3.2Ec**). These results are consistent with asynchronous transmitter release from cones being Ca^{2+} dependent (Rieke & Schwartz, 1996). The decrease in sEPSC frequency results from a reduction in vesicular release rate, whilst the reduction of baseline noise, which was also suppressed by light, probably results from a reduction in the open probability of channels due to a fall in free glutamate concentration in the synaptic cleft (Chapter 2 and see appendices). The rise in baseline noise in darkness, or on washout of cobalt, would thus result from an increase in single-channel fluctuations in response to a background level of free glutamate. This would be consistent with the Gaussian distribution of the baseline noise, which was fitted by utilizing the distribution of the outward current noise components (**Figs. 3.1C & 3.2C**) (Chapter 2).

2) Postsynaptic suppression of sEPSCs and baseline noise by CNQX

Next, I investigated the postsynaptic suppression of sEPSCs and baseline noise by applying CNQX, an antagonist of non-NMDA receptors. **Figure 3.3A** shows the effect of 500 nM CNQX. This relatively low concentration of CNQX induced an outward current, consistent with blocking postsynaptic AMPA receptors (Chapter 1). Time-expanded traces show that 500 nM CNQX

reduced the peak amplitude rather than the frequency of sEPSCs (**Fig. 3.3B**). Higher concentrations of CNQX (10 μM) completely suppressed sEPSCs (inset). The probability density histograms (**Fig. 3.3C**: left) show a reduction of inward current events due to reduced sEPSC amplitudes. A corresponding reduction in baseline noise variance reduces the outward current density (**Fig. 3.3C**: right), as would be expected if CNQX antagonized the action of free glutamate in the synaptic cleft. The time-course of averaged sEPSCs in control and with CNQX is shown in **Fig. 3.3D**. Whilst the mean amplitude was reduced by CNQX, there was no change in the sEPSC decay phase. The cumulative frequency histogram from this data shows no significant reduction of sEPSC frequency by CNQX (**Fig. 3.3Ea**: $P>0.11$) but there was a significant reduction of mean amplitude (**Fig. 3.3Eb**, from 15.7 pA to 10.5 pA). The frequency showed no significant change in 4 cells ($P>0.4$). However, the amplitude was significantly reduced (**Fig. 3.3Ec**).

3) Suppression of sEPSCs, baseline noise and light responses by L-APB

To determine the presynaptic role of group III mGluRs in cone to HC synaptic transmission, I studied the action of L-APB, an agonist of group III mGluRs, on H1 HCs. L-APB, however, is known to have postsynaptic actions, in modulating the inward rectifier potassium channel via cyclic GMP dependent kinase (Dixon & Copenhagen, 1997) and in activating voltage-activated Ca^{2+} channels (Linn et al., 1999). To avoid these postsynaptic actions, H-7, a non-selective protein kinase inhibitor was added to the patch-pipette solutions. Whole-cell recordings with H-7 did not show any detectable effect on HC whole-cell currents, sEPSCs or light responses (data not shown). Furthermore, the holding potential of HCs was kept more negative to –55 mV to avoid large changes in voltage-activated Ca^{2+} conductance. **Figure 3.4A** shows the effect of applying 20 μM L-APB, with the HC equilibrated with H-7 in the patch-pipette solution, on the whole-cell current in the dark. L-APB induced an outward current with a clear reduction in sEPSC frequency (**Fig. 3.4Ba** and **b**), similar to the effect of cobalt or light. The probability density histograms show a reduction of inward current events, due to the suppression of sEPSCs (**Fig. 3.4C**, left) and a

reduction in outward probability density indicating a reduction of baseline noise variance (**Fig. 3.4C**, right). **Figure 3.4D** shows the time-course of averaged sEPSCs before and during application of L-APB. There was a slight reduction in amplitude, but little change in decay phase. The cumulative frequency histograms show a marked reduction in sEPSC frequency induced by L-APB from 147 Hz to 25 Hz (**Fig. 3.4Ea**) and a slight suppression of mean peak amplitude from 28.2 pA to 20.2 pA (**Fig. 3.4Eb**). This slight reduction in amplitude may be due to incomplete blockade, by H-7, of the known post-synaptic action of L-APB on HCs (Dixon & Copenhagen, 1997). L-APB significantly suppressed the mean frequency by 52.7 ± 6.0 % ($p<0.001$) in 19 cells and also significantly suppressed the mean amplitude by 15.5 ± 2.1 % ($p<0.001$) (**Fig. 3.4Ec**). The major effect of 20 μM L-APB under these conditions therefore, is to suppress the transmitter release process, having a similar action to red light or cobalt on sEPSC frequency and amplitude. Lower doses of APB were also effective, 2 μM L-APB suppressed the frequency of sEPSCs by 42.5 ± 22.3 % (n=3).

Figure 3.5A shows the effect of 20 μM L-APB on H1 HC light-induced outward current responses. L-APB suppressed the red light responses, accompanied by a reduction in sEPSC frequency. The time-course of outward DC current changes followed the sEPSC frequency changes (**Fig. 3.5B**). L-APB reduced the frequency of sEPSCs by 74 % (from 101 Hz to 7.5 Hz, filled squares) and reduced the amplitude of light responses by 83.3 % (from 54.1 pA to 9.6 pA, open circles). The reduction of sEPSC frequency and light responses showed a clear correlation (correlation coefficient: 0.90), suggesting that L-APB limits the amplitude of light responses by suppressing the transmitter release process from cone synaptic terminals.

4) The effect of APB is antagonized by MAP4

To confirm that L-APB was acting via a group III mGluR, I examined whether MAP4, a selective antagonist of group III mGluRs, antagonized the effects of L-APB. **Figure 3.6A** shows an application of 500 μM MAP4 made during superfusion of an H1 HC with 20 μM L-APB. The

fast-sweep recordings in each condition are shown in **Fig. 3.6B**. The initial sEPSC frequency in control was 117.6 ± 4.3 Hz and was reduced to 17.9 ± 1.1 Hz by L-APB. Co-application of 500 μM MAP4 partially restored the frequency to 44.1 ± 4.4 Hz, and subsequent washout of MAP4 to 20 μM L-APB alone reduced the frequency to 15.5 ± 0.8 Hz. Some recovery to 69.9 ± 3.2 Hz was then observed on washing out APB (**Fig. 3.6Ca**). The mean peak amplitude was not significantly changed by MAP4, consistent with a presynaptic site of action (**Fig. 3.6Cb**). Averaged results from 4 cells are shown in **Fig. 3.6D**. The sEPSC frequency, reduced by L-APB (mean suppression rate: 29 ± 13 %, $p<0.02$: compared with control) recovered with 500 μM MAP4 ($p<0.01$: compared with L-APB) and the effect of MAP4 was reversible ($p<0.05$). The mean peak amplitude was not significantly changed by L-APB and MAP4 in 4 cells ($p>0.05$), although on recovery from L-APB there was a small increase in the mean peak amplitude ($p>0.04$). Application of MAP4 alone induced an inward current accompanied by a slight, but insignificant, increase in sEPSC frequency (data not shown).

MAP4 (500 μM) also antagonized the reduction of red light responses and sEPSC frequency induced by L-APB (**Fig. 3.7A**). Light responses were reduced by L-APB in proportion to the reduction in sEPSC frequency (**Fig. 3.7B**) and both showed partial recovery on application of MAP4. On washing out the antagonist, there was a more profound reduction in light responses and sEPSC frequency, which showed some recovery on returning to control Ringer. Similar effects were observed in 2 cells.

5) 4-AP reduces the presynaptic effect of L-APB

Two principal mechanisms have been proposed to account for the L-APB induced regulation of transmitter release: (1) suppression of a presynaptic Ca^{2+} conductance (Takahashi et al., 1996) and (2) activation of a presynaptic 4-aminopyridine (4-AP) sensitive K^+ channels (Sladeczek et al., 1993; Cochilla & Alford, 1998). To determine whether L-APB reduces voltage-dependent Ca^{2+} conductance in cones, whole-cell voltage-clamp recordings were obtained from cones in the carp

retinal slice. The current-voltage (*I-V*) relation was measured before and during cobalt or L-APB applications (**Fig. 3.8**). Whilst cobalt was effective in reducing the Ca^{2+} conductance (**Fig. 3.8A**), 20 μM L-APB did not reduce the voltage-dependent Ca^{2+} current in cones (**Fig. 3.8B**).

I therefore examined whether L-APB was acting to suppress a 4-AP-sensitive K^+ current in the presynaptic terminals. **Figure 3.9A** shows an application of 200 μM 4-AP to an H1 HC made during superfusion with 20 μM L-APB. This induced an inward current, consistent with 4-AP acting to reduce the presynaptic inhibition induced by mGluR activation. Fast sweep recordings in each condition are shown in **Fig. 3.9B**. The sEPSC frequency, reduced by L-APB, showed a significant recovery close to the control level with 200 μM 4-AP. The frequency, in the presence of L-APB, increased from 182 ± 9 Hz to 239 ± 9 Hz on application of 4-AP (**Fig. 3.9Ca**). On washing out 4-AP, this was reduced to 154 ± 8 Hz and on returning to control Ringer recovered to 190 ± 78 Hz. The mean peak amplitude, however, showed no significant change with 4-AP (**Fig. 3.9Cb**), suggesting a presynaptic action. Results averaged from 4 cells are shown in **Fig. 3.9D**. The reduction in sEPSC frequency induced by L-APB (74.6 ± 3.3 %, $p<0.05$) showed a significant recovery with 200 μM 4-AP ($p<0.01$) (**Fig. 3.9Da**). Washout of 4-AP significantly reduced the mean frequency ($p<0.01$). The mean peak amplitude was significantly decreased by the initial application of L-APB ($p<0.01$, $n = 4$) (**Fig. 3.9Db**), but showed no further significant changes on application or following washout of 4-AP ($p>0.07$, $n = 4$).

The APB-induced reduction of H1 HC red light responses was also reversed by 4-AP (**Fig. 3.10A**). The outward current response to light was initially reduced by L-APB and then showed some recovery, accompanied by an inward current, on application of 4-AP. Light responses were reduced by L-APB in proportion to the reduction in sEPSC frequency (**Fig. 3.10B**) and both showed recovery on application of 4-AP. A significant recovery resulted on application of 4-AP, consistent with L-APB activation of presynaptic mGluRs reducing transmitter release by increasing a 4-AP sensitive K^+ conductance.

Since the activation of group III metabotropic glutamate receptors has been shown to reduce

intracellular cAMP, which then modulates kinase activity to effect an increase in presynaptic K^+ conductance (Sladeczek et al., 1993; Cochilla & Alford, 1998), I tested whether elevating cAMP reversed the action of L-APB. Application of 100 μM of the membrane-permeable analogue of cAMP, 8-bromo-cAMP, during perfusion with 20 μM APB, did not, however, induce any significant recovery of sEPSC frequency as observed with 4-AP. In some recordings, 100 μM 8-bromo-cAMP induced inward currents in H1 HCs, indicating an opposing action to L-APB, but I could not exclude non-specific effects, for example phosphodiesterase inhibition, leading a rise in cGMP and thus depolarizing cone synaptic terminals and increasing glutamate release.

3.4 Discussion

1) Analysis of H1 HC sEPSCs determines presynaptic vs postsynaptic modulation of synaptic transmission.

The analysis of sEPSCs, in both frequency and amplitude, provides a novel methodology for determining whether synaptic transmission from cones to HI HCs is modulated at either presynaptic or postsynaptic sites. Presynaptic modulation, involving a change in the rate of quantal release of transmitter from cone synaptic terminals, results in a change in sEPSC frequency without any change in mean peak amplitude. Thus, I detected a reduction in the frequency, due to hyperpolarization of the synaptic terminals or suppression of Ca^{2+} influx with red light or cobalt, respectively, with no corresponding reduction in mean amplitude. Postsynaptic modulation, on the other hand, involves no change in the frequency, but does effect a change in amplitude. Accordingly, with CNQX, which blocks AMPA receptors in H1 HC, I detected a reduction in sEPSC amplitude without any corresponding change in frequency. Analysis of voltage noise in ON or OFF-bipolar cells has been used to estimate the transmitter release rate from photoreceptors (Ashmore & Falk, 1982; Ashmore & Copenhagen, 1983) but since this synapse seems to be specialized to reduce the transmission of synaptic noise events discrete quantal sEPSC events arising from the transmitter release process from rods and cones could not be detected. Recent study of the immunocytochemical localization of mGluR6 at photoreceptor to ON-bipolar cell synapses shows a distribution on the ON-bipolar cell dendrites distant to the transmitter release sites of rods and cones (Vardi et al., 2000). This suggests the presence of a synaptic filter, specialized to reduce any fast sEPSC-like events in bipolar cells due to vesicular glutamate release, which would otherwise disrupt single-photon detection, or the high sensitivity, of the rod visual system. HC postsynaptic dendrites, however, are very closely apposed to the cone transmitter release sites (Saito et al., 1985; Vardi et al., 2000) resulting in the presence of discrete sEPSCs in HCs, possessing very rapid kinetics (Chapter 2).

2) Identification of the mGluR on cone presynaptic terminals.

L-APB significantly reduced H1 HC sEPSC frequency and slightly decreased their mean peak amplitude. The remarkable reduction of sEPSC frequency by L-APB indicates the suppression of transmitter release from cone presynaptic terminals as being the predominant mechanism of action. The slight reduction of sEPSC amplitude may indicate either a reduction of postsynaptic AMPA receptor sensitivity, possibly by some action by elevating cGMP via the postsynaptic mGluR (Dixon & Copenhagen, 1997). The presynaptic action is consistent with the expression of PR-sensitive mGluRs on cone presynaptic terminals, functioning as negative feedback to reduce transmitter release. The EC_{50} value of L-APB is in the range of 0.06-1 μM for mGluR 4, 6 and 8, but more than 100 μM for mGluR7 (Cartmell and Schoepp, 2000). Since I found that concentrations of 2 – 20 μM L-APB were effective in reducing sEPSC frequency by 47.3 ± 6.0 %, this suggests that the presynaptic action of APB may be mediated by mGluR4, 6 or 8, but not by mGluR7. MAP4 failed to antagonize the effect of L-APB on retinal ON bipolar cells expressing mGluR6 (Thoreson et al., 1997) and there is no immunocytochemical evidence for the expression of mGluR6 on cone presynaptic terminals (Vardi et al., 2000), excluding the contribution of mGluR6. MAP4 has been shown to be an antagonist at mGluR4 with IC_{50}>500 μM (Knöpfel et al., 1995), whilst for mGluR8 the IC_{50} is greater than 25 μM (Saugstad et al., 1997), in expression systems. I cannot as yet distinguish between mGluR4 and 8 from present pharmacological evidence, but the immnocytochemical evidence could suggest mGluR8 (Koulen et al., 1999).

Koulen et al. (1999) demonstrated the expression of mGluR8 on mammalian cone presynaptic terminals, and its activation by L-APB induced a fall in Ca^{2+} concentration. Group III mGluRs suppress transmitter release in two principal ways: (1) by suppressing the presynaptic voltage-activated Ca^{2+} conductance by direct G-protein-channel interaction (Takahashi et al., 1996; Dolphin, 1998) or (2) by activation of presynaptic 4-aminopyridine (4-AP) sensitive K^+ channels, by a cAMP-mediated second messenger pathway (Cartmell & Schoepp, 2000). The present results would be consistent with the action of L-APB being mediated by mGluR8 or mGluR4 linked to a

reduction in cAMP, which reduces cAMP-dependent kinase activity resulting in an increase in voltage-dependent K^+ conductance, in cone presynaptic terminals. This would hyperpolarize the terminals, which are relatively depolarized in the dark, resulting in a reduction in quantal transmitter release. I found that L-APB had no direct effect on cone voltage-activated Ca^{2+} conductance, so the fall in Ca^{2+} concentration observed on exposure of cones to L-APB (Koulen et al., 1999) may be resulted from a secondary effect due to hyperpolarization (reducing voltage-activated Ca^{2+} conductance) of the presynaptic terminals.

Glutamate is also known to activate a Cl^--dependent transporter current in cones, which is insensitive to APB (Grant & Werblin, 1996) and mediates a presynaptic action of glutamate at the cone terminals (Sarantis et al., 1988; Tachibana & Kaneko, 1988). Since the reversal potential of Cl^- in cones is more positive to their membrane potential in the dark, glutamate depolarizes cones by this mechanism. This constitutes a positive feedback mechanism, proposed to increase the gain for the conversion of changes in light intensity into changes in glutamate release (Sarantis et al., 1988). The mGluR-mediated suppression of vesicular glutamate release, reported here, constitutes a negative feedback mechanism acting to limit the release rate of glutamate. Perhaps the mGluR-mediated negative-feedback pathway is required to prevent the regenerative potential development, or excessive glutamate release by the positive-feedback pathway, mediated by the glutamate transporter current.

3) Negative feedback mediated by mGluRs functioning as autoreceptors.

The present results suggest the possibility of autoreception, such that glutamate released from cones acts via mGluR8 or mGluR4 to reduce the transmitter release process by increasing the voltage-sensitive K^+ conductance in red cone presynaptic terminals. This negative feedback via group III mGluRs might regulate the tonic release of glutamate in the dark. With red light stimulation, the rate of glutamate release is reduced by hyperpolarization of the presynaptic terminals, so the negative feedback would accordingly decrease as the level of free glutamate, and

hence mGluR activation, is reduced. Precise functions of mGluRs in regulating postsynaptic light responses of both HC and bipolar cells remain to be determined. The mGluR antagonist, MAP4, induced only a small, but insignificant, increase in sEPSC frequency when applied in the absence of L-APB. This suggests that the presynaptic mGluR is not highly activated in light-adapted retinal slices when the vesicular release rate, and hence free glutamate, is low. Whether mGluR activation is higher in the dark-adapted condition, when vesicular glutamate release is high, remains to be determined.

Certainly, this negative feedback, limiting the glutamate release process, would play an important role in preventing possible excitotoxic levels of glutamate accumulating at this synapse. A further possible functional role could be to restrict any accumulation of free glutamate, and thus reduce baseline noise due to single-channel fluctuations. This form of presynaptic inhibition probably only applies to the cone visual system in which optimal light detection is not a priority. If rods possessed a similar mechanism, this would tend to reduce the change in glutamate release per mV change in presynaptic potential (Falk, 1989; Shiells & Falk, 1995), and thus reduce visual sensitivity. Whether mGluRs are expressed on rod presynaptic terminals, and whether they mediate positive or negative feedback on transmitter release, remains to be shown.

Chapter 4. Blocking AMPA receptor desensitization prolongs spontaneous EPSC decay times and depolarizes H1 horizontal cells in carp retinal slices.

4.1 Introduction

I have shown that α-amino-3-hydroxy-5-methylisoxazole-4-propionic acid (AMPA) type ionotropic glutamate receptors mediate their spontaneous excitatory postsynaptic currents (sEPSCs) and responses to light in carp retinal slices (Chapter 2; Hirasawa et al., 2001). The decay time constant of sEPSCs reflected the time-course of channel closure. Other factors, which could have influenced the decay time constant, for example, the clearance of glutamate from the synaptic cleft by uptake, were considered. Voltage-clamp recording of sEPSCs was facilitated using dopamine to uncouple the HCs, which reduces their gap-junctional conductance, decreasing their input conductance. This, however, had a dual action, also reducing AMPA receptor desensitization. Heptanol, which has been used to uncouple gap junctions in other systems (Pérez-Armendariz et al., 1991), was therefore used instead of dopamine in the present study. This allowed voltage-clamp recording of sEPSCs and analysis of the effect of blocking desensitization by CTZ on their amplitude, frequency and kinetics.

Receptor desensitization in spiking neurons contributes to the shaping of postsynaptic currents, decreasing EPSC decay time constants (Jones & Westbrook, 1996). AMPA receptor desensitization in isolated HCs is very fast, occurring with a time constant of 1 – 2 ms (Eliasof & Jahr, 1997; Lu et al., 1998). Desensitization can be defined as the reduced ability of a receptor to elicit a postsynaptic response in the presence of a maintained agonist concentration, as occurs, for example, at the nicotinic acetylcholine receptor. Cyclothiazide (CTZ), a selective blocker of AMPA receptor desensitization (Yamada & Tang, 1993), has widely been used to study the effect of AMPA receptor desensitization. Yang et al. (1998) reported that CTZ depolarized HCs, but did not correlate this with its effect on the kinetics of the postsynaptic currents. In this chapter, I show the importance of receptor desensitization in shaping the sEPSC time-course.

4.2 Materials and Methods

1) Retinal slice preparation and superfusion

Slices of retina were prepared as described in Chapter 2, and they were superfused with Ringer's solution containing (mM): 102 NaCl, 2.6 KCl, 1 $CaCl_2$, 1 $MgCl_2$, 28 $NaHCO_3$, 5 glucose and 5 HEPES, adjusted by NaOH to pH 7.5 when bubbled with 95 % O_2 and 5 % CO_2. Heptanol (Sigma), an uncoupling agent for gap junction, was dissolved directly into the superfusate for voltage clamp recording. GYKI52466 (Sigma) and cyclothiazide (CTZ, RBI Ltd.) were dissolved in DMSO (final concentration: less than 0.1 %) and then added to the superfusate. Perfusion speed was 1.4 ml/min and volume of the chamber was 500 µl. The slices were viewed using an upright microscope (BX50WI, Olympus) with infrared illumination (>850 nm) and monitored on a CRT display with a CCD camera (C5985, Hamamatsu Photonics). All experiments were conducted at room temperature (21-23°C).

2) Light stimulation and identification of cells

Retinal slices were similarly illuminated by red- and blue-diffuse light emitting diodes (LED's) as described in Chapter 2. The horizontal cells and their subtypes were also identified by their characteristic morphology and spectral responses as described in Chapter 2. The intensity of light stimulation was usually 0.1-1.5×10^6 quanta/µm^2/s, which induce maximum light responses of HCs.

3) Whole-cell recording

Patch pipettes for whole-cell recording were fabricated from standard-walled borosilicate glass (Clark Electromedical). The patch pipette intracellular solution contained (mM): 70 cesium methanesulfonate ($CsMeSO_4$), 30 CsCl, 1 $MgCl_2$, 5 EGTA, 1 Mg-ATP, 1 Na-GTP, 10 HEPES adjusted to pH 7.2 by CsOH. Patch-pipettes had resistances of 3-6 MΩ and sEPSCs were usually recorded from cells with high input resistances (>100 MΩ). Series resistances were ideally less than 12 MΩ. Whole cell current clamp and voltage clamp recordings were obtained using an Axopatch 1-D amplifier (Axon Instruments). No series resistance compensation was employed

except otherwise described. Signals were filtered at 2-5 kHz and digitized at 8-10 kHz.

4) Pressure-application of glutamate.

Glutamate-induced responses were recorded in response to focal pressure applications from a patch-pipette filled with 0.5 mM glutamate in Ringer solution onto the H1 HCs, under visual control. 3 mM cobalt was added to the external control solution to block synaptic transmission. 20-100 ms pressure (20 psi) pulses were applied to the patch-pipette.

5) Analysis

sEPSCs were analysed by setting a threshold detection level between 4-10 pA, defined as twice the standard deviation (sigma) of the baseline noise in darkness, for details shown in the Chapter 2. The selected threshold level was kept constant for the entire analysis of the cell. All events larger than this level were included if they had a rise time <1 ms and if they did not arise from the decaying phase of the previous event. The peak of sEPSCs was detected semi-automatically with a moving rectangle (Origin 6.0 software, Microcal Ltd). The height of the rectangle was set at about 3 pA, and width was set at about 1-3 ms for interval measurements of sEPSC events and 10-20 ms for their peak measurements not to detect overlapped peak. The decay time constant of sEPSCs was obtained by fitting the decay phase with a single exponential curve. The curve fitting was achieved using a nonlinear least-square error algorithm. The statistical data were shown as means ± standard errors.

6) Uncoupling agents of gap junctions

In the previous sections, I applied dopamine to reduce electrical coupling between HCs (Chapters 2 & 3). Dopamine is known to also modulate the kinetics of glutamate receptors on HCs by blocking desensitization (Schmidt et al., 1994). I, therefore, examined other ways of blocking gap junctional coupling. Firstly, 8-bromo-cAMP and dibutyryl-cAMP, analogs of cAMP which are known to uncouple gap junctions between HCs, were introduced from internal patch solution or applied from external solution. Introducing these cAMP analogs (1 mM) from internal

patch solutions, however, failed to increase the input resistance of HCs in the slice preparation. External application of these analogs (100 μM) was also insufficient to observe sEPSC in HCs. Secondly, carbenoxolone (100 μM), a glycyrrhetinic acid analog known to uncouple gap junctions (Vaney et al., 1998), failed to increase the input resistance of HCs in slice preparations and, therefore, sEPSCs were not observed. Thirdly, 2.5 mM heptanol, an alcohol which uncouples gap junctions (Pérez-Armendariz et al., 1991), prominently increased the input resistance of HCs, and sEPSCs were clearly observed. I, therefore, judged that the application of heptanol was the best protocol to record HC sEPSCs under voltage clamp.

4.3 Results

1) CTZ depolarizes H1 HCs with enhancement of light responses

The effect of cyclothiazide (CTZ) on the membrane potential of H1 HCs in the slice preparation was studied in current clamp mode. Under these conditions, with the recorded cell electrically coupled to neighbouring cells, the membrane potential results from the sum of potential changes in the electrically-coupled network. Cells lying deeper in the slice have a more intact photoreceptor input (Shiells & Falk, 2000) and thus are relatively more depolarized than the recorded cell lying on the surface, and so contribute a depolarizing, inward, current via the gap junctions. Cs^+ was used in the patch-pipette solution to reduce K^+ conductance, which made little difference to the membrane potential, since reducing K^+ conductance in the recorded cell would have little effect on the sum of potential changes contributed by the network. CTZ (100 μM) depolarized H1 HCs from –27.5 ± 8.2 mV to –14.8 ± 5.6 mV in 4 cells (the mean depolarization: 12.8 ± 2.8 mV) (**Fig. 4.1A**). In addition, CTZ also increased the amplitude of the photoresponses (**Fig. 4.1B**). This suggests an increase in light sensitivity, consistent with a rise in glutamate receptor sensitivity on blocking their desensitization. **Figure 4.1C** shows light responses scaled to the same peak amplitudes. The time-course of the light responses showed little change with CTZ. The transient depolarizations at light offset, probably generated presynaptically in the cones, were increased in proportion to the increase in hyperpolarizing light responses, consistent with both effects resulting from a rise in postsynaptic AMPA channel sensitivity on blocking desensitization.

2) Physiological properties of sEPSCs of H1 HCs observed in the presence of heptanol

For voltage clamp recording of sEPSCs from H1 HCs in the slice preparation, I suppressed the electrical coupling between HCs by applying 2.5 mM heptanol. The effect of heptanol on the postsynaptic current of an H1 HC is shown in **Fig. 4.2A**. Heptanol increased the input resistance of the cell from 14 MΩ (at point 1 in Fig. 2A) to 210 MΩ (at point 2). On average, heptanol increased the input resistance of H1 HCs from 20.4 ± 2.8 MΩ to 148 ± 23 MΩ (n=12), similar to,

but more effective than dopamine (Chapter 1). The light responses were almost completely suppressed by heptanol, which was accompanied by an outward shift in the whole-cell current (from *a* to *b* in **Fig. 4.2**) and the appearance of discrete sEPSCs. This suppression of light responses suggests that blocking gap-junctional coupling isolates the recorded cell on the surface of the retinal slice from deeper cells, which have a more intact synaptic input from photoreceptors. In dogfish retinal slices, ON-bipolar cells recorded on the surface of the slices had small light responses (10-20 pA), whilst deeper cells had much larger light responses (100-200 pA), due to a more intact rod input (Shiells & Falk, 2000). The outward current probably arises from the suppression of an inward current entering the recorded cell via gap junctions, from more depolarized HCs (with a more intact cone input) deeper in the slice. So the reduction in light response by heptanol, in the HC on the surface of the slice, derives from the reduction in electrotonic spread of the light response within the HC syncytium. The outward current induced by heptanol application was followed a slow recovery, an inward current, which probably derives from the suppression of K^+ conductance as the electrically isolated cell equilibrated with Cs^+. This improvement in space-clamp, reducing leak currents, allows the recording of discrete sEPSCs. Alcohols, in particular, ethanol, have been shown to reduce AMPA receptor currents in other CNS neurons, but at much higher concentrations (50-200 mM) (Wang et al., 1999). Heptanol (2.5 mM), used here to uncouple gap junctions (Pérez-Armendariz et al., 1991) would, therefore, be unlikely to have any direct postsynaptic effect on the H1 HC AMPA channels. This was confirmed by heptanol failing to block H1 HC responses to pressure applications of glutamate in the presence of Co^{2+} to block synaptic transmission (**Fig. 4.2B**).

Discrete sEPSCs were observed on isolating the recorded H1 HC with heptanol-containing Ringer's solution (**Fig. 4.3A**). The polarity of sEPSCs was reversed at around 0 mV (**Fig. 4.3A**: n=3), consistent with measurements of their reversal potential shown in Chapter 2. The mean decay time constant of sEPSCs was 0.59 ± 0.06 ms (n=8) and the single quantal conductance obtained from their mean peak amplitude was 497 ± 62 pS (n = 8). The sEPSCs were blocked by

20 μM GYKI52466, an antagonist of AMPA receptors (**Fig. 4.3B**: n=5). Cobalt (100 μM) suppressed the sEPSC frequency, similar to the effect of light, but did not affect the mean peak amplitude (**Fig. 4.3Cb and c**), which indicates that Ca^{2+} dependent transmitter release was not markedly affected by heptanol. Similar effects were seen in 3 cells. The rising and decaying phase of the averaged sEPSC time-course in cobalt containing Ringer (the dotted line shown by the inset to **Fig. 4.3Cb**) was quite similar to that in control (solid line). The physiological properties of sEPSCs measured in the presence of heptanol were almost identical to those examined in Chapter 2 (mean decay time constant was 0.71 ± 0.07 ms, single quantal conductance change was 482 ± 59 pS) using dopamine to block gap-junctional coupling. This suggests that heptanol does not significantly alter the underlying physiological properties of the postsynaptic AMPA receptors. However, I cannot completely exclude some presynaptic effect of heptanol, which is known to modulate voltage dependent Ca^{2+} currents in pancreatic beta cells (Pérez-Armendariz et al., 1991) and could, potentially, alter the transmitter release process from cones.

3) CTZ increased the decay time constant of H1 HC sEPSCs

The effect of 100 μM CTZ on H1 HC sEPSCs was studied in the presence of heptanol. **Figure 4.4A** shows sEPSCs averaged in control and with CTZ, and were fitted with single exponential functions describing their decay phases (grey lines). These averaged sEPSCs are shown superimposed (aligned) on the right. CTZ prolonged the decay time constant of sEPSCs. The plots of peak amplitude versus decay time constant of sEPSCs are shown in **Fig. 4.4B**. CTZ significantly increased the decay time constant of sEPSCs from 0.60 ± 0.08 ms to 1.25 ± 0.18 ms (2.1 ± 0.4-fold: $p<0.01$: n=5). Their decay time constant showed a positive correlation with amplitude, indicating that membrane filtering due to cable properties was not prolonging the decay time constant. CTZ did not significantly induce any change in mean sEPSC frequency (22.3 ± 19.1 % : $p > 0.36$, n=5) or change in mean peak sEPSC amplitude (15.9 ± 8.8 % : $p > 0.17$, n=5). There was no change in either the sEPSC interval or amplitude distribution (**Fig. 4.4Ca and b**), which indicates that transmitter release was not significantly altered by CTZ in heptanol solution.

These results are contrary to the report that CTZ increases mEPSC frequency of CA1 hippocampal neurons, which suggested some presynaptic effect acting to increase transmitter release (Diamond & Jahr, 1995).

The millisecond-order decay time-constant of the sEPSCs in CTZ suggests the rapid removal of transmitter from postsynaptic receptors. I tried to detect any contribution of glutamate uptake to the decay time constant of sEPSCs. Inhibition of glutamate uptake transporters in the presence of heptanol, using dihydrokainate (DHK) or L-trans-PDC (150-200 μM), failed to significantly prolong the sEPSC decay time constants (without significant changes; 0.65 ± 0.05 ms (control), 0.79 ± 0.20 ms (with PDC); $p>0.49$, $n=3$; 0.78 ± 0.22 ms (control), 0.86 ± 0.23 ms (with DHK): $p>0.08$, $n=2$). No change in decay time constant was observed with these uptake inhibitors in the presence of CTZ. Blocking desensitization of the AMPA receptors, rather than some action on glutamate uptake, seems to be the principal mechanism leading to their prolonged time-course.

4.4 Discussion

1) CTZ-induced depolarization and suppression of AMPA receptor desensitization.

CTZ increased the decay time constant of sEPSCs by about 2-fold. The inward current carried by each sEPSC would therefore be increased by a similar degree. Since there was no change in frequency or mean sEPSCs peak amplitude, this would lead to depolarization of the H1 HCs. Quantitatively, the increase in current influx induced by CTZ can be estimated from the results shown in **Fig. 4.1.** The depolarization induced by glutamate released from cones, $V_{transmitter}$ is described by the following equation,

$$V_{transmitter} = V_d - V_{bright} \qquad (1)$$

where V_{bright} is a membrane potential under bright light (when transmitter release is suppressed) and V_d the resting potential of HC in darkness (when transmitter release is high). $V_{transmitter}$ can also be described as follows,

$$V_{transmitter} = -\frac{I}{G_{AMPA}} \qquad (2)$$

where I is a total influx of current through AMPA receptors in darkness and G_{AMPA} is the total conductance of AMPA receptors on HCs. From equations (1) and (2), the following equation can be obtained;

$$I = G_{AMPA} \cdot (V_{bright} - V_d) \qquad (3)$$

Observed values, V_{bright} and V_d, in control solution in **Fig. 4.1**, were –32.7 mV and –26.2 mV, respectively. V_{bright} and V_d in CTZ were –28.2 mV and –17.8 mV, respectively. Therefore, I in control ($I_{control}$) and I in CTZ (I_{CTZ}) were -6.5 G_{AMPA} pA and -10.4 G_{AMPA} pA, respectively. Therefore, I can estimate that the macroscopic current influx passing the membrane of an H1 HC was increased by 1.6-fold with CTZ. The mean value of the macroscopic current influx was

increased by 1.8 ± 0.3-fold (n=4), corresponding well with the 2-fold increase in sEPSC decay time constant. The prolonged sEPSC decay time constant reflects an underlying increase in the open probability of AMPA receptor channels. The CTZ-induced depolarization can therefore be accounted for by an increased current influx due to a more prolonged sEPSC time-course on blocking AMPA receptor desensitization.

There was little change in the kinetics of the light responses, which were potentiated by CTZ. This is because the rise and decay phases of the horizontal cell light response, which follow the time-course of the cone synaptic input, are much slower than the kinetic changes observed at the level of the sEPSCs on blocking desensitization. A doubling of the sEPSC decay time constant to 1.25 ms would, clearly, have little detectable effect on the macroscopic current time-course, changing over a time-scale of hundreds of ms.

2) Factors determining the sEPSC decay time constant.

The decay time constant of sEPSCs showed a positive correlation with peak amplitude, indicating that they were not filtered by the cable properties of the cell membrane. A negative correlation would indicate a poor space-clamp (Spruston et al., 1993). The positive relationship between the decay time constant and the peak amplitude might suggest a dependency of amplitude on the rate of glutamate diffusion from receptors in the synaptic cleft (Glavinovic & Rabie, 1998). CTZ prolonged the decay time constant of sEPSCs by blocking desensitization of the AMPA receptor-channels. We cannot, however, exclude whether the change in sEPSC kinetics derives from an increase in deactivation, or channel closing time. Other work, showing that CTZ blocks AMPA receptor desensitization (rather than changing the deactivation kinetics of the channels), would favour desensitization over deactivation (Shen et al., 1999; Koike et al., 2000). Glutamate uptake does not affect the sEPSC decay phase, since inhibitors of glutamate transporters, dihydrokainate or L-trans-PDC, failed to prolong the decay time constant. Shen et al. (1999) reported that the pharmacological properties of AMPA receptors of carp HCs are similar to those

obtained at AMPA receptors assembled from flop variants in expression systems. CTZ has a much less potent action on the flop type, compared to its action in blocking desensitization of flip type AMPA receptors. The maximal effect is obtained at 300 μM on the flop type, so 100 μM used in the present experiments may not have completely blocked desensitization. However, over the first few ms of the response to glutamate, comparable to the sEPSC timescale, 100 μM CTZ was completely effective in blocking desensitization (Koike et al., 2000). The small increase in sEPSC decay time constant by a factor of 2 with CTZ suggests that the degree of desensitization of H1 HC AMPA type receptors is much less prominent than, for example, kainate receptors of cone-driven OFF-bipolar cells (DeVries & Schwartz, 1999). Rod-driven HCs (Shiells et al., 1986), or rod-driven OFF-bipolar cells (Shiells & Falk, 1994), on the other hand, did not show any desensitization to glutamate. Desensitization in the rod system would clearly disrupt dim light detection, whereas in the cone system the function of glutamate receptor desensitization may be to improve resolution in the time domain. The H1 HC AMPA receptor desensitization would conserve high sensitivity in the dark without inducing any prominent change in their light response timecourse. This might function to prevent their excessive depolarization in the dark-adapted condition and extend their response operating range.

Chapter 5. General discussion

Analysis of sEPSCs on H1 HCs reveals the asynchronous vesicular transmitter release from cone photoreceptors

Whole-cell patch clamp recording of HCs from retinal slices revealed sEPSC events with high time resolution, while voltage clamp recording by double barrelled micro-electrodes (Low et al., 1991; Yamada et al., 1992) failed to detect rapid sEPSC events, probably due to filtering by the high resistance micro-electrodes. The two following reasons can be added for recordings of HC sEPSCs. First, HC dendrites closely face to the cone transmitter release sites (Saito et al., 1985; Vardi et al., 2000). Recent study of the immunocytochemical localization of iononotropic glutamate receptor subunits (GluR1, 2, 2/3 and 4) at cone pedicles also shows that HC dendrites face to cone synaptic ribbons, while OFF-BC dendrites contact at basal junctions at cone pedicles (Haverkamp et al., 2000). Moreover, immunocytochemical localization of mGluR6 at PR to ON-BC synapses shows that the ON-bipolar cell dendrites are distant to the transmitter release sites of PRs (Vardi et al., 2000). These evidences suggest that the synaptic filter of BCs would reduce fast sEPSC-like events resulted from vesicular glutamate release, which could not occur in HCs. Second, AMPA receptors capable to generate rapid sEPSCs play as postsynaptic receptors on HCs. Actually, the noise level of ON-BC postsynaptic current is much less than that of OFF-BC postsynaptic current (Wu et al., 2000). This suggests that mGluRs on ON-BC, which show relatively slow conductance change due to a second messenger system, may contribute to the synaptic filtering of rapid synaptic events by vesicular transmitter action (Wu et al., 2000).

Discrete sEPSC on H1 HCs in carp retina, of which frequency is suppressed by light stimulus, should be the direct evidence for an asynchronous vesicular transmitter release from cones. Usually, in the vertebrate retina, an analysis of voltage noise at bipolar cells can provide the feature of graded transmitter release rate from PRs (Ashmore & Copenhagen (1983)). Their voltage noise analysis, however, needed a statistical analysis based on Campbell's theorem to describe the quantitative phenomenon of synaptic transmission, because of the failure of discrete quantal events. In contrast, an analysis of sEPSCs on HCs can provide the feature of vesicular transmitter release

from PRs without a statistical analysis, and therefore should be useful to describe the aspect of vesicular transmitter release from PRs.

Ribbon synapse in photoreceptors

In contrast to conventional synapse releasing neurotransmitter transiently, ribbon synapse in PRs release transmitter continuously in the dark and reduce the release rate in response to the graded changes in the membrane potential. Their specialized physiological properties are determined by the differences of structure and molecular mechanism. Ribbon synapse possesses a special structure called 'synaptic ribbon', which is running above a linear active zone. Since many vesicles accumulate at the base of the synaptic ribbon (Gray & Pease, 1971), it is considered that the synaptic ribbons contribute to the capture of synaptic vesicles from the cytosol and to the transportation of them to the active zone. Synaptic ribbon, mediating vesicle capture and its transportation, is crucial for continuous transmitter release. Moreover, ribbon synapses of PRs and BCs express a different member of synaptic vesicle-associated proteins. Firstly, ribbon synapses lack synapsins, synaptic vesicle-associated proteins found in all conventional synapses (Morgans et al., 2000). Secondly, ribbon synapse expresses syntaxin 3 for an essential component of the core fusion complex, whilst conventional synapse expresses syntaxin 1 (Morgans et al., 1996). Thirdly, ribbon synapse in PRs specially expresses a major protein component called RIBEYE which may contribute to the synaptic vesicle fusion (Schmitzs et al., 2000). Although these synaptic vesicle-associated proteins are considered to be crucial for graded neuronal signaling, their physiological function is still elusive. sEPSC analysis on HCs should also be applicable to investigate the molecular mechanisms of transmitter release from PR ribbon synapses.

Presynaptic transmitter release regulation by activation of mGluRs

Conventional analysis of postsynaptic potential cannot determine the modulation site of graded potential synapse. First, the analysis of postsynaptic voltage fluctuation is not useful to determine the synaptic modulation site, because it will be reduced by both of pre- and postsynaptic inhibition. Actually, the voltage fluctuation of ON-ganglion cells, in the presence of tetrodotoxin, is suppressed by both of L-APB (changing presynaptic quantal rate) and CNQX (changing postsynaptic quantal amplitude) (Freed, 2000). In contrast, sEPSC analysis of HC is a novel and useful method to determine the modulation site in PR-HC synaptic transmission, because sEPSC frequency and amplitude can be regulated by the vesicular transmitter release rate from presynapse and the postsynaptic receptor sensitivity respectively, as shown in Chapter 3. I demonstrated that mGluR agonist suppressed vesicular transmitter release from PRs using sEPSC analysis. APB-induced frequency suppression of sEPSC indicates that the activation of mGluR can play a role in the presynaptic regulation of vesicular transmitter release from PRs. sEPSC frequency regulation by mGluR can contribute to the auto-feedback mechanism of glutamate release from PRs, although its modulation mechanism in detail is still elusive. Nitric oxide (Savchenko et al., 1997) or somatostatin (Akopian et al., 2000) is considered to regulate transmitter release from photoreceptors. sEPSC analysis on HCs can provide the quantitative feature for vesicular transmitter release and, therefore, should be useful to describe the presynaptic modulation in the outer retina. The analysis of sEPSC frequency and amplitude should thus provide a novel and useful method to determine the modulation site of PR-HC synaptic transmission.

It is needed to determine whether L-APB suppresses transmitter release from cone PRs directly or indirectly. Two kinds of mechanism can be proposed for the effects of L-APB.

First is a direct regulation to PRs, as discussed in Chapter 3. I have no direct evidence for the modulation of L-APB on voltage dependent Ca^{2+} or K^{+} channels on PRs. However, the recovery of sEPSC frequency by 4-AP may indicate that L-APB suppressed transmitter release via 4-AP sensitive pathway but not direct suppression of presynaptic Ca^{2+} conductance.

Second is an indirect regulation to PRs via second order neurons through negative feedback pathway. Two possible pathways can be considered: 1) GABA-ergic negative feedback pathway or 2) GABA independent feedback pathway (Verweij et al., (1996)). In the accessory olfactory bulb, the granule cell mGluR2 can regulate GABA transmission to the mitral cell (Hayashi et al., 1993). In my experiments, however, both of picrotoxin and bicuculline, antagonists of GABA receptors, failed to recover the sEPSC frequency suppressed by L-APB. Therefore, GABA-ergic feedback system may not contribute to the transmitter release regulated by mGluR. GABA independent-negative feedback, sifting the voltage range of Ca^{2+} current of cone PR to suppress transmitter release (Verweij et al., (1996)), may also be activated by L-APB. However, it is unlikely, since L-APB had no effect on voltage dependent Ca^{2+} current of cone PRs (**Fig. 3.8**).

As described above, the regulatory mechanism of transmitter release by L-APB remains to be clear. Further investigation is needed to determine the mGluR-mediated transmitter release regulation at PR-HC synapse.

Postsynaptic AMPA receptor desensitization to graded potential signalling of HCs

In Chapter 4, the CTZ induced-prolongation of sEPSC decay time indicates that AMPA receptor on HCs can be desensitized to glutamate during synaptic transmission. The effects of CTZ, depolarizing HCs and prolonging sEPSC decay time, suggest the importance of AMPA receptor desensitization to maintain the HC resting potential and to regulate the operating range of HC light responses. AMPA receptor desensitization of HCs, therefore, regulates the current influx activated by glutamate and should be important to regulate operating range of HCs. The postsynaptic regulation by receptor desensitization can control the graded light response of HCs.

Dopamine, released from interplexiform cells, can suppress the receptor desensitization on HCs (Schmidt et al., 1994), which therefore can account for the potentiation of HC glutamate response (Knapp & Dowling, 1989). AMPA receptor desensitization should contribute to the prevention of the glutamate response of HCs from maximal response, and therefore makes room for

the synaptic potentiation by neuromodulators.

Concluding remarks

Main findings in the present study are as follows. First, an analysis of sEPSC on HCs, of which frequency is reduced by light stimulation, revealed the feature of asynchronous vesicular transmitter release from PRs (Chapter 2). Second, the frequency of vesicular transmitter release can be modulated by a presynaptic regulation of mGluRs, resulting in the regulation of HC light responses (Chapter 3). Third, the postsynaptic AMPA receptor on HCs is desensitized by glutamate released from PRs, resulting in the regulation of HC light responses (Chapter 4). The asynchronous transmitter release from PRs should be essential for the graded light response of HCs, because the release rate can be modulated gradually and successively by light stimulation. This asynchronous and vesicular transmitter release could be specialized for graded transmitter release at ribbon synapses. Moreover, the analyses of sEPSC on HCs clearly showed that the HC light response was regulated by both of pre- and postsynaptic factors; presynaptic transmitter release and postsynaptic receptor sensitivity.

Different from conventional intracellular recordings, sEPSC study on HCs can reveal 1) the vesicular transmitter release rate from PRs (by analysing sEPSC frequency) and 2) the closure kinetics of postsynaptic AMPA receptor (by analysing sEPSC decay time course). The sEPSC analysis of HCs should be useful to investigate not only the vesicular synaptic transmission at PR-HC synapse, but also the elementary postsynaptic process for graded potential signalling.

Appendices

1. Introduction of the products of Lorentzians to fit the power spectrum of postsynaptic current of HCs

I will show the introduction of the products of Lorentzians to fit the power spectrum of postsynaptic current of HCs in **Fig. 2.9**. In general, time course of each elementary process of synaptic events can be described by a single exponential curve if opening time of channels is much faster than closing time (e.g., Anderson & Stevens, 1973). In contrast, since sEPSC in HC shows rise time (opening time) comparable to decay time (closing time), elementary synaptic events in HCs can be approximated as follows,

$$g(t) = a[\exp(-t/\tau_d) - \exp(-t/\tau_r)] \qquad (1)$$

where τ_d and τ_r were decay and rise time constants respectively, and a is an amplitude factor.

The Fourier transform of equation (1) is given as follows,

$$g(f) = a\left[\left(\frac{1}{i\omega + \frac{1}{\tau_d}}\right) - \left(\frac{1}{i\omega + \frac{1}{\tau_r}}\right)\right] \qquad (2)$$

where $\omega=2\pi f$ ($f=1/2\pi\tau$) and i for the imaginary unit.

Power spectral density $S(f)$ of synaptic noise current composed of a number of elementary current (sEPSCs), arriving at a mean rate ν, is written by the following equation (e.g., DeFelice, L.J. "Introduction to Membrane Noise", Plenum Press, New York and London, 1981)

$$S(f) = 2\nu|g(f)|^2 \qquad (3)$$

The power spectral density is obtained from equations (2) and (3),

$$S(f) = \frac{S_0}{\left(1+\left(\frac{f}{f_d}\right)^2\right)\left(1+\left(\frac{f}{f_r}\right)^2\right)} \qquad (4)$$

where $S_0 = 2a^2\nu(\tau_d-\tau_r)^2$ and $f_d=1/(2\pi\tau_d)$, $f_r=1/(2\pi\tau_r)$.

Since power spectrum of postsynaptic current of HCs was fitted well with the products of Lorentzians (**Fig. 2.9**), the baseline noise component (probably attributable to continuous channel noise) may also have similar kinetics to sEPSC events.

2. sEPSC and baseline noise

According to the original scheme of synaptic transmission proposed by Katz and colleagues, the amplitude of postsynaptic response is resulted from liner summation of miniature synaptic events. If their classical proposal were valid to describe the PR-HC synaptic transmission, sEPSC might have been defined from absolute zero current level but not baseline level. However, I assumed that the definition of sEPSC from baseline noise level was appropriate by the following reasons. Firstly, an outward component of baseline noise, of which variance is suppressed by light stimulus or cobalt, was fitted with Gaussian distribution function, indicating that the baseline noise variance is resulted from random continuous noise. Secondly, sEPSC amplitude in the dark was almost constant during light stimulation or in the presence of cobalt, indicating that quantal content is constant. Since the quantal content is unlikely to be changed by the manipulations to reduce transmitter release rate, the constant quantal content indicates that the measurement of sEPSC from baseline level is proper.

Then, how is the outward DC holding current occurred by the manipulations to reduce the transmitter release, such as light stimulation and the application of cobalt ? I assumed that the outward DC holding current was attributable to the continuous closure of postsynaptic receptors,

which would hyperpolarize the cells. A major part of baseline noise in the dark can be attributed to the continuous AMPA channel noise, probably activated by residual glutamate in the synaptic cleft, because the suppression of the postulated baseline noise was accompanied by the outward holding current. Supporting this, single channel conductance estimated from the variance change of baseline noise was similar to that of non-NMDA receptor channels as shown below.

The single channel conductance was estimated from the variance of baseline noise originating from receptor channel noise and the mean current level, both of which were reduced by red light stimulation. The variances of baseline noise in darkness and red light shown in **Fig. 2.3Bb** and **c** were 16.8 pA^2 and 7.3 pA^2, respectively. The outward current elicited by red light stimulation was 30 pA. Therefore, the single channel current was -0.32 pA, estimated from the modification of conventional stationary noise analysis as shown by the following equation,

$$i = \frac{\sigma_d^2 - \sigma_r^2}{I}$$

where i is a single channel current of receptor channels, I is an outward current elicited by red light stimulation, σ^2_d and σ^2_r are variances of baseline noise in darkness and red light. The single channel conductance of 8 pS was obtained from the single channel current divided by the electromotive force (= a potential difference between the holding potential of -40 mV and the reversal potential of 0 mV). The mean value from 14 cells was 16.4 ± 1.8 pS. This is in good agreement with the single channel conductance of non-NMDA glutamate receptor channel derived from studies on isolated HCs (10-30 pS: Lasater, 1990; 7 pS: Schmidt, 1997).

In the present analysis, however, I cannot exactly define the transmitter release rate, because high frequent sEPSC made it difficult to discriminate from baseline noise completely. Recently, Neher and Sakaba (2001) developed a new deconvolution analysis to estimate transmitter release rate, with a nonlinear current component resulting from the delayed clearance of glutamate from the synaptic cleft, at the Calyx of Held synapse. Their newly developed deconvolution method resolves the time course of neurotransmitter release. Such a novel analysis may be applicable to

determine the aspects of transmitter release at PR-HC synapses.

References

Anderson, C. R. & Stevens, C. F. (1973) Voltage clamp analysis of acetylcholine produced end-plate current fluctuations at frog neuromuscular junction. *Journal of Physiology*, **235**, 655-691.

Anwyl, R. (1999) Metabotropic glutamate receptors: electrophysiological properties and role in plasticity. *Brain Research Review*, **29**, 83-120.

Ashmore, J.F. & Copenhagen, D.R. (1983) An analysis of transmission from cones to hyperpolarizing bipolar cells in the retina of the turtle. *Journal of Physiology*, **340**, 569-597.

Ashmore, J.F. & Falk, G. (1982). An analysis of voltage noise in rod bipolar cells of the dogfish retina. *Journal of Physiology*, **332**, 273-297.

Akopian, A., Johnson, J., Gabriel, R., Brecha, N. & Witkovsky, P. (2000) Somatostatin modulated voltage-gated K^+ and Ca^{2+} currents in rod and cone photoreceptors of the salamander retina. *Journal of Neuroscience*. **20**, 929-936.

Bekkers, J. M. & Stevens, C. F. (1989) NMDA and non-NMDA receptors are co-localized at individual excitatory synapses in cultured hippocampus. *Nature*, **341**, 230-233.

Bekkers, J. M., Richerson, G. B. & Stevens, C. F. (1990) Origin of variability in quantal size in cultured hippocampal neurons and hippocampal slices. *Proceedings of the National Academy of Sciences USA*, **87**, 5359-5362.

Brandstätter, J.H., Koulen, P., Kuhn, R., van der Putten, H. & Wässle, H. (1996) Compartmental localization of a metabotropic glutamate receptor (mGluR7): two different active sites at a retinal synapse. *Journal of Neuroscience*. **16**, 4749-4756.

Byzof & Trifonov (1968) The response to electric stimulation of horizontal cells in the carp retina. *Vision Research*, **8**, 817-822.

Byzof & Trifonov (1981) Ionic mechanisms underlying the nonlinearity of horizontal cell membrane. *Vision Research*, **21**. 1573-1581.

Cartmell, J. & Schoepp, D.D. (2000) Regulation of neurotransmitter release by metabotropic glutamate receptors. *Journal of Neurochemistry*,**75**, 889-907.

Clements J. D. & Silver, R. A. (2000) Unveiling synaptic plasticity: a new graphical and analytical approach. *Trends in Neurosciences*, **23**, 105-113.

Cochilla, A.J. & Alford, S. (1998) Metabotropic glutamate receptor-mediated control of transmitter release. *Neuron*, **20**, 1007-1016.

Copenhagen, D.R. & Jahr, C. (1989) Release of endogenous excitatory amino acids from turtle photoreceptors. *Nature*, **341**, 536-539.

Del Castillo & Katz, B. (1954) Quantal components of the end-plate potential. *Journal of Physiology*, **124**, 574-585.

DeFelice, L.J. (1981) Introduction to Membrane noise, Plenum Press, New York and London.

DeVries, S.H. & Schwartz, E.A. (1999) Kainate receptors mediate synaptic transmission between

cones and 'Off' bipolar cells in a mammalian retina. *Nature*, **397**, 157-160.

De la Villa, Kurahashi, T. & Kaneko, A. (1995) L-glutamate-induced responses and cGMP-activated channels in three subtypes of retinal bipolar cells dissociated from the cat. *Journal of Neuroscience,* **15**, 3571-3582.

Diamond, J.S. & Jahr, C.E. (1995) Asynchronous release of synaptic vesicles determines the time course of the AMPA receptor-mediated EPSC. *Neuron*, **15**, 1097-1107.

Dixon, D.B. & Copenhagen, D.R. (1997) Metabotropic glutamate receptor-mediated suppression of an inward rectifier current is linked via a cGMP cascade. *Journal of Neuroscience*, **17**, 8945-8954.

Djamgoz, M.A.B. (1984) Electrophysiological characterization of the spectral sensitivities of horizontal cells in cyprinid fish retina. *Vision Research*, **24**, 1677-1687.

Djamgoz, M.B.A., Archer, S.N. & Vallerga, S, (1995) Neurobiology and Clinical Aspects of the Outer Retina. Chapman & Hall.

Dolphin, A.C. (1998). Mechanisms of modulation of voltage-dependent calcium channels by G-proteins. *Journal of Physiology,* **506**, 3-11.

Downing, J.E.G., Djamgoz, M.B.A. & Bowmaker, J.K. (1986) Photoreceptors of a cyprinid fish, the roach: morphological and spectral characteristics. *Journal of Comparative Physiology A*, **159**, 859-868.

Downing, J.E.G. & Djamgoz, M.B.A. (1989) Quantitative analysis of cone photoreceptor-horizontal cell connectivity patterns in the retina of cyprinid fish: electron microscopy of functionally identified and HRP-labelled horizontal cells. *Journal of Comparative Neurology*, **289**, 537-553.

Dowling, J.E. & Ripps, H. (1973) Effect of magnesium on horizontal cell activity in the skate retina. *Nature*, **292**, 101-103.

Edwards, F.A., Konnerth, F.A., Sakmann, B. & Takahashi, T. (1989) A thin slice preparation for patch clamp recording from neurons of the mammalian central nervous system. *Pflüger Archive*, **414**, 600-612.

Eliasof, S. & Jahr, C.E. (1997) Rapid AMPA receptor desensitization in catfish cone horizontal cells. *Visual Neuroscience*, **14**, 13-18.

Falk, G (1989) Signal transmission from rods to bipolar and horizontal cells: a synthesis. *Progress in Retinal and Eye Research*, Ed. by N. N. Osborne & J. Chader (Pergamon Press) **8**, 255-279.

Fatt, P. & Katz, B. (1952) Spontaneous subthreshold activity at motor nerve ending. *Journal of Physiology*, **117**, 109-128

Freed, M. (2000) Rate of quantal excitation to a retinal ganglion cell evoked by sensory input. *Journal of Neurophysiology*, **83**, 2956-2966.

Frerking, M. & Nicoll, R.A. (2000) Synaptic kainate receptors. *Current Opinion in Neurobiology,* **10**, 342-351.

Furukawa, T., Yamada, M., Petruv, R., Djamgoz, M.B.A. & Yasui, S. (1997) Nitric oxide,

2-amino-4-phosphonobutyric acid and light/dark adaptation modulate short-wavelength-sensitive synaptic transmission to retinal horizontal cells. *Neuroscience Research*, **27**, 65-74.

Geiger, J.R.P., Melcher, T., Koh, D.S., Sakmann, B., Seeburg, P.H., Jonas, P. & Monyer, H. (1995) Relative abundance of subunit mRNAs determines gating and Ca^{2+}permeability of AMPA receptors in principal neurons and interneurons in rat CNS. *Neuron*, **15**, 193-204.

Grant, G.B. & Werblin, F.S. (1996) A glutamate-elicited chloride current with transporter-like properties in rod photoreceptors of the tiger salamander. *Visual Neuroscience*, **13**, 135-144.

Gray, E.G. & Pease, H.L. (1971) On understanding the organization of the retinal receptor synapses. *Brain Research*, **35**, 1-15.

Glavinovic, M.I. & Rabie, H.R. (1998). Monte Carlo simulation of spontaneous miniature excitatory postsynaptic currents in rat hippocampal synapse in the presence and absence of desensitization. *Pflüger Archive*, **435**, 193-202.

Hare, W.A. & Owen, W.G. (1992) Effects of 2-amino-4-phosphonobutyric acid on cells in the distal layers of the tiger salamander's retina. *Journal of Physiology*, **445**, 741-757.

Haverkamp, S., Grünert, U. & Wässele, H. (2000) The cone pedicle, a complex synapse in the retina. *Neuron*, **27**, 85-95.

Hirasawa, H., Shiells, R.A. & Yamada, M. (2001). Analysis of spontaneous EPSCs in retinal horizontal cells of the carp. *Neuroscience Research (in press)*.

Hayashi, Y., Momiyama, A., Takahashi, T., Oishi, H., Ogawa-Meguro, R., Shigemoto, R., Mizuno, N. & Nakanishi, S. (1993) Role of metabotropic glutamate receptor in synaptic modulation in the accessory olfactory bulb. *Nature*, **366**, 687-690.

Hollmann, M. & Heinemann, S. (1994) Cloned glutamate receptors. *Annulal Review of Neuroscience*, **17**, 31-108.

Ishida, A.T., Kaneko, A. & Tachibana, M. (1984) Responses of solitary retinal horizontal cells from Carassius auratus to L-glutamate and related amino acids. *Journal of Physiology*, **358**, 169-182.

Ishida, A.T. & Neyton, J. (1985) Quisqualate and L-glutamate inhibit retinal horizontal-cell responses to kainate. *Proceedings of the National Academy of Sciences USA*, **82**, 1837-1841.

Jones, M.V. & Westbrook, G.L. (1996) The impact of receptor desensitization on fast synaptic transmission. *Trends in Neuroscience*, **19**, 96-101.

Juusola, M., French, A. S., Uusitalo, R. O. & Weckström, M. (1996) Information processing by graded-potential transmission through tonically active synapses. *Trends in Neurosciences*, **19**, 292-297.

Knapp, A.G. & Dowling, J.E. (1987) Dopamine enhances excitatory amino acid-gated conductances in cultured retinal horizontal cells. *Nature*, **325**, 437-9.

Kandel, E. R., Schwartz, J.H. & Jessell, T. M. (1991) Principles of Neural Science, 3rd edition. Norwalk, CT: Appleton and Lange.

Kaneko, A. & Shimazaki, H. (1975) Effects of external ions on the synaptic transmission from photoreceptors to horizontal cells in the carp retina. *Journal of Physiology*, **252**, 509-522.

Kaneko, A. & Tachibana, M. (1985) Electrophysiological measurement of the spectral sensitivity of three types of cones in the carp retina. *Japanese Journal of Physiology*. **35**, 355-365.

Kaneko, A. & Yamada, M. (1972) S-potentials in the dark-adapted retina of the carp. *Journal of Physiology*, **227**, 261-273.

Knöpfel, T., Lukic, S., Leonard, T., Flor, P.J., Kuhn, R. & Gasparini, F. (1995) Pharmacological characterization of MCCG and MAP4 at the mGluR1b, mGluR2 and mGluR4a human metabotropic glutamate receptor subtypes. *Neuropharmacology*, **34**, 1099-1102.

Koike, M., Tsukada, S., Tsuzuki, K., Kijima, H. & Ozawa, S. 2000. Regulation of kinetic properties of GluR2 AMPA receptor channels by alternative splicing. *Journal of Neuroscience*, **20**, 2166-2174.

Koulen, P., Kuhn, R., Wässele, H. & Brandstatter, J.H. (1999) Modulation of intracellular calcium concentration in photoreceptor terminals by a presynaptic metabotropic glutamate receptor. *Proceedings of the National Academy of Sciences USA*, **96**, 9909-9914.

Lasater, E.M. & Dowling, J.F. (1982) Carp horizontal cells in culture respond selectivity to L-glutamate and its agonists. *Proceedings of the National Academy of Sciences USA*, **79**, 936-940.

Lasater, E.M. (1990) Properties of non-NMDA excitatory amino acid-activated channels in isolated retinal horizontal cells. *Journal of Neuroscience*, **10**, 1654-1663.

Linn, C.L. & Gafka, A.C. (1999) Activation of metabotropic glutamate receptors Modulates the voltage-gated sustained calcium current in a teleost horizontal cell. *Journal of Neurophysiology*, **81**, 425-434.

Low, J.C., Yamada, M. & Djamgoz, M.B.A. (1991) Voltage clamp study of electrophysiologically-identified horizontal cells in carp retina. *Vision Research*, **31**, 437-449.

Lu, T., Shen, Y. & Yang, X-L. (1998) Desensitization of AMPA receptors on horizontal cells isolated from crucian carp retina. *Neuroscience Research*, **31**, 123-135.

Maple, B.R., Werblin, F.S. & Wu, S.M. (1994) Miniature excitatory postsynaptic currents in bipolar cells of the tiger salamander retina. *Vision Research*, **34**, 2357-2362.

Matsumura, M., Okinami, S. & Ohkuma, M. (1981) Synaptic vesicle exocytosis in goldfish photoreceptor cells. *Albrecht von Graefes Arch Klin Ophthalmol*, **215**, 159-170.

Miyachi, E-I. & Murakami, M. (1989) Decoupling of horizontal cells in carp and turtle retinae by intracellular injection of cAMP. *Journal of Physiology*, **419**, 213-224.

Morgans, C. W., Brandstätter, J.H., Kellerman, J., Kuhn, R., Betz, H. & Wässle, H. (1996) A SNARE complex containing syntaxin 3 is present in ribbon synapses of the retina. *Journal*

of Neuroscience, **16**, 6713-6721.

Morgans, C. W. (2000) Neurotransmitter release at ribbon synapses in the retina. *Immunology and Cell Biology*, **78**, 442-446.

Murakami, M., Ohtsu, K, & Otsuka, T. (1972) Effects of chemicals on receptors and horizontal cells in the retina. *Journal of Physiology*, **227**, 899-913.

Nakajima, Y., Iwakabe, H., Akazawa, C., Nawa, H., Shigemoto, R., Mizuno, N. & Nakanishi, S. (1993). Molecular characterization of a novel retinal metabotropic glutamate receptor mGluR6 with a high agonist selectivity for L-2-amino-4-phosphonobutyrate. *Journal of Biological Chemistry,* **268**, 11868-11873

Nawy, S., Sie, A. & Copenhagen, D.R. (1989) The glutamate analog 2-amino-4- phosphonobutyrate antagonizes synaptic transmission from cones to horizontal cells in the goldfish retina. *Proceedings of the National Academy of Sciences USA*, **86**, 1726-1730.

Nawy, S.& Jahr, C.E. (1990) Suppression by glutamate of cGMP-activated conductance in retinal bipolar cells. *Nature*, **325**, 967-972.

Neher, E. & Sakaba, T. (2001) Combining deconvolution and noise analysis for the estimation of transmitter release rates at the calyx of held. *Journal of Neuroscience*, **21**, 444-461.

O'Dell, T.J. & Christensen, B.G. (1989) Horizontal cells isolated from catfish retina contain two types of excitatory amino acid receptors. *Journal of Neurophysiology*, **61**, 1097-1109.

Paternain, A., Morales, M. & Lerma, J. (1995) Selective antagonism of AMPA receptors unmasks kainate receptor-mediated responses in hippocampal neurons. *Neuron,* **14**, 185-189.

Paulsen, O. & Heggelund, P. (1994) The quantal size at retinogeniculate synapses determined from spontaneous and evoked EPSCs in guinea-pig thalamic slices. *Journal of Physiology*, **480**, 505-511.

Pérez-Armendariz, M., Roy, C., Spray, D.C. & Bennett, M.V.L., (1991). Biophysical properties of gap junctions between freshly dispersed pairs of mouse pancreatic beta cells. *Biophysical Journal*, **59**, 76-92.

Reike, F. & Schwartz, E.A. (1996) Asynchronous transmitter release: control of exocytosis and endcytosis at the salamander rod synapse. *Journal of Physiology*, **493**, 1-8.

Saito, T., Kujiraoka, T., Yonaha, T. & Chino, Y. (1985) Reexamination of photoreceptor-bipolar connectivity patterns in carp retina: HRP-EM and golgi-EM studies. *Journal of Comparative Neurology*, **236**, 141-160.

Sarantis, M., Everett, K. & Attwell, D. (1988) A presynaptic action of glutamate at the cone output synapse. *Nature*, **332**, 451-453.

Saugstad, J.A., Kinzie, J.M., Shinohara, M.M., Segerson, T.P. & Westbrook, G.L. (1997) Cloning and expression of rat metabotropic glutamate receptor 8 reveals an distinct pharmacological profile. *Molecular Pharmacology*, **51**, 119-125.

Savchenko, A., Barnes, S. & Kraner, R. (1997) Cyclic-nucleotide-gated channels mediate synaptic feedback by nitric oxide. *Nature*, **390**, 694-698.

Scanziani, M., Gahwiler, B.H. & Thompson, S.M. (1995) Presynaptic inhibition of excitatory synaptic transmission by muscarinic and metabotropic glutamate receptor activation in th hippocampus : are Ca^{2+} channels involved? *Neuropharmacology*, **34**, 1549-1557.

Segal, J.R., Ceccarelli, B., Fesce, R. & Hurlbut, W.P. (1985) Miniature endplate potential frequency and amplitude determined by an extension of Campbell's theorem. *Biophysical Journal*, **47**, 183-202.

Schmitzt, F., Königstorfer, A. & Südhof, T.C. (2000) RIBEYE, a component of synaptic ribbons: A protein's journey through evolution provides insight into synaptic ribbon function. *Neuron*, **28**, 857-872.

Schmidt, K.F., Kruse, M. & Hatt, H. (1994) Dopamine alters glutamate receptor desensitization in retinal horizontal cells of perch (*Perca fluviatilis*). *Proceedings of the National Academy of Sciences USA*, **91**, 8288-8291.

Schmitt, K.F. (1997) Properties of glutamate-gated ion channels in horizontal cells of the perch retina. *Vision Research*, **37**, 2023-2028.

Shen, Y., Lu, T. & Yang, X.-L. (1999) Modulation of desensitization at glutamate receptors in isolated crucian carp horizontal cells by concanavalin A, cyclothiazide, aniracetam and PEPA. *Neuroscience*, **89**, 979-990.

Shiells, R.A., Falk, G. & Naghshineh, S. (1981) Action of glutamate and aspartate analogues on rod horizontal and bipolar cells. *Nature*, **294**, 592-594.

Shiells, R.A., Falk, G. & Naghshineh, S. (1986) Ionophoretic study of the action of excitatory amino acids on rod horizontal cells of the dogfish retina. *Proceedings of the Royal Society of London B*, **227**, 121-135.

Shiells, R.A. & Falk, G. (1990) Glutamate receptors of rod bipolar cells are linked to a cyclic GMP cascade via a G-protein. *Proceedings of the Royal Society of London B*, **242**, 91-94.

Shiells, R.A. (1994) Glutamate receptors for signal amplification. *Current Biology,* **4**, 917-918.

Shiells, R.A. & Falk, G. (1994) Responses of rod bipolar cells isolated from dogfish retinal slices to concentration-jumps of glutamate. *Visual Neuroscience*, **11**, 1175-1183.

Shiells, R.A. & Falk, G. (1995) Signal transduction in retinal bipolar cells. *Progress in Retinal and Eye Research*, Ed. by N. N. Osborne & J. Chader (Pergamon Press) **14**, 223-247.

Shiells, R.A. & Falk, G. (2000) Activation of Ca^{2+}-calmodulin kinase II induces desensitization by background light in dogfish retinal 'on' bipolar cells. *Journal of Physiology*, **528**, 327-338.

Silver, R.A., Traynelis, S. F. & Cull-Candy, S.G. (1992) Rapid-time-course miniature and evoked excitatory currents at celebellar synapses *in situ*. *Nature*, **355**, 163-166.

Silver, R.A., Colquhoun, D., Cull-Candy, S.G. & Edmonds, B. (1996) Deactivation and desensitization of non-NMDA receptors in patches and the time course of EPSCs in rat cerebellar granule cells. *Journal of Physiology*, **493**, 167-173.

Sladeczek, F., Momiyama, A. & Takahashi, T. (1993) Presynaptic inhibitory action of a

metabotropic glutamate receptor agonist on excitatory transmission in visual cortical neurons. *Proceedings of the Royal Society of London B*, **242**, 297-303.

Spruston, N., Jaffe, D.B., Williams, S.H. & Johnston, D., 1993. Voltage- and space-clamp errors associated with the measurement of electrotonically remote synaptic events. *Journal of Neurophysiology*, **70**, 781-802.

Stell, W.K., Lighthood, D.P., Wheeler, T.G. & Leeper, H.F. (1975) Goldfish retina; functional polarization of cone horizontal cell dendrites and synapses. *Science*, **190**, 989-990.

Tachibana, M. (1985) Permeability changes induced by l-glutamate in solitary retinal horizontal cells isolated from Carassius auratus. *Journal of Physiology*, **358**, 153-167.

Tachibana, M. & Kaneko, A. (1988) L-glutamate-induced depolarization in solitary photoreceptors: A process that may contribute to the interaction between photoreceptors *in situ*. *Proceedings of the National Academy of Sciences USA*, **85**, 5315-5319.

Takahashi, K.-I. & Copenhagen, D.R. (1992) APB suppresses synaptic input to retinal horizontal cells in fish : a direct action on horizontal cells modulated by intracellular pH. *Journal of Neurophysiology*, **67**, 1633-1642.

Takahashi, T., Forsythe, I.D., Tsujimoto, T., Barnes-Davies, M. & Onodera, K. (1996) Presynaptic calcium current modulation by a matabotropic glutamate receptor. *Science*, **274**, 594-597.

Thoreson, W.B., Gottesman, J., Jane, D.E., Tse H-W., Watkins, J.C. & Miller, R.F. (1997) Two phenylglycine derivatives antgonize responses to L-AP4 in On bipolar cells of the amphibian retina. *Neuropharmacology*, **36**, 13-20.

Tomita, T., Kanako, A., Murakami, M. & Pautler, E.L. (1967) Spectral sensitivity curves of single cones of carp. *Vision Research*, **7**, 519-531.

Tomita, T. (1970) Electrical activity of vertebrate photoreceptors. *Quarterly Reviews of Biophysics*, **3**, 179-222.

Tong, G. & Jahr, C.E. (1994) Multivesicular release from excitatory synapses of cultured hippocampal neurons. *Neuron*, **12**, 51-59.

Trifonov, Y.A. (1968) Study of synaptic transmission between photoreceptors and horizontal cells by means of electrical stimulation in the retina, *Biofizica*, **13**, 809-817.

Vaney, D.I., Nelson, J.C. & Pow, D.V. (1998) Neurotransmitter coupling through gap junctions in the retina. *Journal of Neuroscience*, **18**, 10594-10602.

Vardi, N., Duvoisin, R., Wu, G. & Sterling, P. (2000). Localization of mGluR6 to dendrites of ON bipolar cells in primate retina. *Journal of Comparative Neurology*, **423**, 402-412.

Verweij, J., Kamermans, M. & Spekreijse, H. (1996) Horizontal cells feed back to cones by shifting the cone calcium-current activation range. *Vision Research*, **36**, 3943-3953.

Yamada, K.A. & Tang, C-M. (1993) Benzothiadiazides inhibit rapid glutamate receptor desensitization and enhance glutamatergic synaptic currents. *Journal of Neuroscience*, **13**, 3904-3915.

Yamada, M., Fraser, S.P., Furukawa, T., Hirasawa, H., Katano, K., Djamgoz, M.B.A. & Yasui, S.

(1999) Effects of nitric oxide, light adaptation and APB on spectral characteristics of H1 horizontal cells in carp retina. *Neuroscience Research*, **35**, 309-319.

Yamada, M., Low, J.C. & Djamgoz, M.B.A. (1992) Chromaticity of synaptic inputs to H1 horizontal cells in carp retina: analysis by voltage-clamp and spectral adaptation. *Experimental Brain Research*, **89**, 465-472.

Yamada, M. & Yasui, S. (1988) Measurement of DC and AC spectral sensitivities of retinal horizontal cells by "voltage clamp by light". *Journal of Neuroscience Methods*, **24**, 65-72.

Yang, J.H., Maple, B., Gao, F., Maguire, G. & Wu, S. (1998) Postsynaptic responses of horizontal cells in the tiger salamander retina are mediated by AMPA-preferring receptors. *Brain Research*, **797**, 125-134.

Yasui, S. & Yamada, M. (1989) H1 horizontal cells of carp retina have different postsynaptic mechanisms to mediate short- versus long-wavelength visual signals. *Experimantal Brain Research*, **74**, 256-262.

Yasui, S., Yamada, M. & Djamgoz, M.B.A. (1990) Dopamine and 2-amino-4- phosphonobutyrate differentially affect spectral responses of H1 horizontal cells in carp retina. *Experimental Brain Research*, **83**, 79-84.

Wang, M.Y., Rampil, I.J. & Kendig, J.J. (1999) Ethanol directly depresses AMPA and NMDA glutamate currents in spinal cord motor neurons independent of actions on GABA A or glycine receptors. *Journal of Pharmacology and Experimental Therapeutics*, **290**, 362-367.

Werblin, F.S. (1978) Transmission along and between rods in the tiger salamander retina. *Journal of Physiology*, **280**, 449-470.

Wu, L.G. & Saggau, P. (1997) Presynaptic inhibition of elicited neurotransmitter release. *Trends in Neurosciences*, **20**, 204-212.

Wu, S.M., Gao, F. & Maple, B.R. (2000) Functional architecture of synapses in the inner retina: Segregation of visual signals by stratification of bipolar cell axon terminals. *Journal of Neuroscience*, **15**, 4462-4470.

Figures

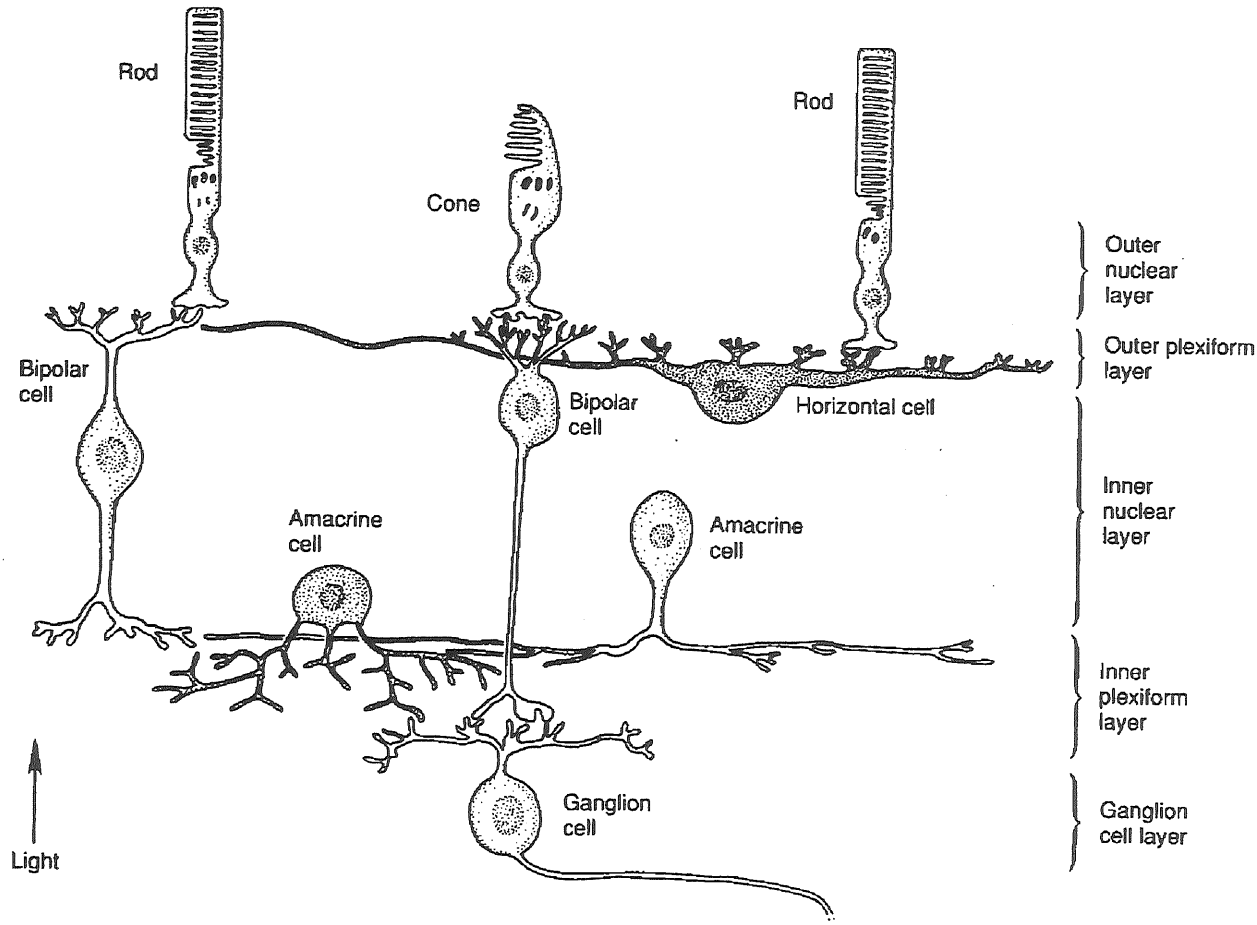

Figure 1.1 Schematic diagram of retinal circuitry. The retina posses five major classes of neurons arranged into three nuclear layers: photoreceptor cells (rods and cones), bipolar cells, horizontal cells, amacrine cells, and ganglion cells. Photoreceptor, bipolar and horizontal cells make synaptic connections with each other in the outer plexiform layer. The bipolar, amacrine and ganglion cells make synaptic contact in the inner plexiform layer. Information flows vertically from photoreceptors to ganglion cells via bipolar cells. Information also flows laterally, mediated by horizontal cells in the outer plexiform layer and amacrine cells in the plexiform layer. (Modified from Kandel et al., Principles of Neural Science, 3rd edition. Norwalk, CT: Appleton and Lange, 1991)

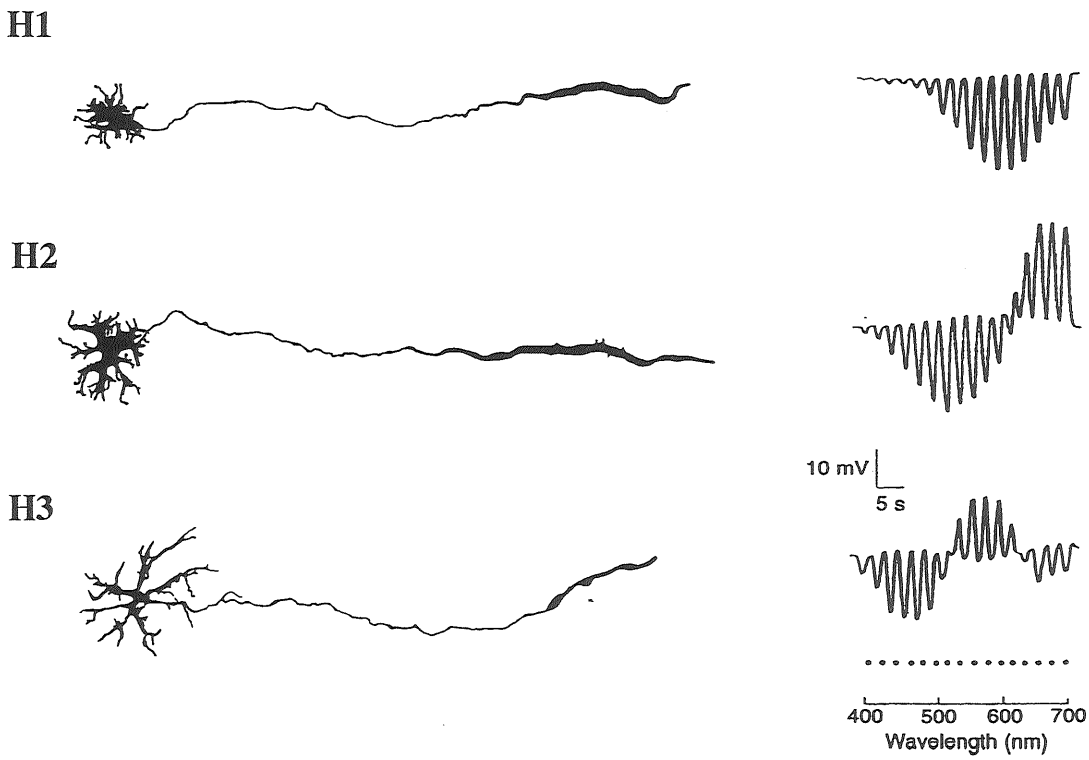

Figure 1.2 Three types of cone-driven Horizontal cells of the fish retina. Left: whole mount view of cone-driven HCs of the goldfish. Right: light–evoked responses of HCs in the retina of the cyprinid fish (roach), showing cone-driven activity. (top) luminosity (H1); (middle) biphasic chromacity type (H2); (bottom) triphasic chromaticity type (H3), all driven by cones with no rod input. Sixteen different spectral stimuli (20 nm intervals) of near-equal quantum content were presented in sequence (dots at right bottom of the figure) to cover the spectral range from 400 nm to 700 nm. (Modified from Djamgoz et al., Neurobiology and Clinical Aspects of the Outer Retina. Chapman & Hall, 1995)

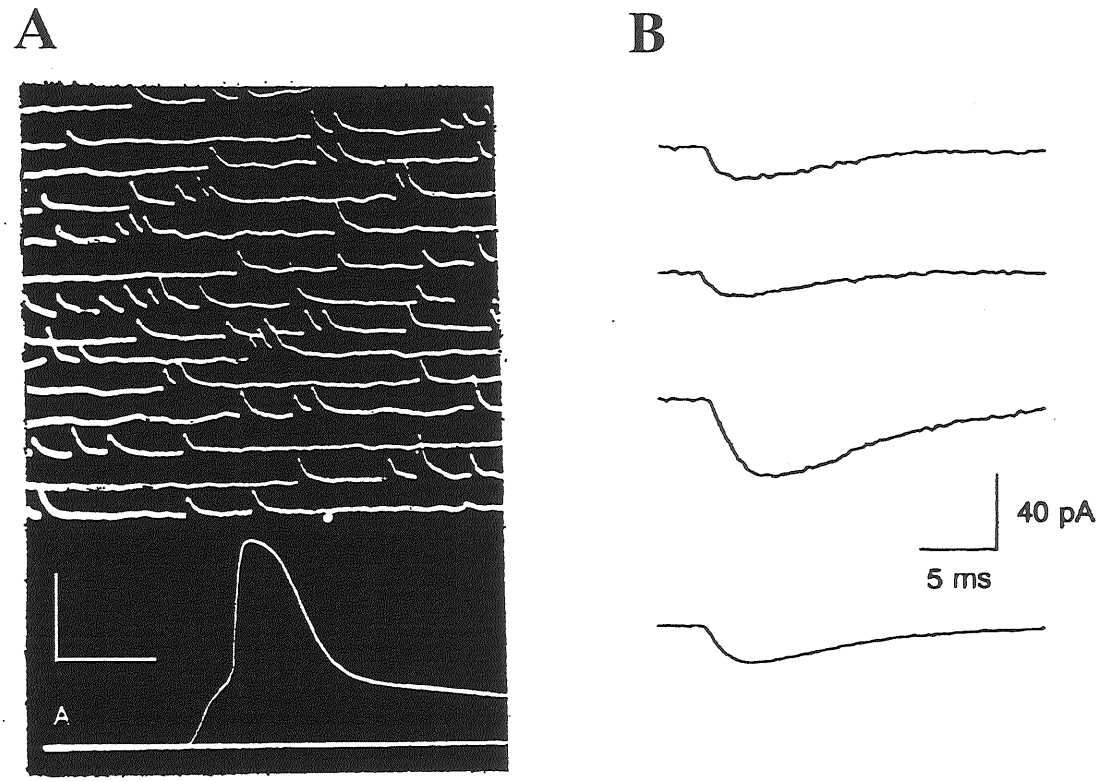

Figure 1.3 Miniature synaptic events recorded from muscle fiber endplate (A) and hippocampal neurons (B).

A. Intracellular recording of spontaneous miniature end-plate potentials (mEPPs) in the muscle fiber. Upper portions were recorded at low speed and high amplification (calibrations 3.6 mV and 46 ms): mEPPs show the localized spontaneous activity at the junctional region. Lower records show the electric response to a nerve impulse, taken at high speed and lower gain (calibrations 50 mV and 2 ms). The stimulus was applied to the nerve at the beginning of the trace. (Modified from Fatt & Katz, 1952)

B. Patch-clamp recording of miniature excitatory postsynaptic currents (mEPSCs) in the hippocampal slice. Three individual mEPSCs (top three traces) and the average of 12 such mEPSCs (bottom trace). (Modified from Bekkers et al., 1990)

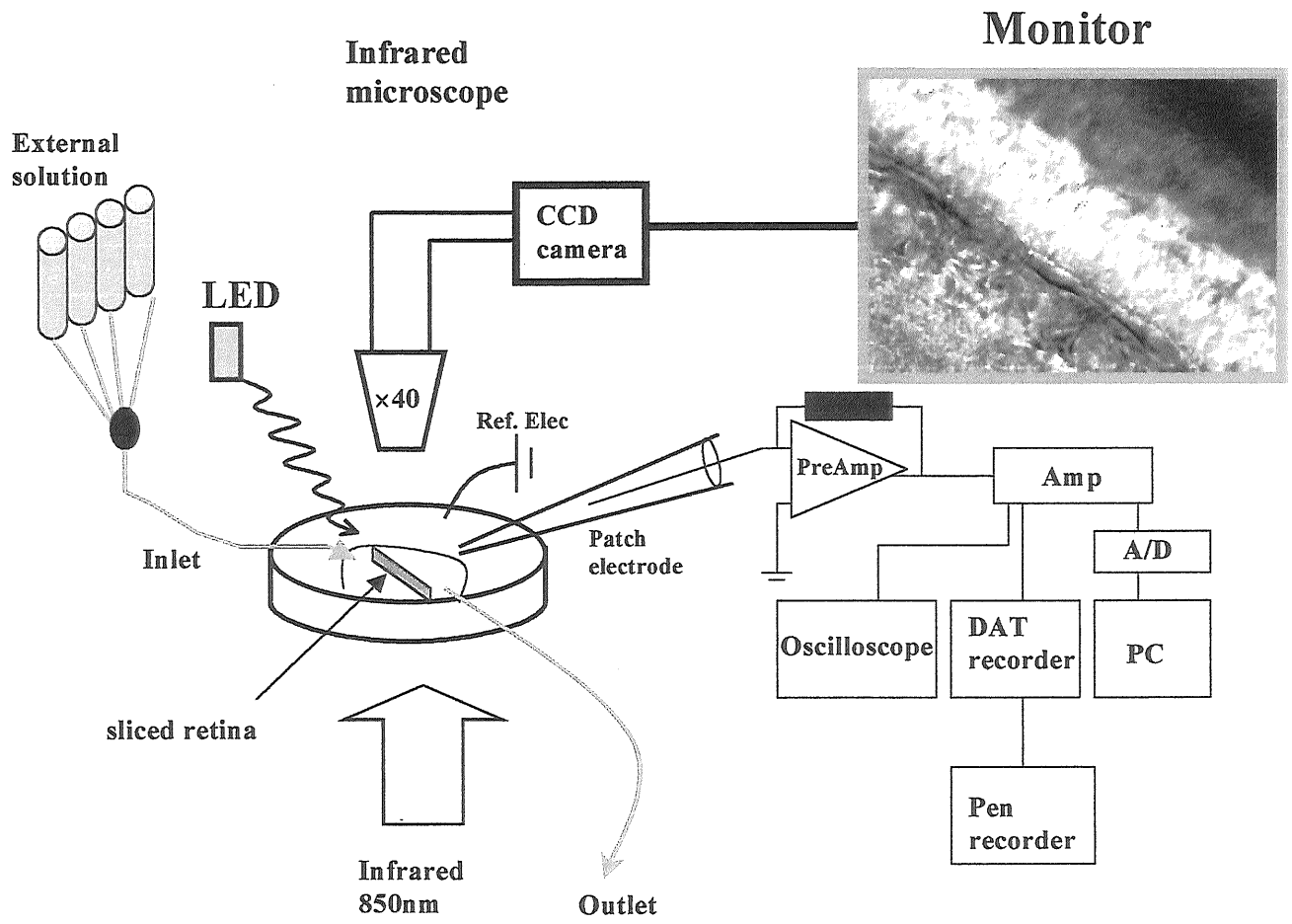

Figure 2.1 Schematic diagram of whole-cell patch-clamp recording systems.

Sliced retina was monitored by an infrared microscope, and perfused with external solution gravity fed from an inlet tube (Inlet). The solution was flowed out from an outlet tube (outlet). Whole cell current recorded by a patch electrode was amplified by a patch clamp amplifier (Amp), and stored in a DAT recorder or a personal computer (PC). The sliced retina was illuminated with red- and blue-diffuse light emitting diodes (LED's). A reference electrode (Ref. Elec) was connected to the bath solution.

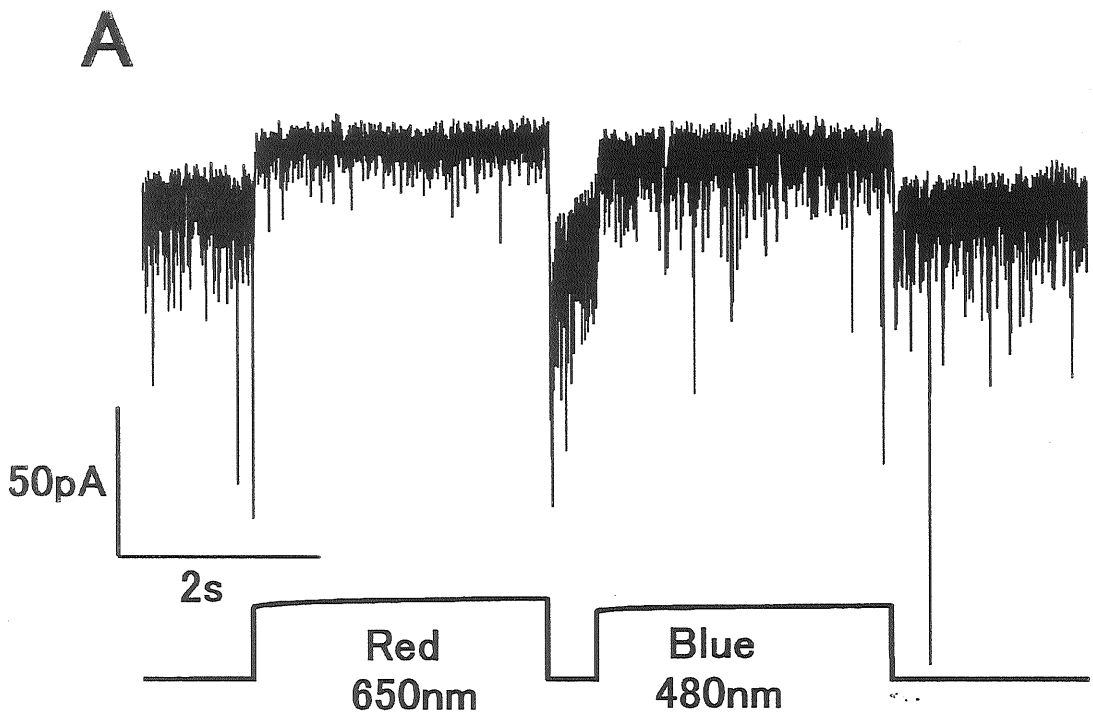
A
50pA
2s
Red
650nm
Blue
480nm

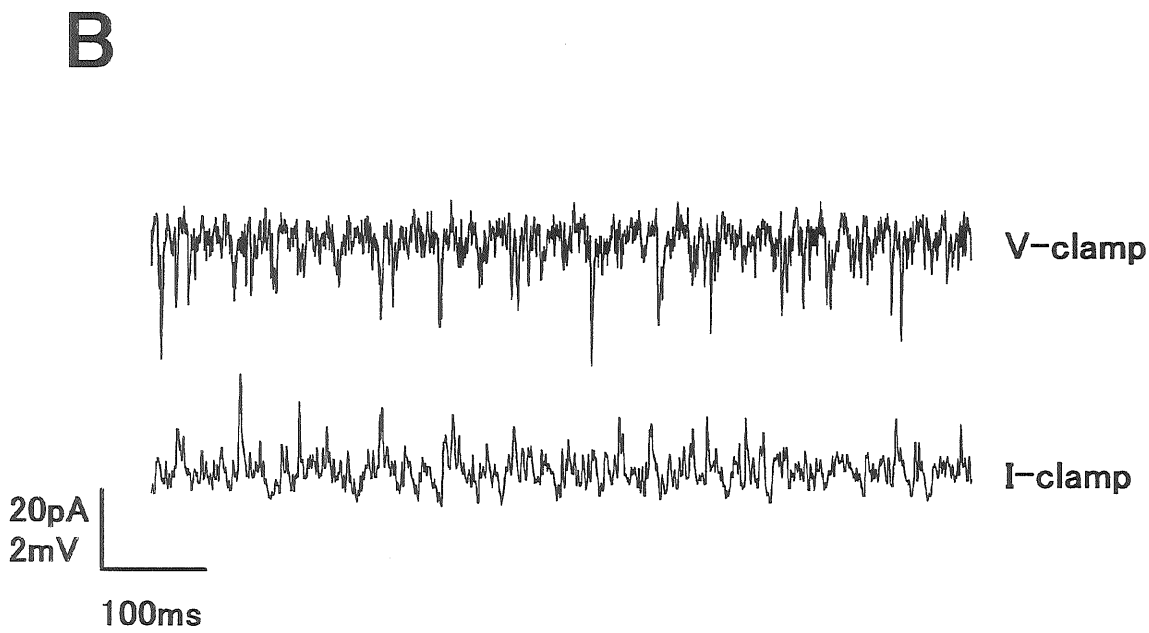
B
V-clamp
I-clamp
20pA
2mV
100ms

Figure 2.2 Light-induced currents from an H1 type horizontal cell (H1 cell) recorded in whole cell mode from carp retinal slice.

A. Current response accompanied with spontaneous rapid inward transients from the cell. The intensity of red and blue light stimuli was adjusted to elicit the same DC amplitudes of outward current. Red and blue light intensities were 5.6×10^5 and 6.2×10^5 quanta/μm^2/s, respectively. Holding potential was –40 mV.

B. The reduction of spontaneous responses by switching from voltage clamp mode to current clamp mode in darkness. Upper trace: The current trace in voltage clamp mode with a holding potential at –49 mV. Lower trace: The voltage trace in current clamp mode with a resting potential at –39 mV.

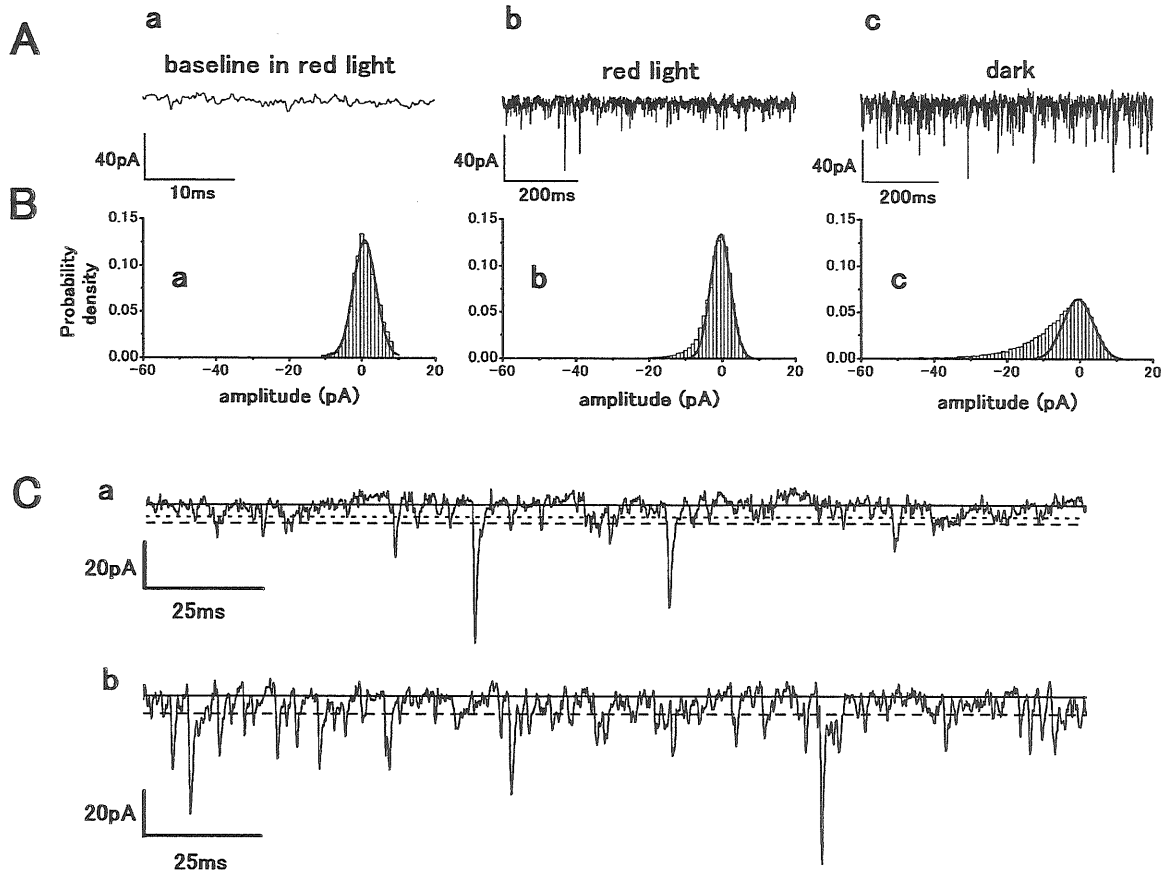

Figure 2.3 Isolation of spontaneous EPSCs (sEPSCs) from baseline noise in an H1 cell of retinal slice.

A. Baseline noise of the cell (a) compared with the cell's sEPSCs recorded under red light stimulation (b) and in darkness (c). Red light intensity was 5.6×10^5 quanta/μm^2/s. Holding potential was –40 mV. Sampling frequency for digitization was 8 kHz.

B. The probability density histograms obtained from current traces in *A*. Zero current level of distribution was set at the point of the maximum of the probability density function. (a) The histogram without sEPSCs shown in *Aa*. Thick line in the histogram: a Gaussian (standard deviation σ = 3.0 pA) chosen to fit the probability density. (b) The histogram of the current trace in red light shown in *Ab*. Thick line in the histogram: a Gaussian (σ = 2.7 pA) chosen to fit the right half of the probability density, considered as the distribution of baseline noise. (c) The histogram from the current trace in darkness shown in *Ac*. Thick line in the histogram: a Gaussian (σ = 4.1 pA) chosen to fit the right half of the probability density, considered as the distribution of baseline noise.

C. Fast sweep current recording with criterion level. (a) The current trace in red light obtained from *Ab*. The thin dotted line: 2 times standard deviation of baseline noise in red light (5.4 pA : from histogram of *Bb*). Thick dashed line: 2 times standard deviation of baseline noise in darkness (8.2 pA : from histogram of *Bc*). (b) The current trace in darkness obtained from *Ac*. The continuous line indicates zero current level. sEPSCs overlapping with the previous sEPSCs were not counted for amplitude measurement, even if they exceeded the criterion level.

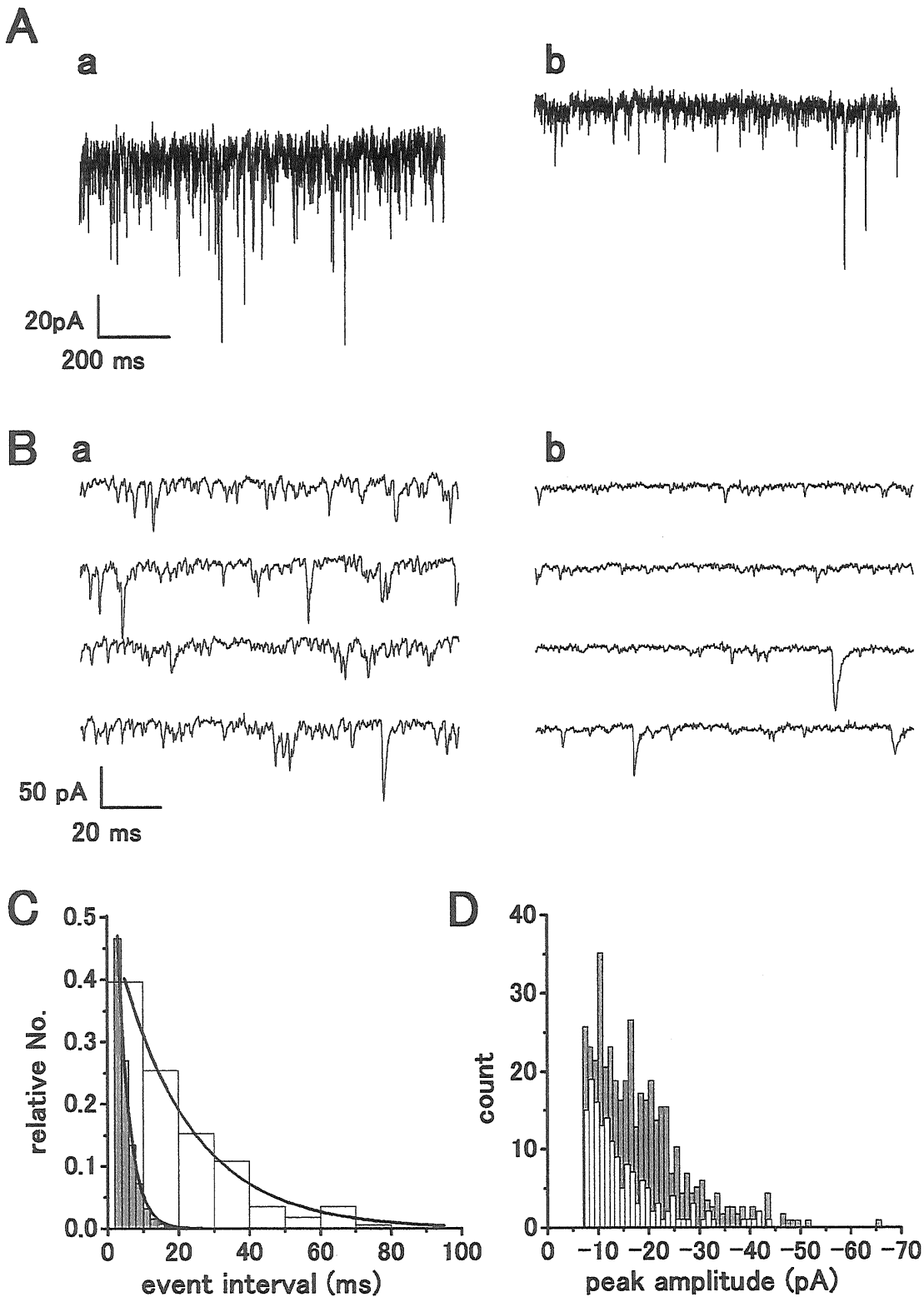
A
a
b
20pA
200 ms
B
a
b
50 pA
20 ms
C
relative No.
0.5
0.4
0.3
0.2
0.1
0.0
0
20
40
60
80
100
event interval (ms)
D
count
40
30
20
10
0
0
−10
−20
−30
−40
−50
−60
−70
peak amplitude (pA)

Figure 2.4 Red light induced suppression of sEPSCs of an H1 cell in retinal slice compared with those in darkness.

A. EPSCs recorded in darkness (a) and under red light stimulation (5.6×10^5 quanta/μm^2/s) (b). The cell was voltage clamped at –40 mV. The red light suppressed the frequency of EPSCs and elicited an outward current of 20 pA.

B. Fast sweep recordings of the current in darkness (a) and under red light (b) shown in *A*.

C. Event interval histograms of the sEPSCs of an H1 cell with holding potential at –40 mV. The filled (2 ms bins) and the open (10 ms bins) columns show the histograms in darkness and red light, respectively. The event interval histograms were fitted by single exponential curves. The mean intervals corresponding to the time constants were 3.2 ms in darkness (n = 544) and 20.3 ms in red light (n = 177), which represent 313 and 49.3 Hz of frequency, respectively.

D. Peak amplitude histograms of sEPSCs of the H1 cell in *C* in darkness (filled) and in red light (open columns). Mean peak amplitudes in darkness (n=488) and in red light (n=159) were 22.8 and 16.9 pA, which yield conductance changes 570 and 423 pS, respectively.

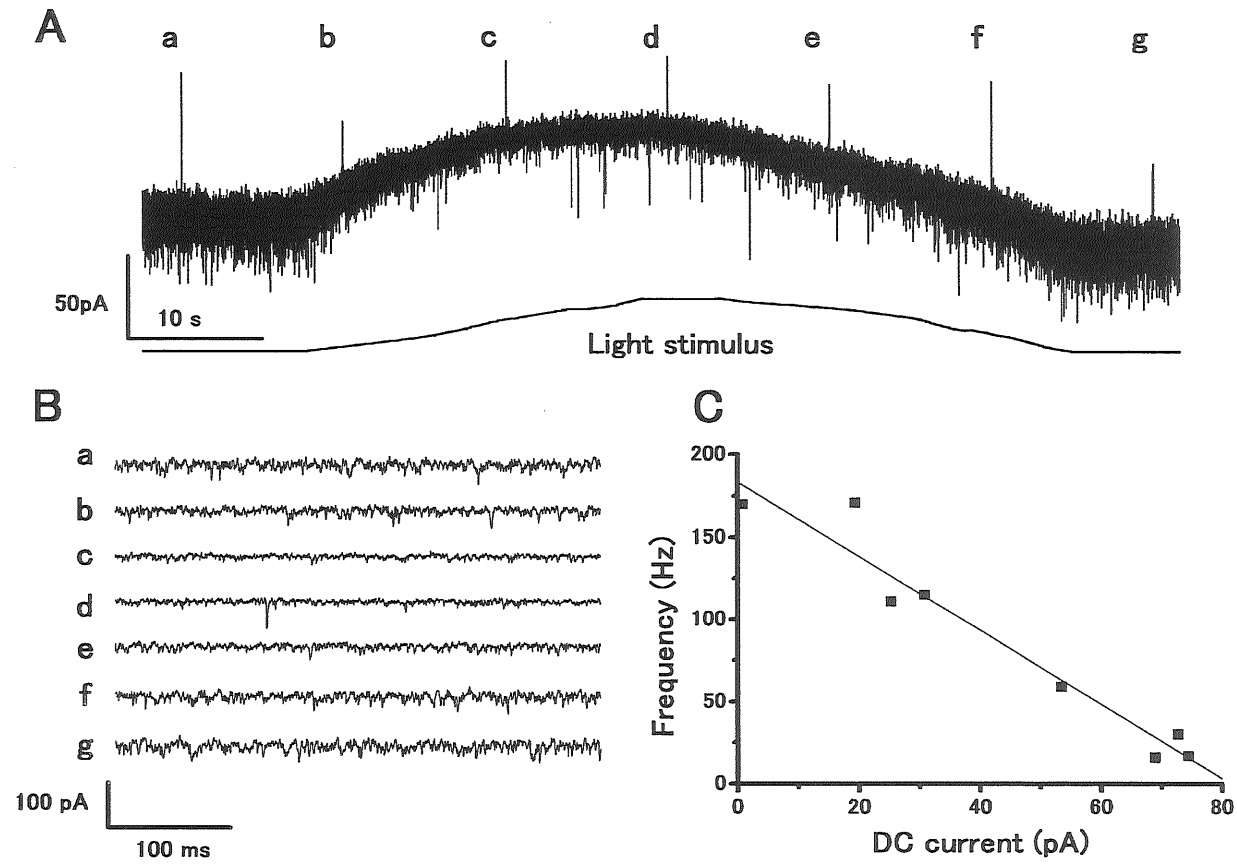

Figure 2.5 Suppression of sEPSCs of an H1 cell by ramp modulation of red light intensity.

A. Upper trace: the gradual change of the outward current in the H1 cell induced by red light. Lower trace: the voltage applied to the red LED (light output was approximately linear with voltage). The maximum light intensity was 6.3×10^5 quanta/μm^2/s. Holding potential: -70 mV. The standard deviation of baseline noise in darkness was 7.0 pA.

B. Fast sweep recordings of the sEPSCs at several time points shown in *A*.

C. Frequency of sEPSCs plotted against outward current, measured from the dark level, induced by red light. The correlation coefficient for the frequency of sEPSCs and outward current was -0.97. The holding potential: -70 mV.

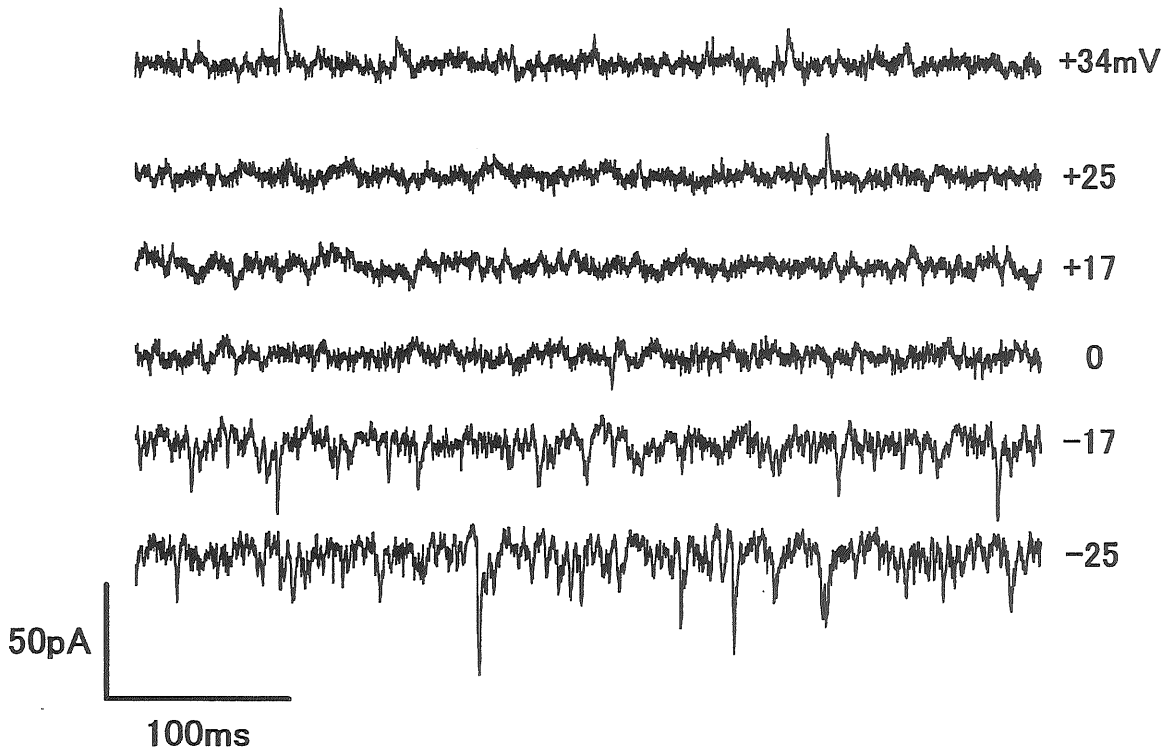

Figure 2.6 The reversal potential of sEPSCs of an H1 cell in retinal slice.

sEPSCs recorded at various holding potentials in darkness (-25, -17, 0, +17, +25 and +34mV). Correction of the holding potential was made by using series resistance compensation. The polarity of sEPSCs was reversed at around 0 mV.

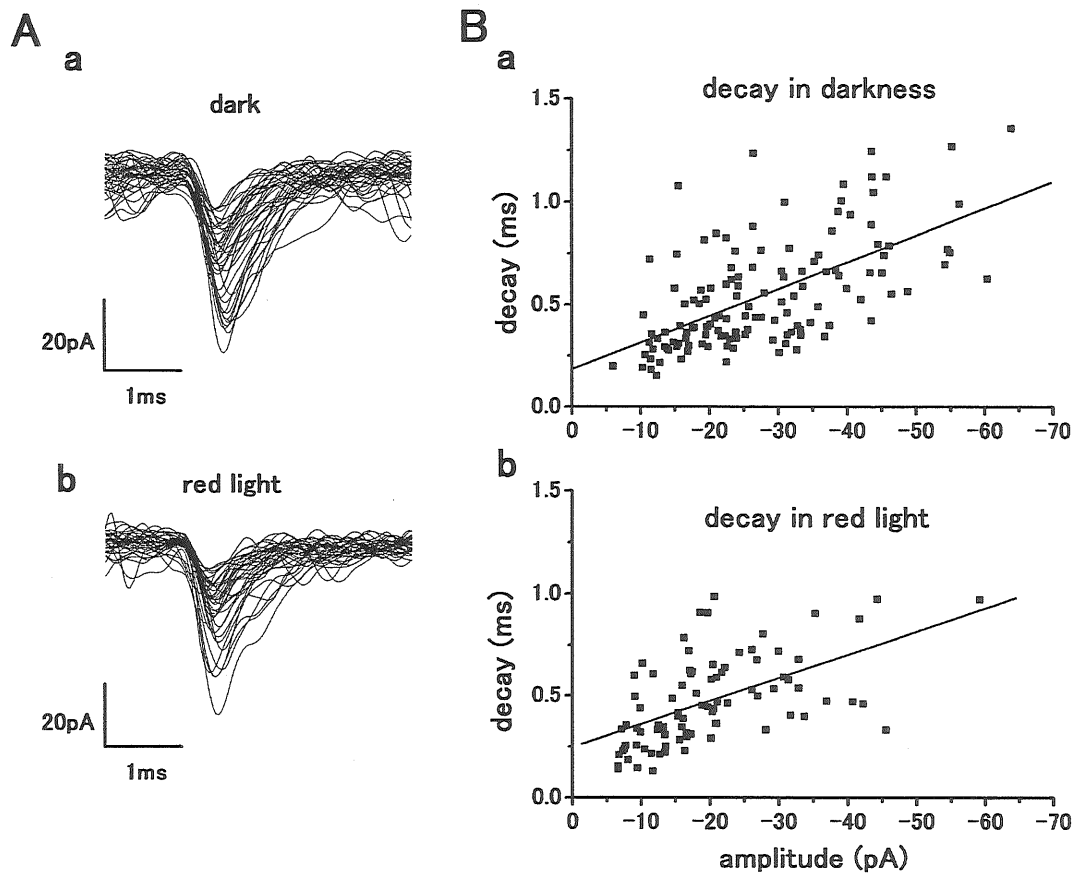

Figure 2.7 Kinetics of sEPSCs of H1 cells in darkness and under red light.

A. (a) Superimposed traces of 42 sEPSCs in darkness in an H1 cell. (b) Superimposed traces of 39 sEPSCs remained under red light.

B. (a) Plot of decay time and peak amplitude of 132 sEPSCs obtained in darkness. A solid line shows the linear fit. Correlation coefficient for decay time and peak amplitude was 0.61. (b) Plot of decay time and peak amplitude of 87 sEPSCs obtained under red light. Correlation coefficient for decay time and peak amplitude was 0.56. There was no significant difference between the decay time constants in darkness and under red light.

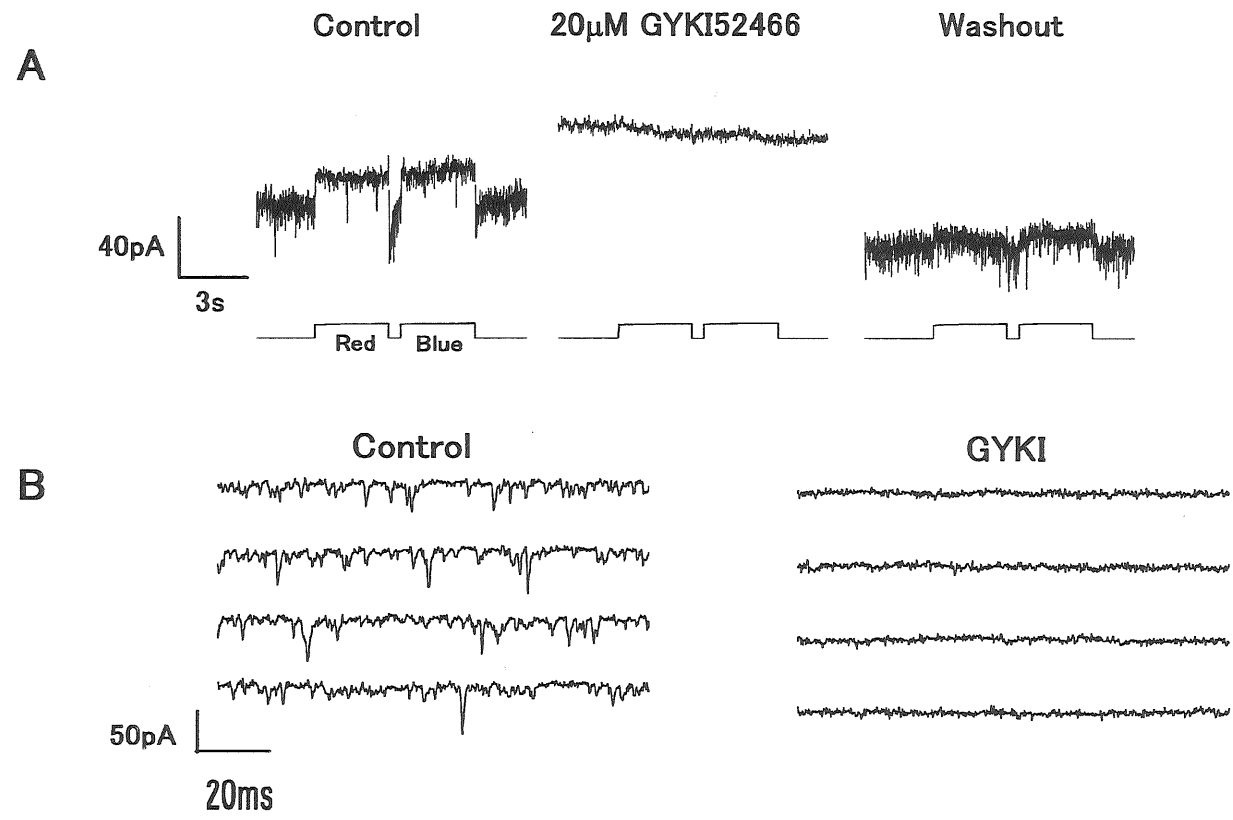

Figure 2.8 Suppression of sEPSCs and light responses of H1 cells by GYKI52466.

A. Upper trace: Current noise of an H1 cell to light stimulation in control Ringer and in the presence of 20 μM GYKI52466 and recovery on wash-out. GYKI52466 almost completely blocked light responses (upward deflections), and its recovery was observed by washing-out. Holding potential: -60 mV. Lower trace: The timing of red (left) and blue (right) stimuli.

B. Fast sweep recordings of the sEPSCs suppressed by 20 μM GYKI52466.

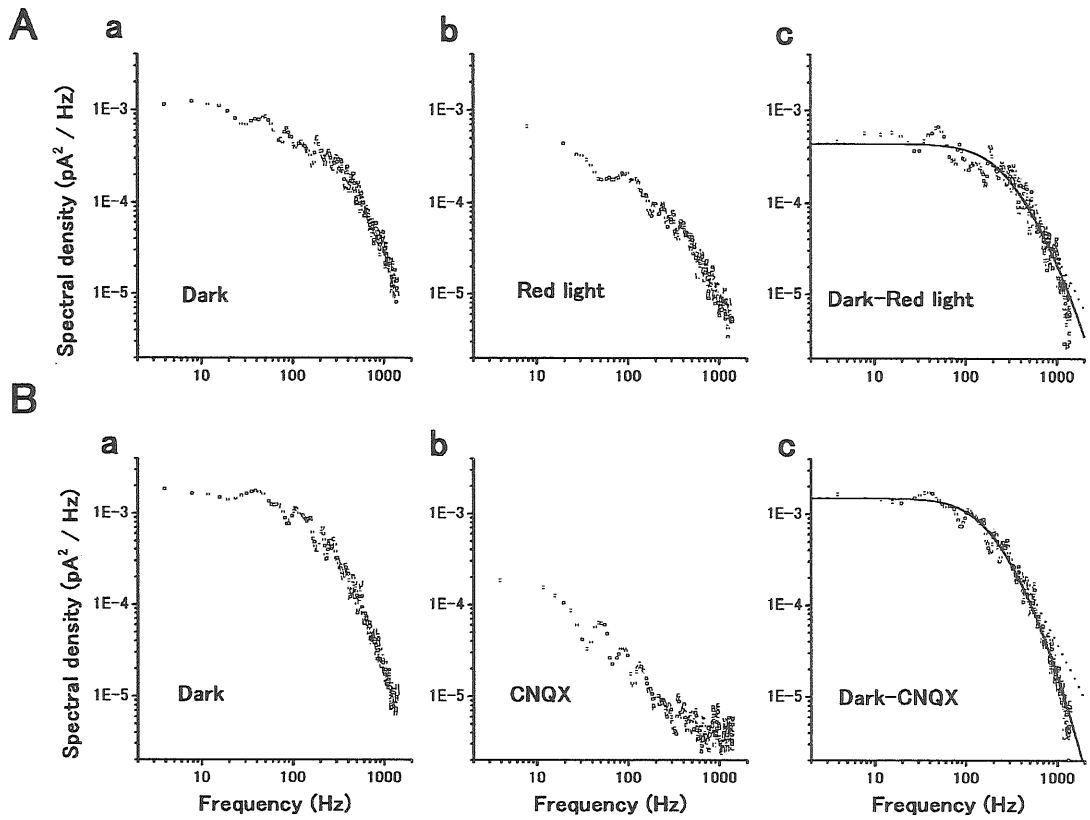

Figure 2.9 Power spectra of sEPSCs in H1 cells suppressed by red light stimulation and CNQX.

A. Power spectrum changed by red light illumination. Power spectrum in darkness (a) and that in red light (b) and the difference spectrum (c) between darkness and red light. Dark - red power spectrum, f_d = 264 Hz, f_r = 1600 Hz. (f_d and f_r : cut-off frequency for decay and rise phase, respectively)

B. Power spectrum changed by 10 μM CNQX. Power spectrum in darkness before (a) and after treatment of CNQX (b) and the difference spectrum (c) between those in darkness and CNQX. Dark - CNQX power spectrum, f_d = 160 Hz, f_r = 905 Hz. Each of the difference power spectrum was obtained by subtracting the spectrum obtained in each test condition from that in darkness, and was fitted by equation (2) in Methods. A single Lorentzian (shown by a dashed line) does not fit well to the high frequency region of power spectrum. In each case, eight samples of 256 ms duration, with low pass filtered at 2 kHz, were averaged using a sampling frequency of 8 kHz

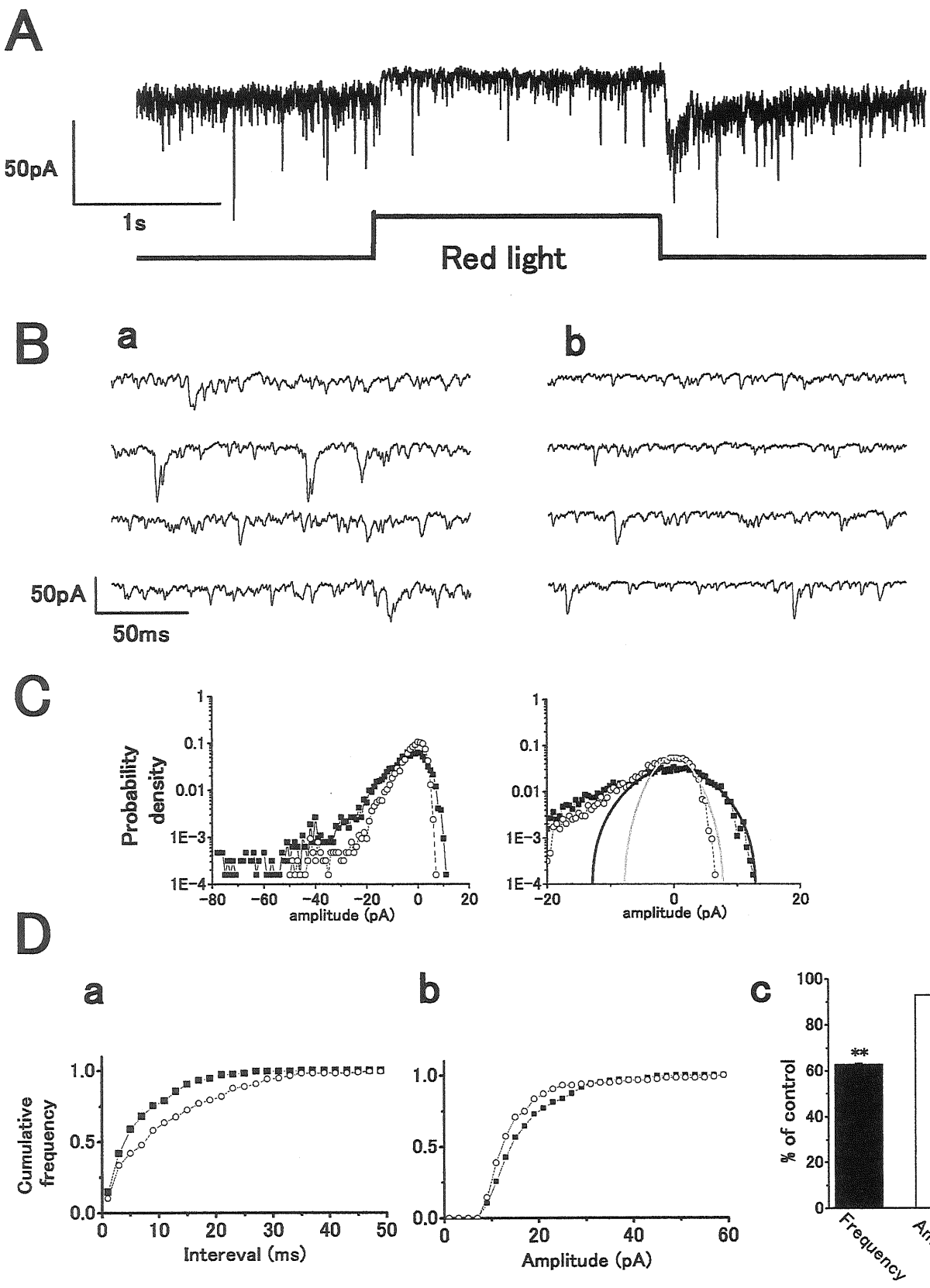
A
50pA
1s
Red light
B
a
b
50pA
50ms
C
Probability density
1
0.1
0.01
1E-3
1E-4
-80
-60
-40
-20
0
20
amplitude (pA)
-20
0
20
amplitude (pA)
D
a
b
c
Cumulative frequency
1.0
0.5
0.0
0
10
20
30
40
50
Intereval (ms)
0
20
40
60
Amplitude (pA)
100
80
60
40
20
0
% of control
**
Frequency
Amplitude

Figure 3.1 Red light illumination reduces the frequency of spontaneous excitatory postsynaptic currents (sEPSCs) without significant reduction of mean peak amplitude in an H1 horizontal cell (HC), recorded from a carp retinal slice.

A. Whole-cell voltage clamp recording from an H1 horizontal cell showing an outward current response to a step of red light with a reduction in sEPSC frequency. 20 μM dopamine was used throughout to block gap junctions to allow recording of sEPSCs (inward current events) (Hirasawa et al., 2001). The intensity of the red light was 6×10^5 quanta/μm^2/s. Holding potential was –52 mV.

B. Fast sweep recordings in darkness (a) and with red light (b).

C. Probability density distribution histograms of postsynaptic current in darkness (filled squares) and red light (open circles) (left). The maxima of the probability density distributions were set to zero current. The same histograms on an expanded amplitude scale to show the baseline noise distribution (right). Gaussian functions fitted the outward current density in darkness (black line, standard deviation: $\sigma = 5.1$ pA) and in red light (gray line, $\sigma = 2.6$ pA).

D. (a) Cumulative probability histograms showing sEPSC interval distribution in darkness (filled squares: 168 events) and in red light (open circles: 116 events). The mean sEPSC intervals were 7.1 ms and 11.5 ms in darkness and in red light, respectively. (b) Cumulative probability histograms of peak amplitude of sEPSCs in darkness (filled squares: 282 events) and in red light (open circles: 171 events). Mean amplitude in red light (15.7 pA) was slightly reduced compared with that in darkness (17.7 pA). (c) Bar chart summarizing the changes in mean frequency (a) and peak amplitude (b) from 3 cells. The red light reduced the frequency of sEPSCs by 37.4 ± 0.1 % ($p<0.001$) but did not change the mean amplitude (7.0 ± 1.9 %; $p>0.05$). Level of significance was: **: $p<0.01$

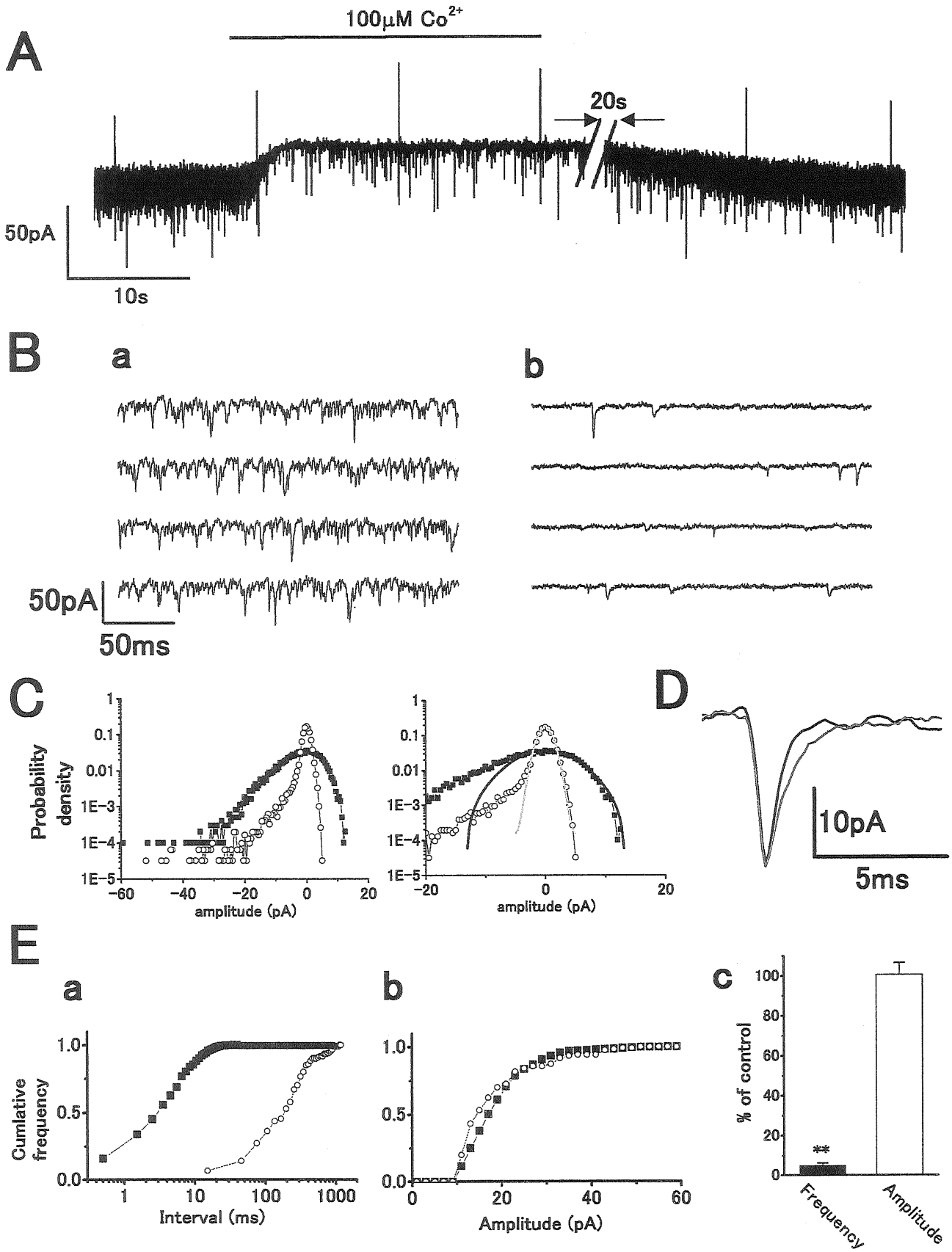
A
100μM Co2+
20s
50pA
10s
B
a
b
50pA
50ms
C
Probability density
amplitude (pA)
amplitude (pA)
D
10pA
5ms
E
a
b
c
Cumlative frequency
Interval (ms)
Amplitude (pA)
% of control
**
Frequency
Amplitude

Figure 3.2 External application of 100 μM cobalt reduces the sEPSC frequency in darkness without any significant reduction in mean amplitude.

A. Whole-cell voltage clamp recording from an H1 horizontal cell showing an outward current response to application of cobalt, showing a reduction in sEPSC frequency. A voltage command pulse of 5 mV was applied every 12 s to monitor input conductance. For illustration, the trace was shortened by 20 s (indicated by the slashes). Holding potential was –44 mV.

B. Fast sweep recordings before (a) and during cobalt application (b).

C. Probability density distribution histograms of postsynaptic current in control (filled squares) and with cobalt (open circles) (left). The maxima of the probability density distributions were set to zero current. The same histogram on an expanded amplitude scale to show the baseline noise distribution (right). Gaussian functions fitted the outward current density in control (black line, $\sigma = 4.7$ pA) and with cobalt (gray line, $\sigma = 1.1$ pA).

D. Time-course of averaged sEPSCs before (black trace, n = 95) and during cobalt application (gray trace, n = 57)

E. Cumulative probability histograms showing sEPSC interval distribution in control (filled squares: 817) and in cobalt (open circles: 116) indicate lower sEPSC event frequency in cobalt. The mean sEPSC intervals were 4.9 ms and 246 ms in control and with cobalt, respectively. (b) Cumulative probability histogram of peak amplitude of sEPSCs in control (filled squares: 413 events) and with cobalt (open circles: 120 events). Mean amplitude in cobalt (18.8 pA) was slightly reduced compared with that in control (19.4 pA). (c) Bar chart summarizing the change of mean frequency (a) and mean peak amplitude (b) from 8 cells. 100 μM cobalt reduced the sEPSC frequency (4.7 ± 1.3 % : $p<0.001$) but did not change the mean amplitude (101 ± 0.1 % : $p>0.8$).

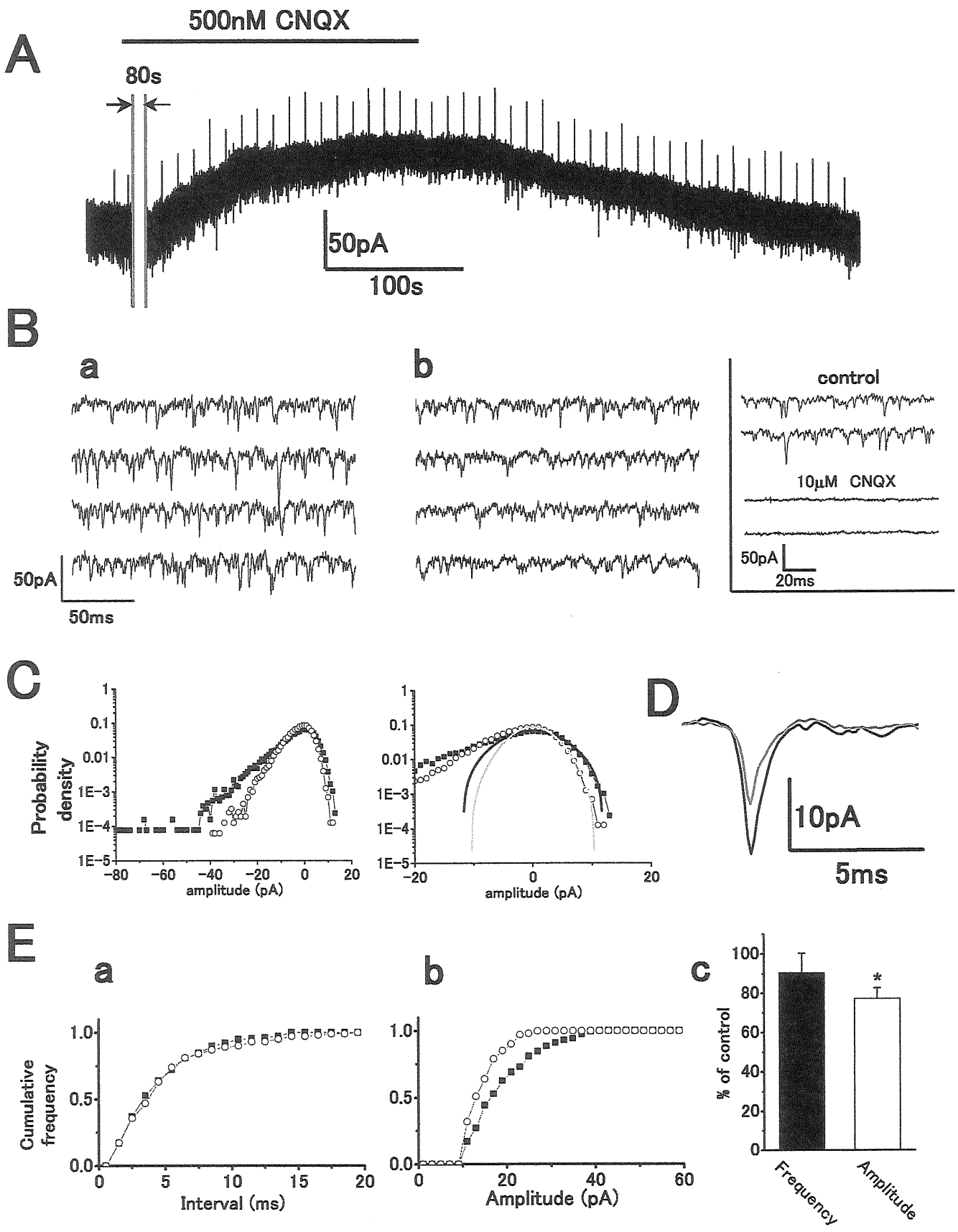
A
500nM CNQX
80s
50pA
100s
B
a
b
control
10μM CNQX
50pA
50ms
20ms
C
Probability density
amplitude (pA)
D
10pA
5ms
E
a
b
c
Cumulative frequency
Interval (ms)
Amplitude (pA)
% of control
Frequency
Amplitude

Figure 3.3 500 nM CNQX reduced the sEPSC mean peak amplitude without any change in frequency.

A. Whole-cell voltage clamp recording from an H1 horizontal cell showing an outward current in response to application of CNQX, with a reduction in sEPSC amplitude. For illustration, 80 s of the recording was removed. A voltage command pulse of 5 mV was applied every 12 s. The initial inward current was probably a solution-switching artifact since this was only observed in 1 out of 4 recordings. Holding potential was –60 mV.

B. Fast sweep recordings, in darkness, before (a) and during CNQX application (b).

C. Probability density distribution histograms of postsynaptic current in darkness (filled squares) and with 500 nM CNQX (open circles) (left). The maxima of the probability density distributions were set to zero current. The same histograms on an expanded amplitude scale to show the baseline noise distribution (right). Gaussian functions fitted the outward current density in control (black line, σ = 5.0 pA) and with CNQX (gray line, σ = 3.4 pA).

D. Time-course of averaged sEPSCs before (black trace, n = 139) and during CNQX application (gray trace, n = 196).

E. Cumulative probability histograms showing sEPSC interval distribution in control (filled squares: 222 events) and with CNQX (open circles: 157 events) indicate no significant change of sEPSC frequency with CNQX. The mean sEPSC intervals were 4.3 ms and 4.7 ms in control and with CNQX, respectively. (b) Cumulative probability histograms of peak amplitude of sEPSCs in darkness (filled squares: 221 events) and with CNQX (open circles: 156 events). Mean amplitude in CNQX (10.5 pA) was reduced compared with that in control (15.7 pA). (c) Bar chart summarizing the change of mean frequency (a) and mean peak amplitude (b) from 4 cells. 500 nM CNQX reduced the sEPSC amplitude (77.3 ± 0.1 % : $P<0.03$) but did not change the mean frequency (90.5 ± 9.9 % : $P>0.4$). Level of significance was: *: $p<0.05$

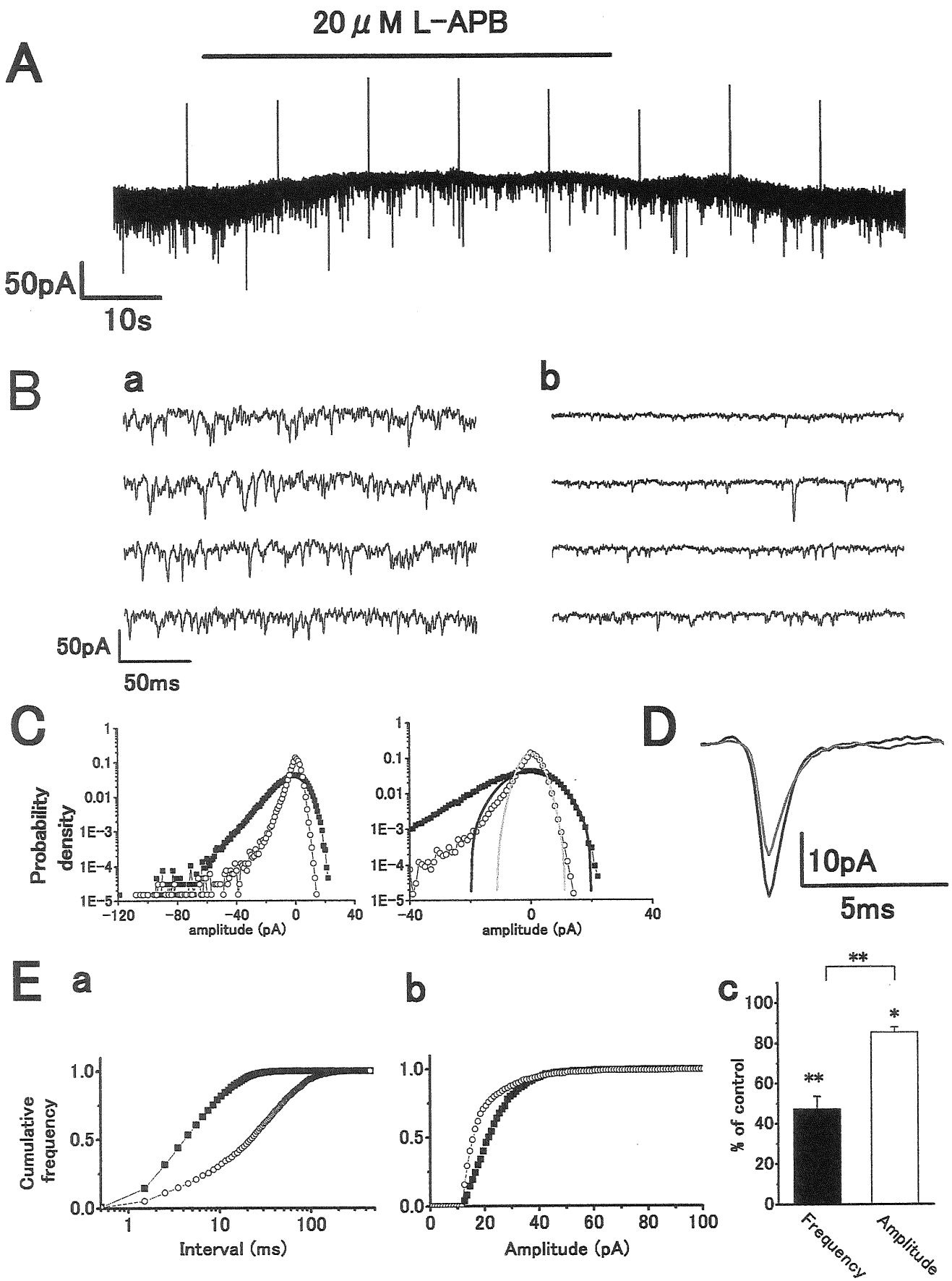
20 μ M L-APB
A
50pA
10s
B
a
b
50pA
50ms
C
Probability density
1
0.1
0.01
1E-3
1E-4
1E-5
−120
−80
−40
0
40
amplitude (pA)
D
10pA
5ms
E
a
b
c
Cumulative frequency
1.0
0.5
0.0
1
10
100
Interval (ms)
0
20
40
60
80
100
Amplitude (pA)
% of control
**
*
Frequency
Amplitude

Figure 3.4 L-APB reduces sEPSC frequency with slight reduction of mean peak amplitude.

A. Whole-cell voltage clamp recording from an H1 horizontal cell in the dark showing an outward current response to application of 20 μM L-APB, with a reduction in sEPSC frequency. The patch-pipette solution contained 100 μM H-7 to block the post-synaptic action of L-APB, mediated by phosphorylation. A voltage command pulse of 5 mV was applied every 12 s. Holding potential was –57 mV.

B. Fast sweep recordings before (a) and during L-APB application (b).

C. Probability density distribution histograms of postsynaptic current in control (filled squares) and with 20 μM L-APB (open circles) (left). The maxima of the probability density distributions were set to zero current. The same histograms on an expanded amplitude scale to show the baseline noise distribution (right). Gaussian functions fitted the outward current density in darkness (black line, σ = 7.5 pA) and with CNQX (gray line, σ = 3.1 pA).

D. Time-course of averaged sEPSCs before (black trace, n = 84) and during L-APB application (gray trace, n = 104).

E. Cumulative probability histograms showing sEPSC interval distribution in control (filled squares: 2935 events) and with L-APB (open circles: 1112 events) indicates reduction of sEPSC frequency with L-APB. The mean sEPSC intervals were 6.8 ms and 34.0 ms darkness and with L-APB, respectively. (b) Cumulative probability histograms of peak amplitude of sEPSCs in control (filled squares: 1249 events) and with L-APB (open circles: 885 events). Mean amplitude in L-APB (20.2 pA) was reduced compared with that in control (28.2 pA). (c) Bar chart summarizing the change of mean frequency (a) and amplitude (b) from 19 cells. 20 μM L-APB reduced the sEPSC frequency by 52.7 ± 6.0 % ($p<0.001$) and slightly reduced the mean amplitude by 15.5 ± 2.1 % ($p<0.001$). The frequency reduction was significantly greater than that of peak amplitude ($p<0.001$).

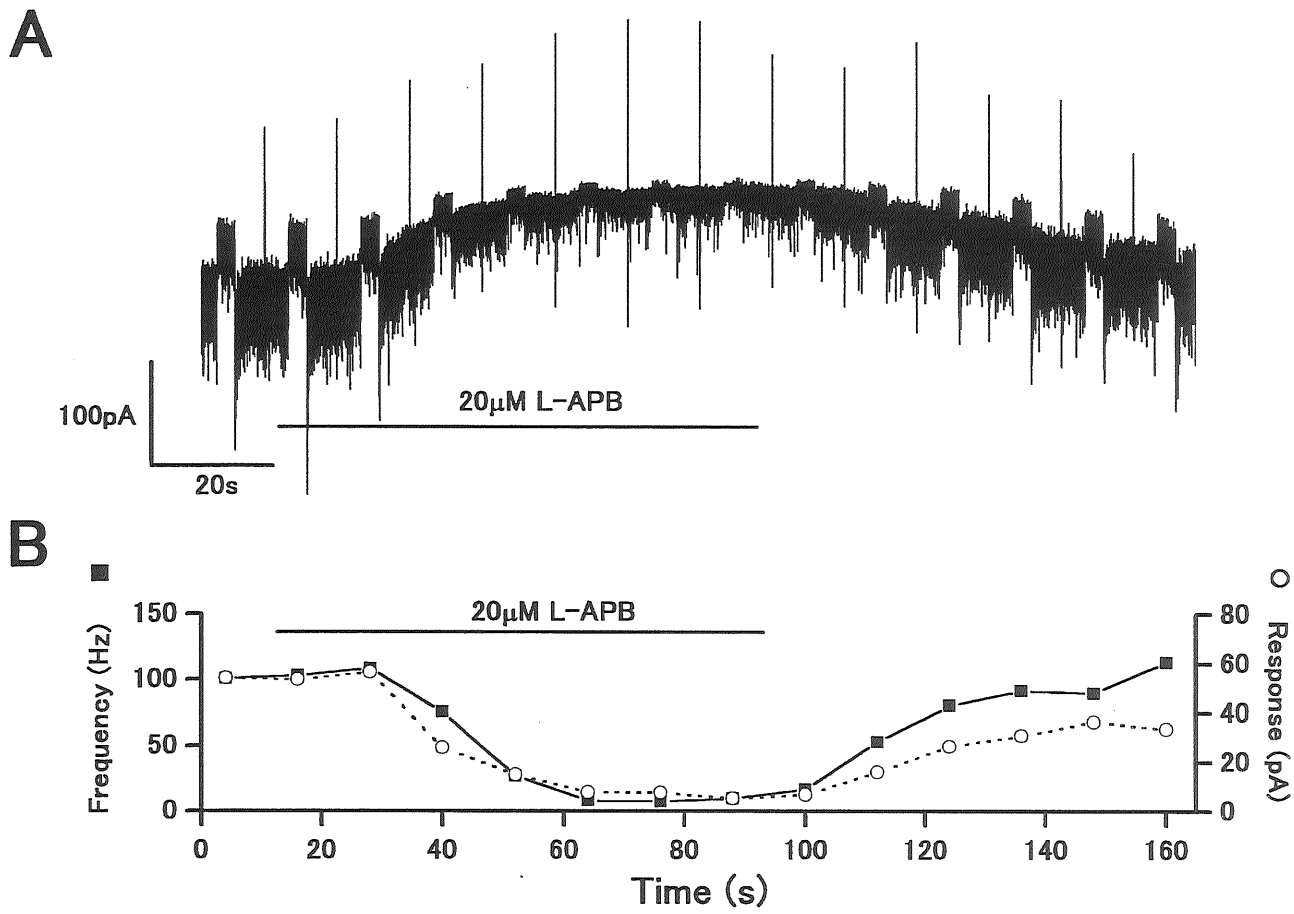

Figure 3.5 The light-induced outward current responses were reduced by L-APB, accompanied by a reduction of sEPSC amplitudes.

A. Whole-cell voltage clamp recording from an H1 horizontal cell showing outward current responses to red light steps (2×10^6 quanta/μm^2/s). An application of 20 μM L-APB induced an outward shift in the whole-cell current. A voltage command pulse of 5 mV was applied every 12 s. Holding potential was –60 mV.

B. Light responses (open circles) and sEPSC frequency (filled squares) showed a reduction over a similar timecourse in response to APB.

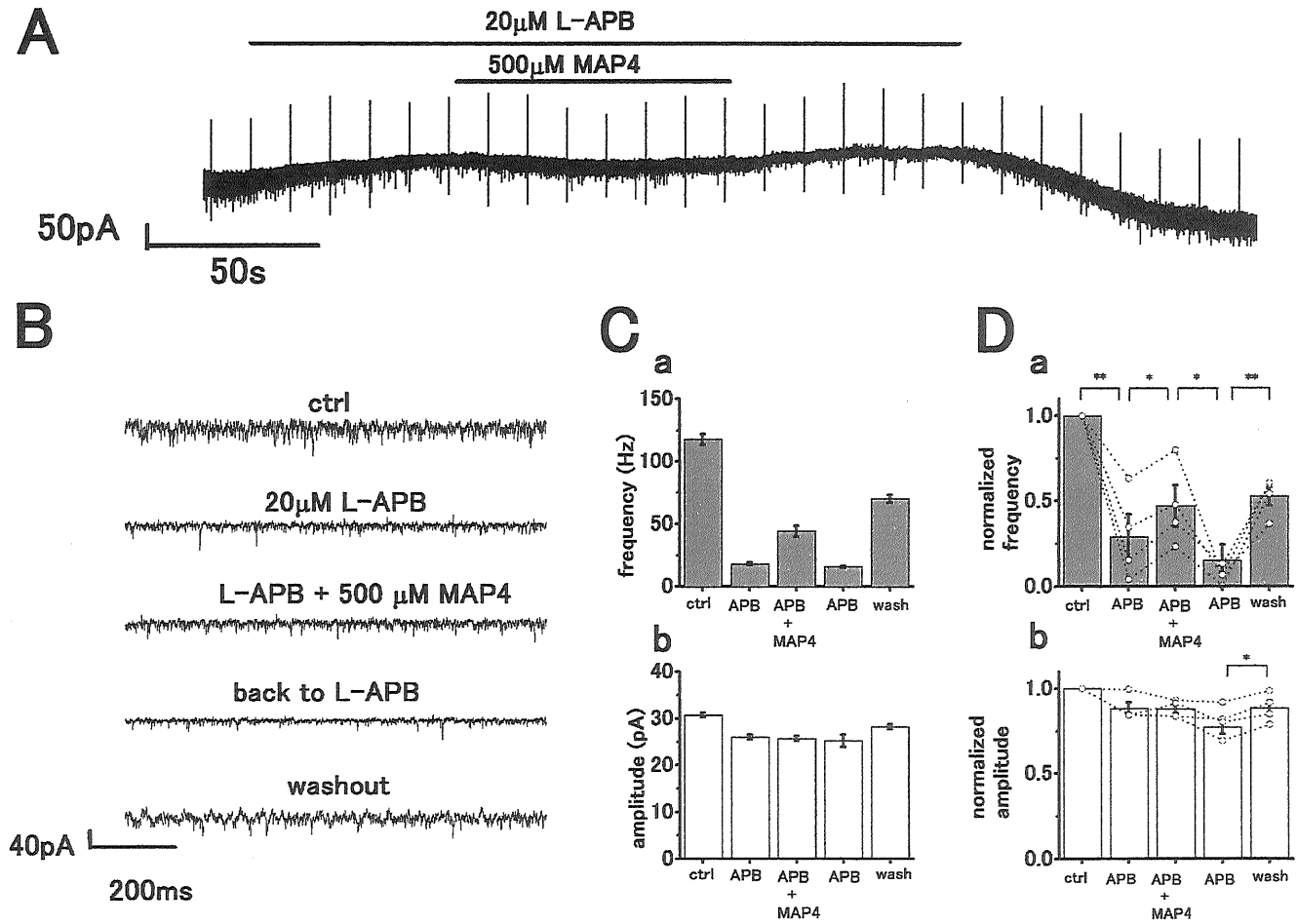

Figure 3.6 The action of L-APB in reducing sEPSC frequency is antagonized by MAP4.

A. Whole-cell voltage clamp recording from an H1 horizontal cell in the dark. 20 μM L-APB induced an outward current accompanied by a reduction in sEPSC frequency. Co-application of 500 μM MAP4 induced an inward current with some recovery of sEPSC frequency. A voltage command pulse of 5 mV was applied every 12 s. Holding potential was –57 mV.

B. Fast sweep recording of current traces in each pharmacological condition shown in A.

C. (a) Bar chart representation of sEPSC frequency under the different pharmacological conditions. MAP4 application partially restored the reduction in sEPSC frequency induced by L-APB. (b) A similar plot showing little change in sEPSC peak amplitudes.

D. Bar charts summarizing the mean changes in sEPSC frequency (a) and peak amplitude (b) from 4 cells. Open circles with dotted lines indicate individual data from single cells. Error bars indicate SEM. Levels of significance were: **: $p<0.01$, *:$p<0.05$

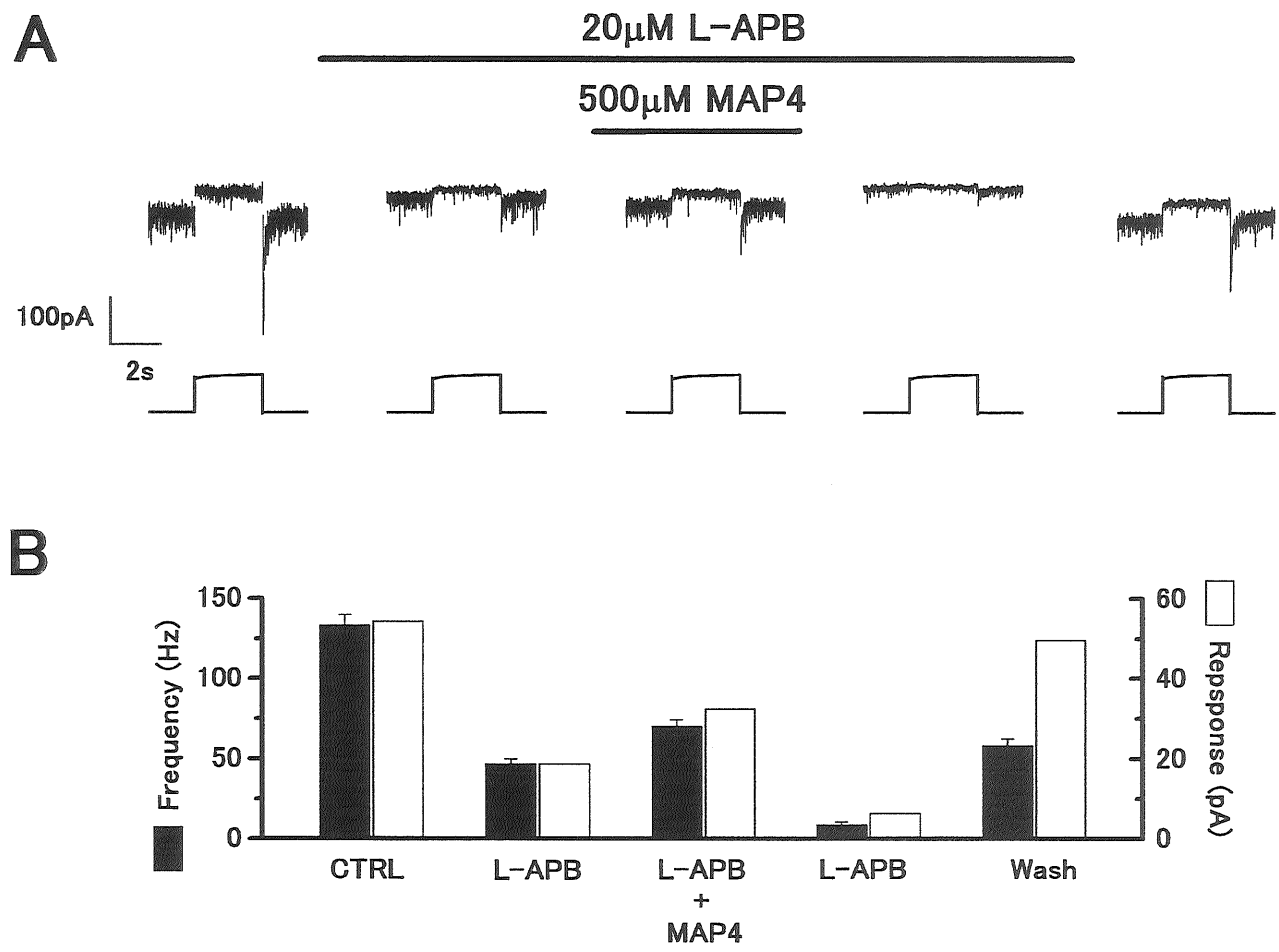

Figure 3.7 MAP4 antagonizes the presynaptic action of L-APB.

A. Outward current responses to red light (2×10^6 quanta/μm^2/s) recorded under whole-cell voltage clamp from an H1 HC. Application of 20 μM L-APB induced an outward current and reduction of the light responses. Co-application of 500 μM MAP4 induced an inward current, accompanied by some recovery of the light responses. Holding potential was –57 mV.

B. The L-APB induced reduction in light response amplitude (open bars) and sEPSC frequency (filled bars) were restored by MAP4.

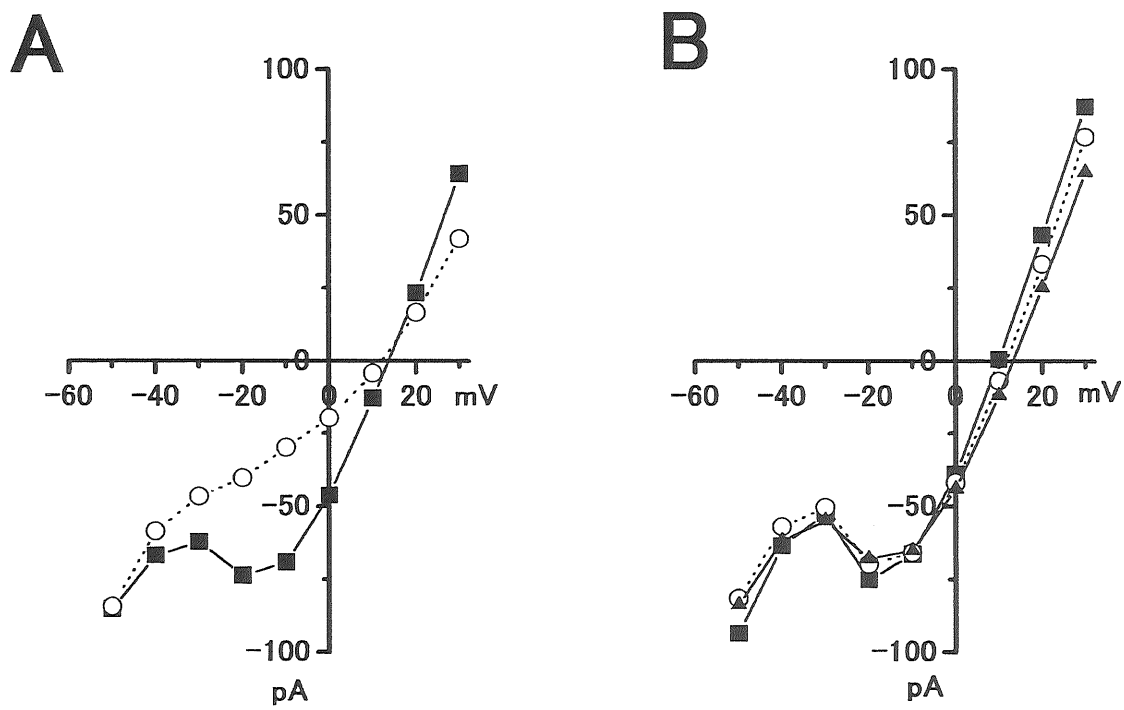

Figure 3.8 20 μM L-APB does not reduce voltage-activated Ca^{2+} conductance in cones.

A. Current-voltage (*I-V*) relations obtained from a whole-cell voltage-clamped cone photoreceptor in the carp retinal slice before (squares) and during (circles) cobalt application, showing a reduction of voltage-sensitive Ca^{2+} conductance by cobalt.

B. *I-V* relationships from the same cone photoreceptor before (circles), during (squares) and on washout (triangles) of a 20 μM APB application to the retinal slice, showing no effect of APB on Ca^{2+} conductance. In both cases, K^+ conductance was suppressed by external application of Cs and TEA.

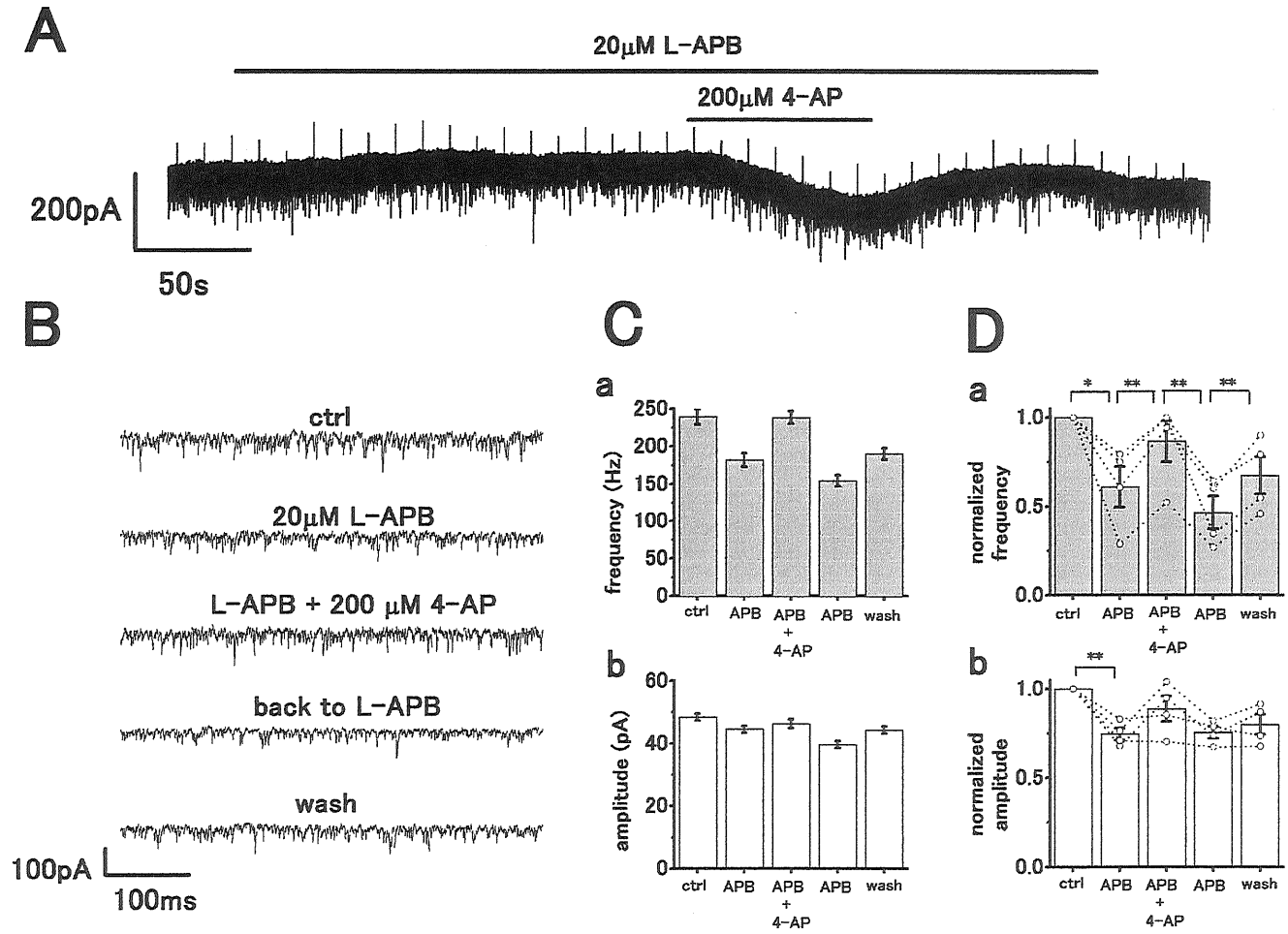

Figure 3.9 Blocking K^+ conductance with 4-AP induces an inward current and recovery of H1 HC sEPSC frequency reduced by L-APB.

A. Whole-cell voltage clamp recording from an H1 horizontal cell in the dark. 20 μM L-APB induced an outward current accompanied by a reduction in sEPSC frequency. Co-application of 200 μM 4-AP induced an inward current. A voltage command pulse of 5 mV was applied every 12 s. Holding potential was –71 mV.

B. Time-expanded sections of the recording in *A* showing reduction in sEPSC frequency with L-APB and then some recovery with 4-AP, accompanying the inward current.

C. Bar charts showing mean sEPSC frequency (a) and mean peak amplitude (b) changes from 4 cells in each pharmacological condition. Error bars indicate SEM.

D. Bar charts summarizing the mean changes in sEPSC frequency (a) and peak amplitude (b) from 4 cells. Open circles with dotted lines indicate individual data from single cells. Error bars indicate SEM. Levels of significance were: **: $p<0.01$, *:$p<0.05$

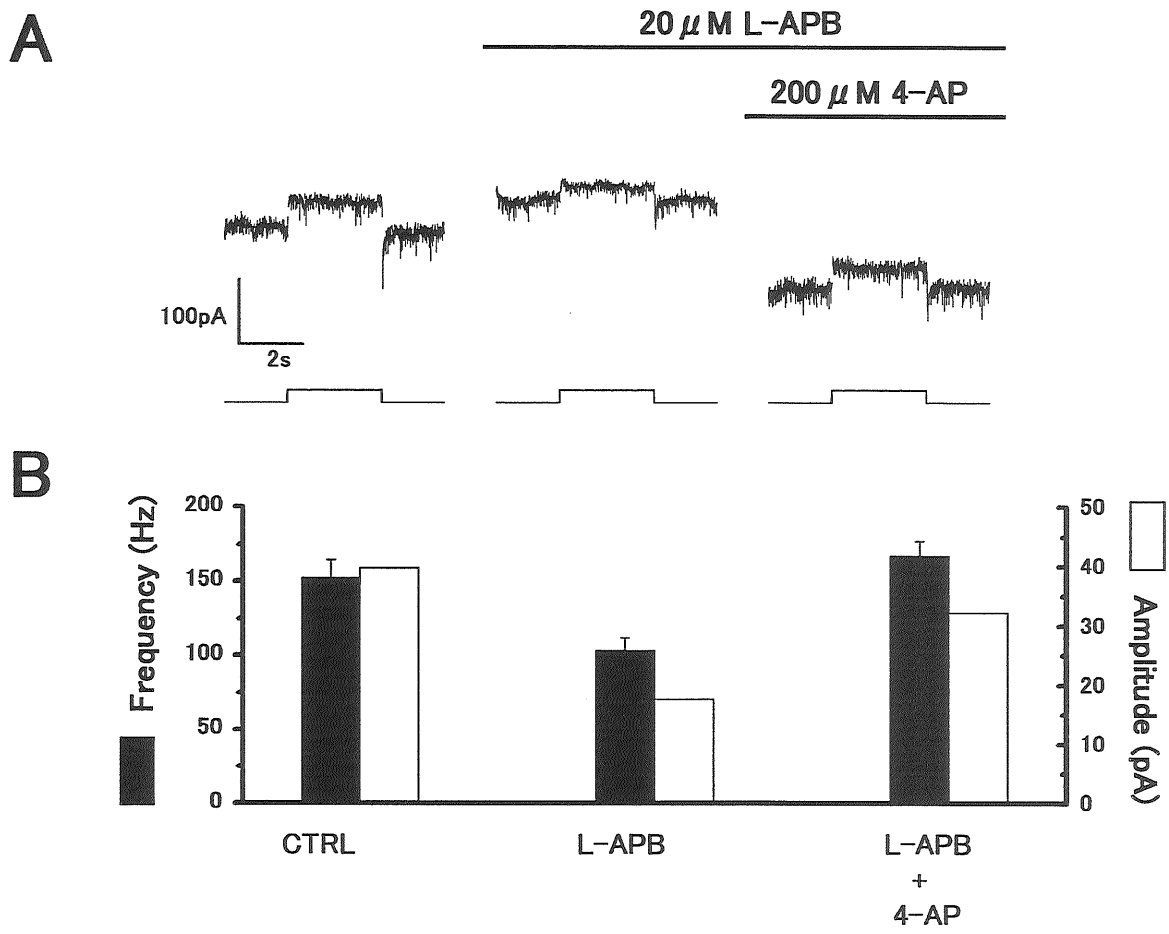

Figure 3.10 Blocking K^+ conductance with 4-AP reverses the APB-induced reduction of H1 HC light responses.

A. Outward current responses to red light (2×10^6 quanta/μm^2/s) recorded under whole-cell voltage clamp from an H1 HC. Application of 20 μM L-APB induced an outward current and reduction of light responses. Co-application of 200 μM 4-AP induced an inward current, accompanied by some recovery of the light responses. Holding potential was –60 mV.

B. The L-APB-induced reduction in light response amplitude (open bars) and sEPSC frequency (filled bars) showed some recovery with 4-AP

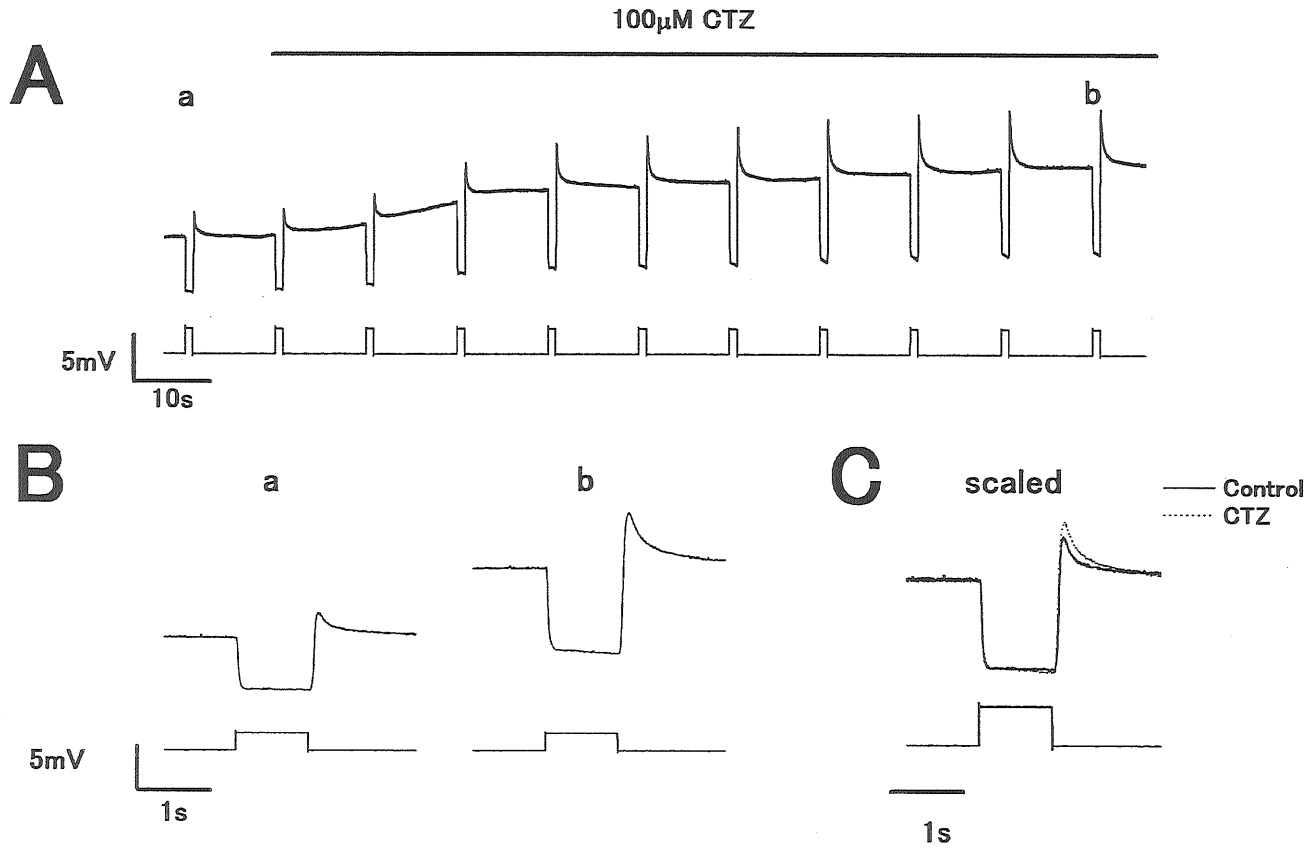

Figure 4.1 100 μM cyclothiazide (CTZ) depolarizes H1 HCs in carp retinal slices, with enhancement of light responses

A. The effect of CTZ-containing Ringer solution on voltage responses of the HC recorded in current clamp mode. A step of red light with 1 s duration was applied every 12 s. Light intensity was adjusted to induce a half-saturating light response (2.8×10^5 quanta/μm^2/s). CTZ depolarized the resting potential from –26.2 mV to –17.8 mV and increased the amplitude of light-evoked membrane hyperpolarization from 6.2 mV to 10.4 mV.

B. Enlarged voltage traces of photoresponses in control (a) and in CTZ (b) in A.

C. Voltage responses in control (solid line) and in CTZ (dotted line) normalized at the peak amplitude.

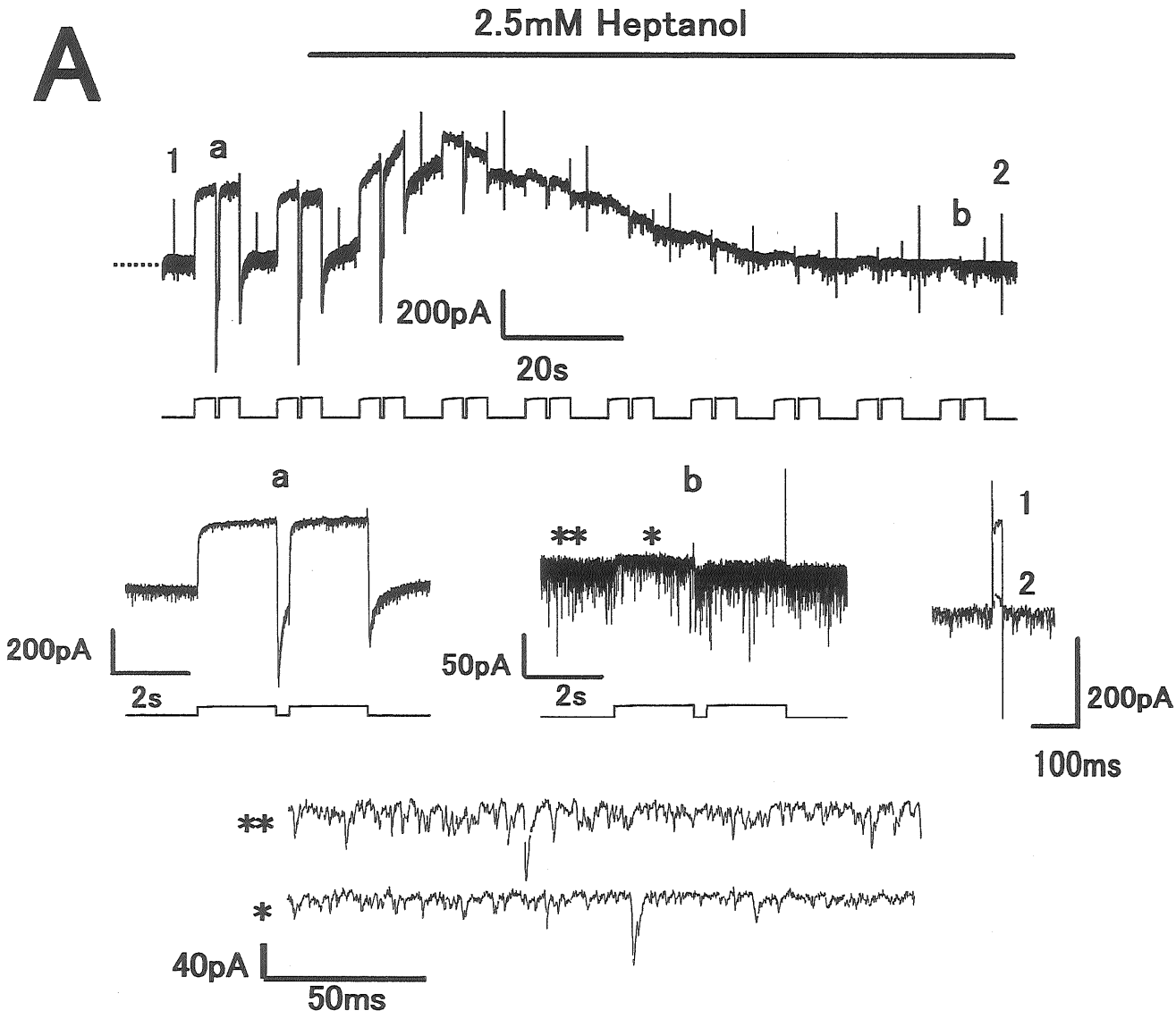
A
2.5mM Heptanol
1
a
2
b
200pA
20s
a
b
1
2
200pA
2s
50pA
2s
200pA
100ms
**
*
40pA
50ms

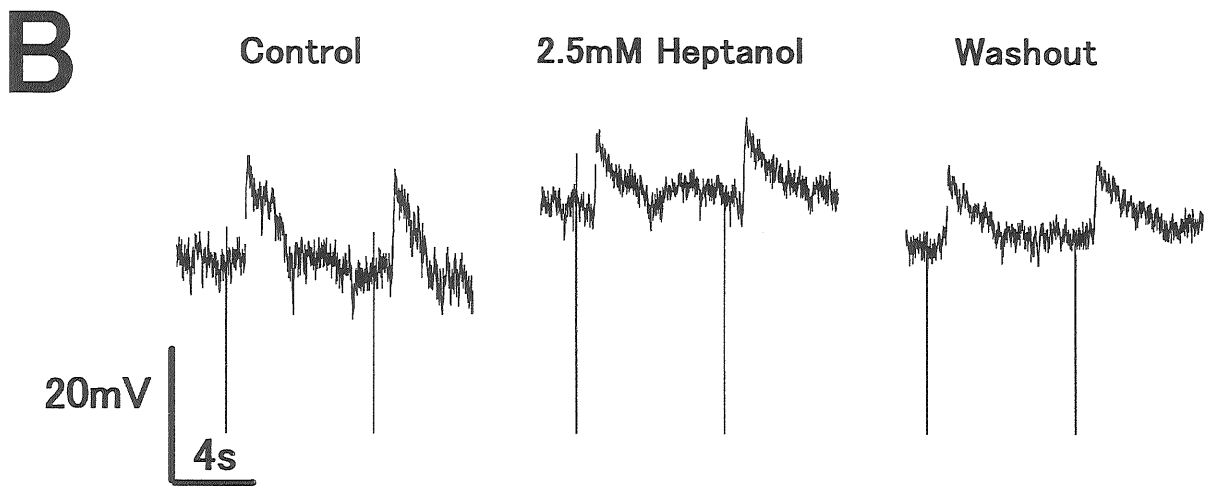
B
Control
2.5mM Heptanol
Washout
20mV
4s

Figure 4.2 Spontaneous excitatory postsynaptic currents (sEPSCs) of an H1 HC in a retinal slice observed in the presence of 2.5 mM heptanol

A. The effect of heptanol on postsynaptic current of the HC recorded in voltage clamp mode. The dotted line at the beginning of the recording indicates zero current level. The lower trace indicates the timing of light-step stimulation (left: red, right: blue). Outward current responses were elicited by a pair of red and blue light stimuli in control solution (a) and in heptanol-containing Ringer solution (b). The light steps elicited outward currents > 200 pA before the application of heptanol. Light intensities of red and blue light stimuli were 1.0 and 1.4×10^6 quanta/μm^2/s, respectively. Membrane conductance was monitored by applying 4 mV of pulses of 20 ms duration every 12 s. (1, 2): The currents induced by 5 mV pulses. The input resistances in control and heptanol were 14 MΩ (1) and 210 MΩ (2), respectively. Series resistance was 10 MΩ. Holding potential was –60 mV. The current traces in darkness (**) and with red light (*) in (b) are shown below on expanded timescales as marked with asterisks.

B. 2.5 mM heptanol fails to block HC depolarizing responses to pressure applications of glutamate. Depolarizing responses to 0.5 mM glutamate were recorded in current clamp mode. 3 mM Co^{2+}, to block synaptic transmission, was present in Ringer's solution. Hyperpolarizing 10 mV command pulses were applied to monitor input resistance, which increased with heptanol, and trigger the pressure applications.

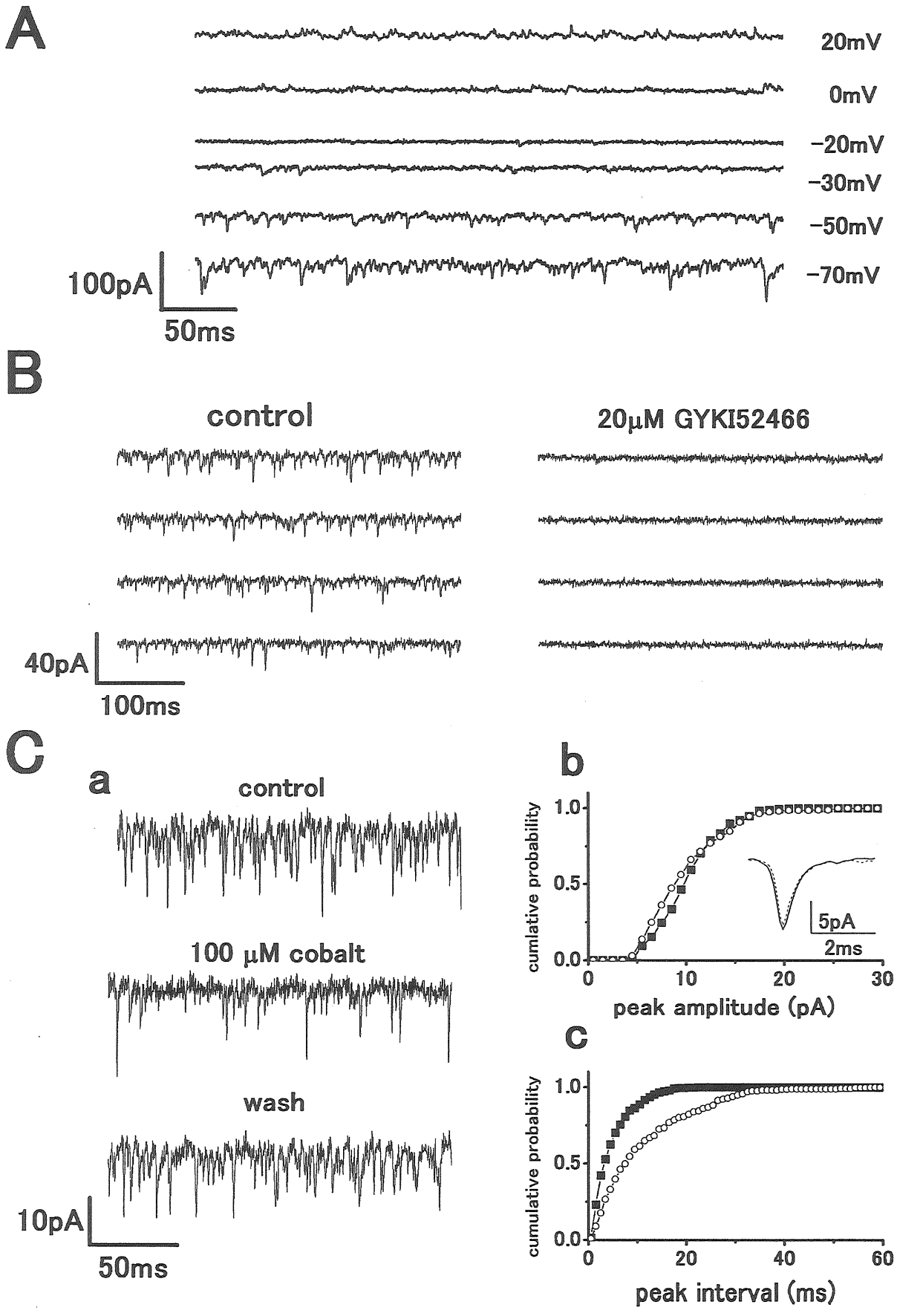
A
20mV
0mV
−20mV
−30mV
−50mV
−70mV
100pA
50ms
B
control
20μM GYKI52466
40pA
100ms
C
a
control
100 μM cobalt
wash
10pA
50ms
b
cumulative probability
1.0
0.5
0.0
0
10
20
30
peak amplitude (pA)
5pA
2ms
c
cumulative probability
1.0
0.5
0.0
0
20
40
60
peak interval (ms)

Figure 4.3 Physiological properties of sEPSCs of H1 HCs in a slice preparation in 2.5 mM heptanol

A. The sEPSCs at several holding potentials. Polarity of sEPSCs reversed at around 0mV.

B. The sEPSCs were blocked by 20 μM GYKI52466.

C. The effect of 100 μM cobalt on sEPSCs. (a) Current traces of sEPSCs. (b) Cumulative probability histograms of peak amplitude of sEPSCs in control (filled squares:, *n* (number of events) = 304) and in cobalt-containing Ringer (open circles: *n* = 205). Mean peak amplitudes of sEPSCs in control and cobalt were 10.4 pA and 9.9 pA, respectively. The inset shows the average sEPSC time-course in control (solid line: *n* = 148) and cobalt (dotted line: *n* = 97) containing Ringer. (c) Cumulative probability histograms of the peak interval of sEPSCs in control (filled squares: *n* = 638) and in cobalt (open circles: *n* = 279). The mean peak intervals of sEPSCs in control and cobalt were 5.2 ms and 10.8 ms, respectively.

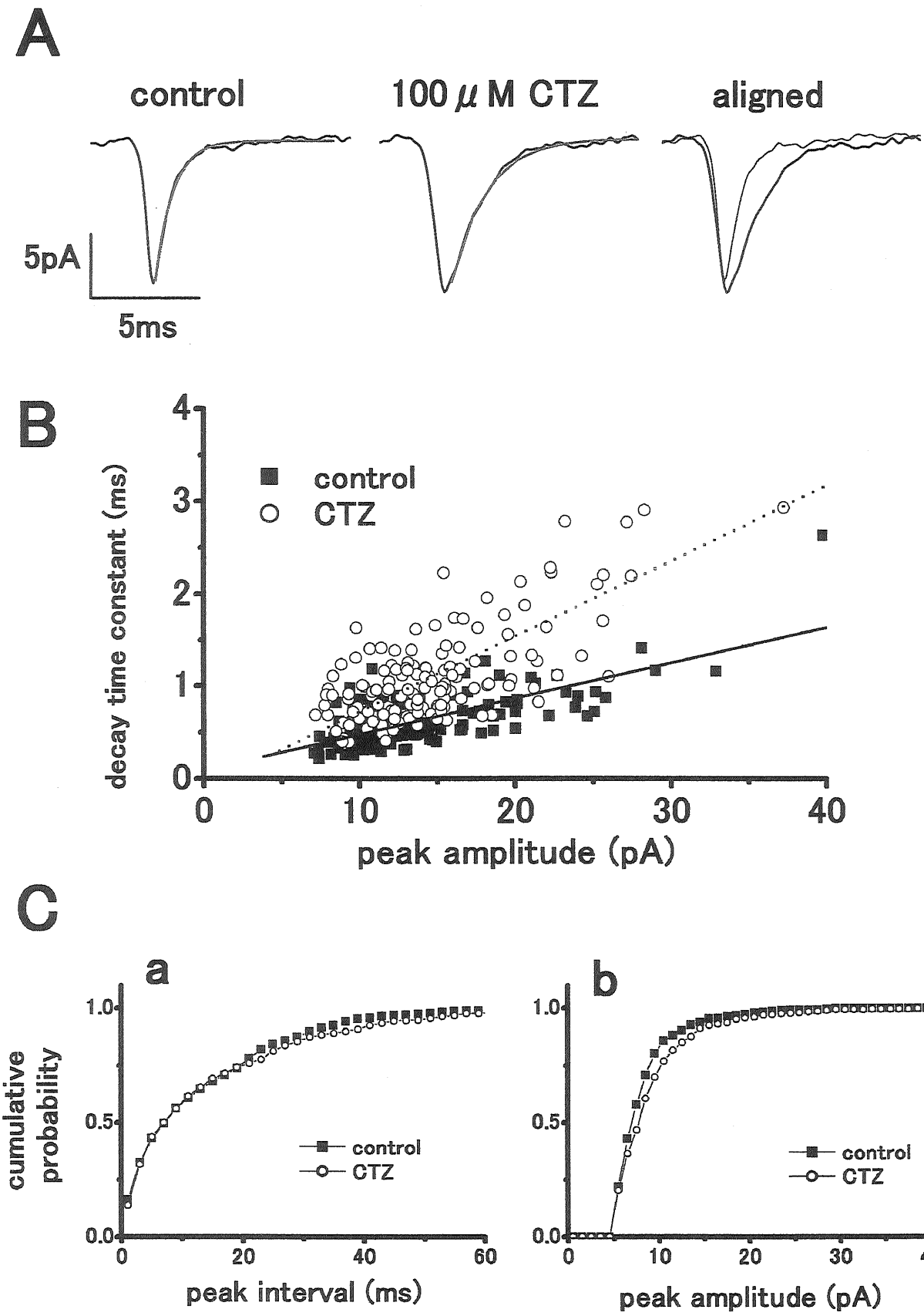
A
control
100 μ M CTZ
aligned
5pA
5ms
B
decay time constant (ms)
control
CTZ
peak amplitude (pA)
C
a
cumulative probability
control
CTZ
peak interval (ms)
b
control
CTZ
peak amplitude (pA)

Figure 4.4 100 μM CTZ increased the decay time constant of sEPSCs of an H1 HC

A. The effect of 100 μM CTZ on H1 HC sEPSCs in the presence of heptanol. The decay phase of sEPSC was fitted with single exponential curve (gray line). Averaged sEPSCs in control (n = 143: left) and CTZ (n = 131: middle) were fitted with single exponentials with time constants of 0.66 ms and 1.41 ms, respectively. Right: Superimposed (aligned) traces in control (thin line) and CTZ (thick line).

B. The plot of peak amplitude versus decay time constant of sEPSCs in control (filled squares) and CTZ (open circles). The data were fitted with linear regression lines by the least square error method (control: solid line, CTZ: dashed line). CTZ significantly increased the mean decay time constant of sEPSCs from 0.63 ms to 1.21 ms.

C. (a) Cumulative probability histograms of peak amplitude of sEPSCs in control (filled squares: n (number of events) = 455) and in CTZ (open circles: n = 400). The mean peak amplitudes of sEPSCs in control and in CTZ were 8.6 pA and 9.5 pA, respectively. (b) Cumulative probability histograms of peak interval of sEPSCs in control (filled squares: n = 750) and in CTZ (open circles: n = 630). The mean interval of sEPSCs in control and CTZ were 13.3 ms and 15.8 ms, respectively.